Abundance Constraints

on Sources of Nucleosynthesis, and on the Chemical Evolution of the Universe and its Components

- Part II -

NIC School 2008

26 Jul 2008

by Roland Diehl

One of the Key Tools of Astrophysics:

Where do specific atomic nuclei and their abundance originate?

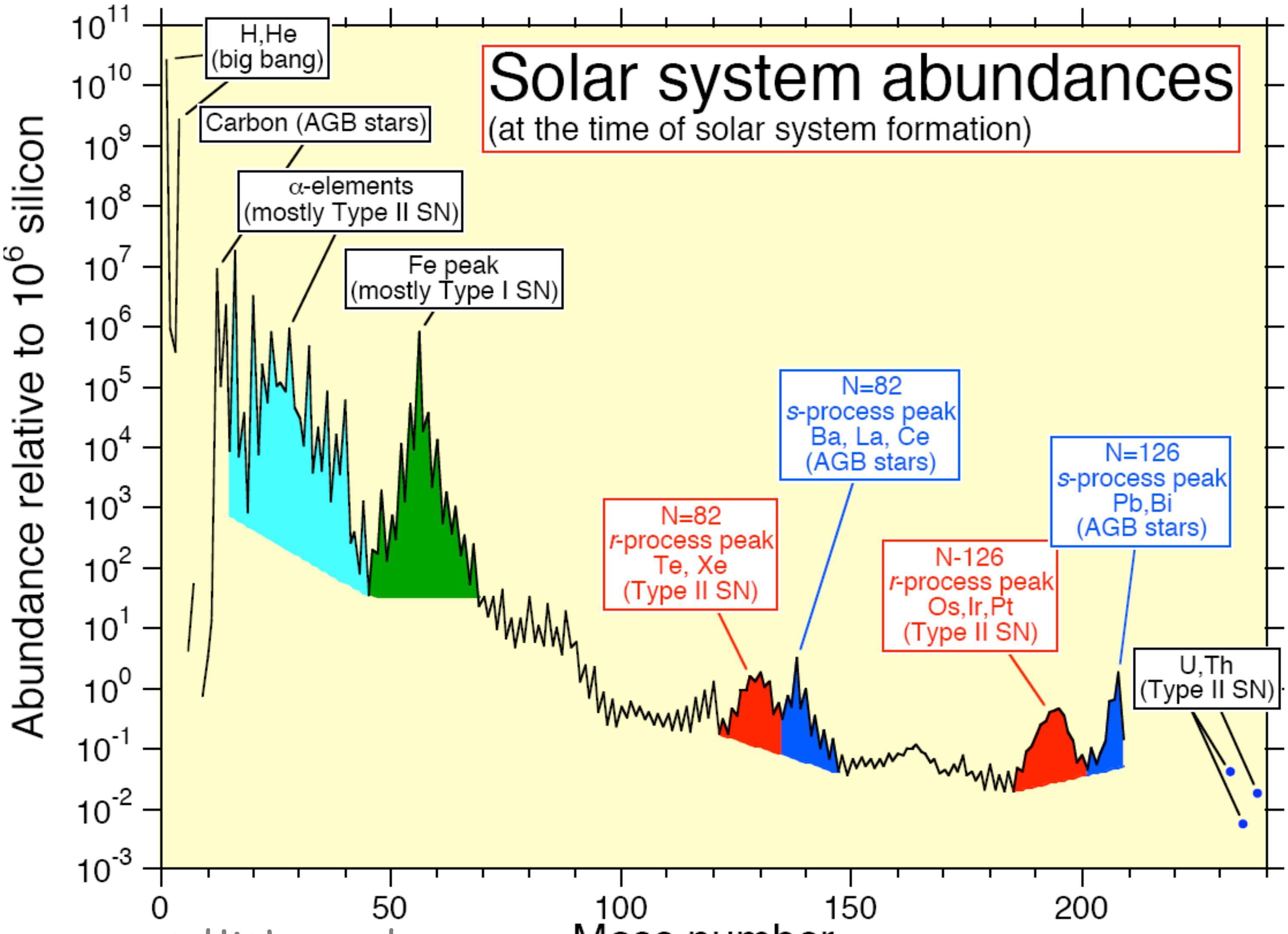

- ... the current 'lithurgy'
  - -> how much do we understand?

Courtesy: Andy Davis

The General Context:

How Do Nucleosynthetis Sources Enrich the Universe with Heavy Elements?

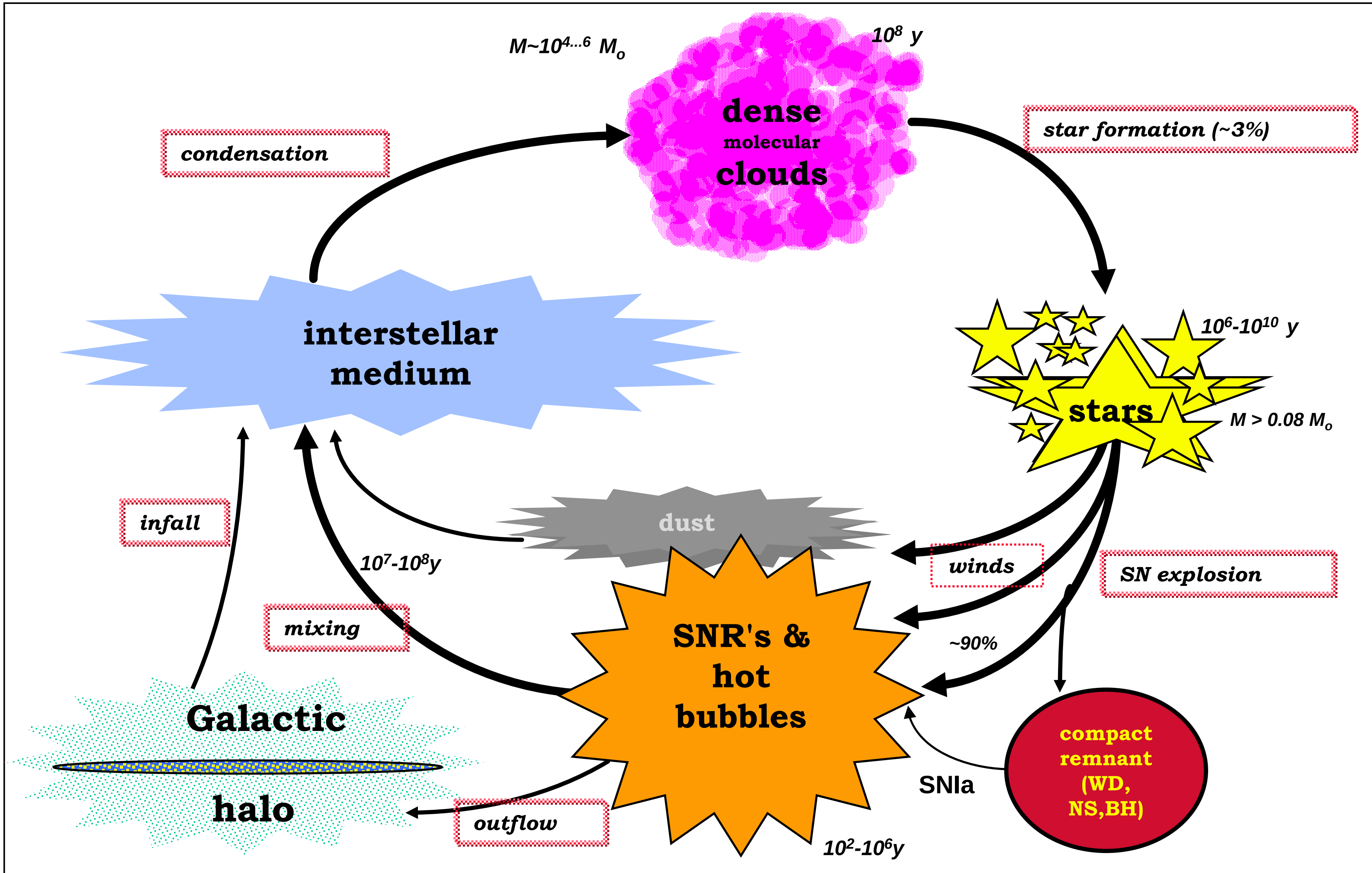

- ☆ Nuclear Reactions in Stars and Supernovae Rearrange Baryons -> New Atoms
- ☆ New Atoms are Mixed into ISM which Forms New Stars & Planets

...today's lecture:

- ☆ Complete the 'abundance-measurement tool' menu
  - ☞ diffuse / larger-scale gamma-ray constraints
  - ☞ meteoritic abundance constraints
  - ☞ more absorption and emission line methods
- ☆ Discuss the abundance-constrained view of universal chemical evolution
  - ☞ stellar-structure & nuclear-burning lessons
  - ☞ nuclear-physics lessons
  - ☞ stellar evolution & yields over the history
  - ☞ galaxy evolution over the history
  - ☞ large-scale universal chemical evolution

» a very broad scope, covering many disiplines of astrophysics...

Diversity of Complementing Observing Methods

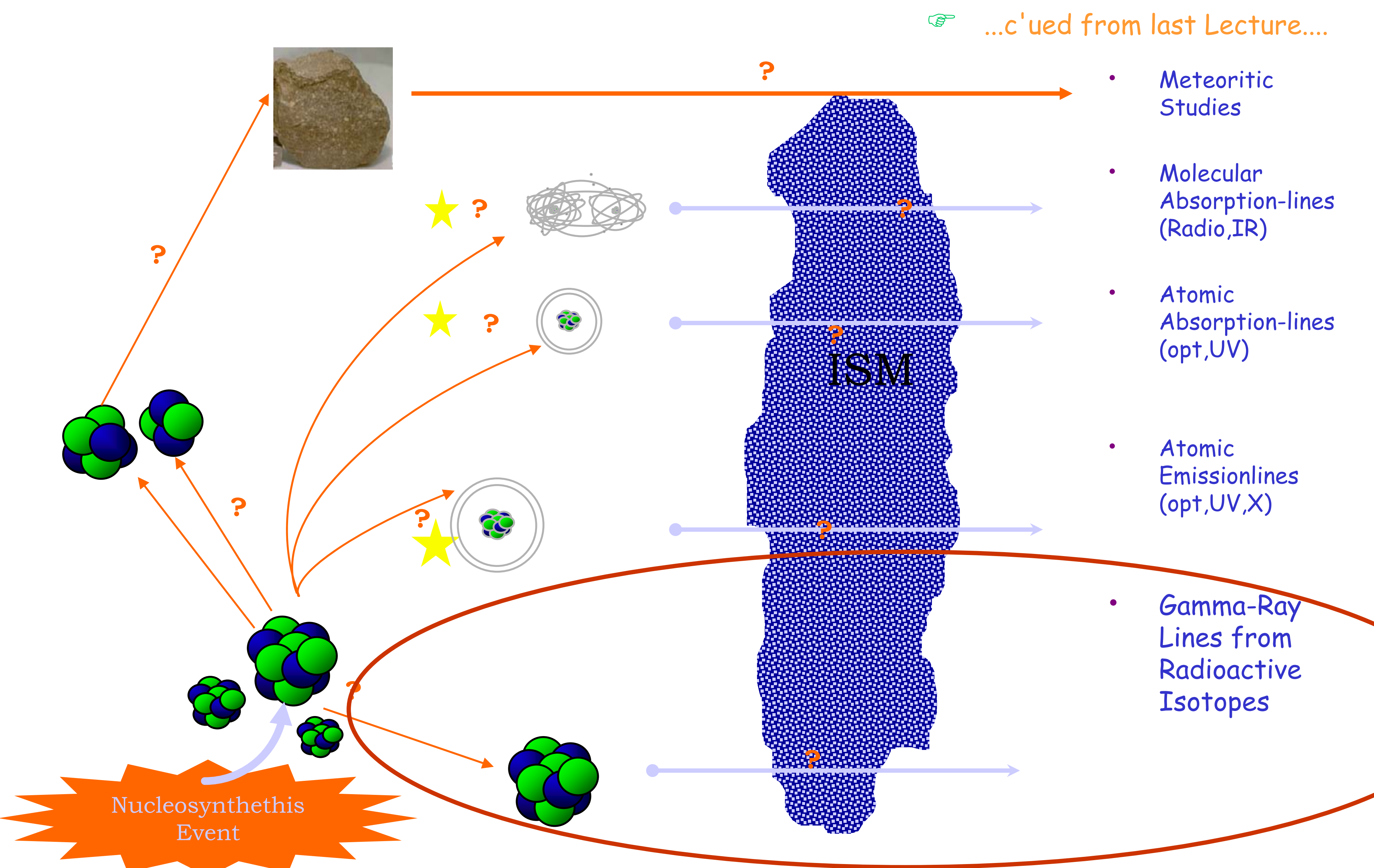

Massive-Star Interiors: Complex Astrophysics Issues

☆ **Massive Stars**

- ☞ Stellar Evolution Phases
- ☞ Mass Loss
- ☞ Convection & Mixing
- ☞ Intermittent Nuclear-Burning Phases

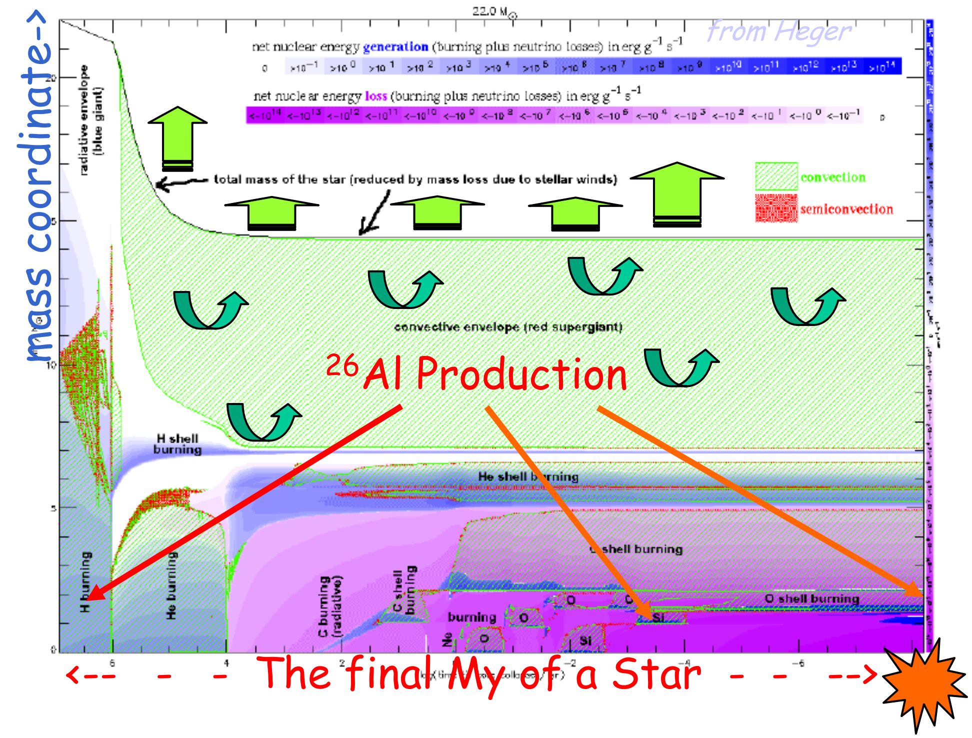

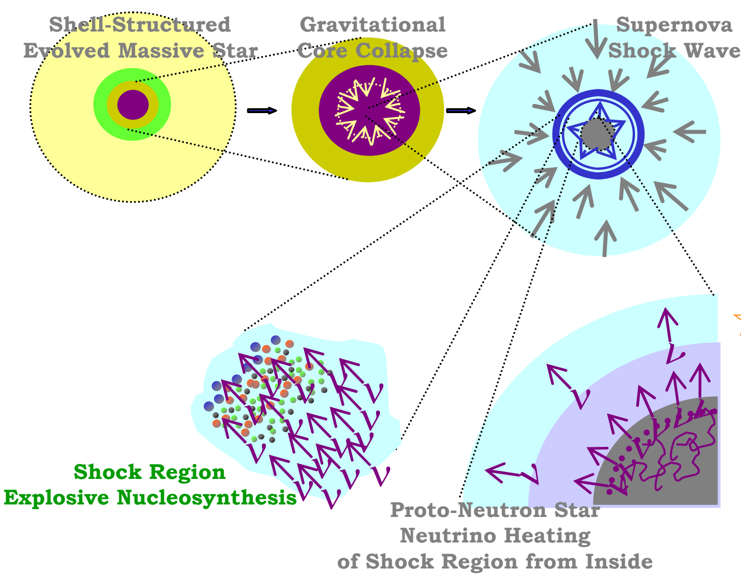

☆ **Supernova Physics**

- ☞ Explosion Trigger
- ☞ Shock Structure and Mixing

Massive-Star Interiors: Complex Astrophysics Issues

- ☆ Massive Stars
  - ☞ Stellar Evolution Phases
  - ☞ Mass Loss
  - ☞ Convection & Mixing

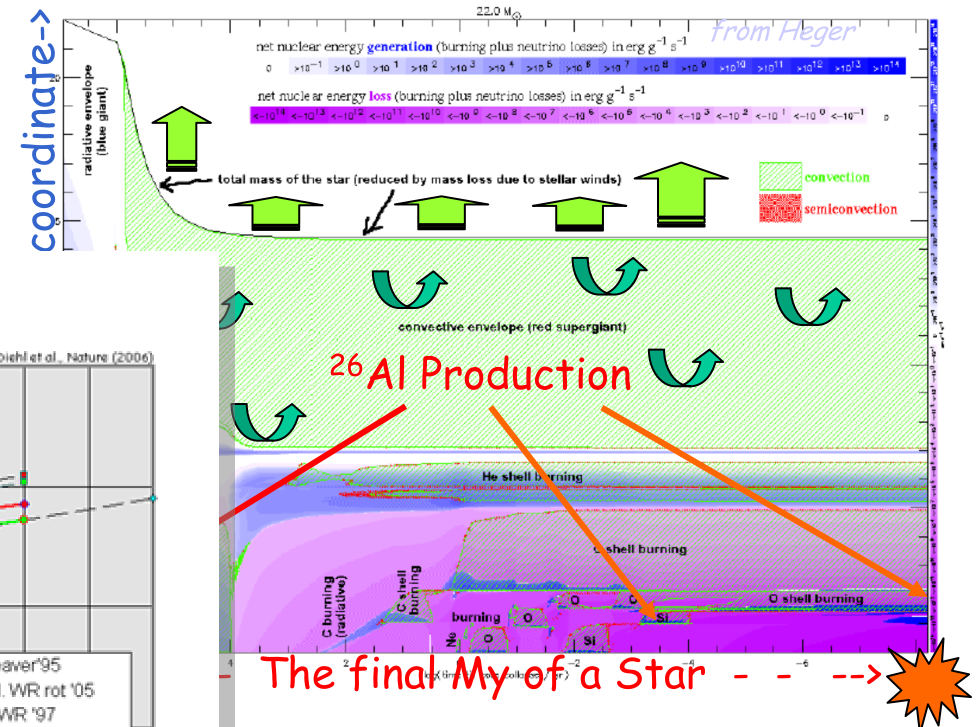

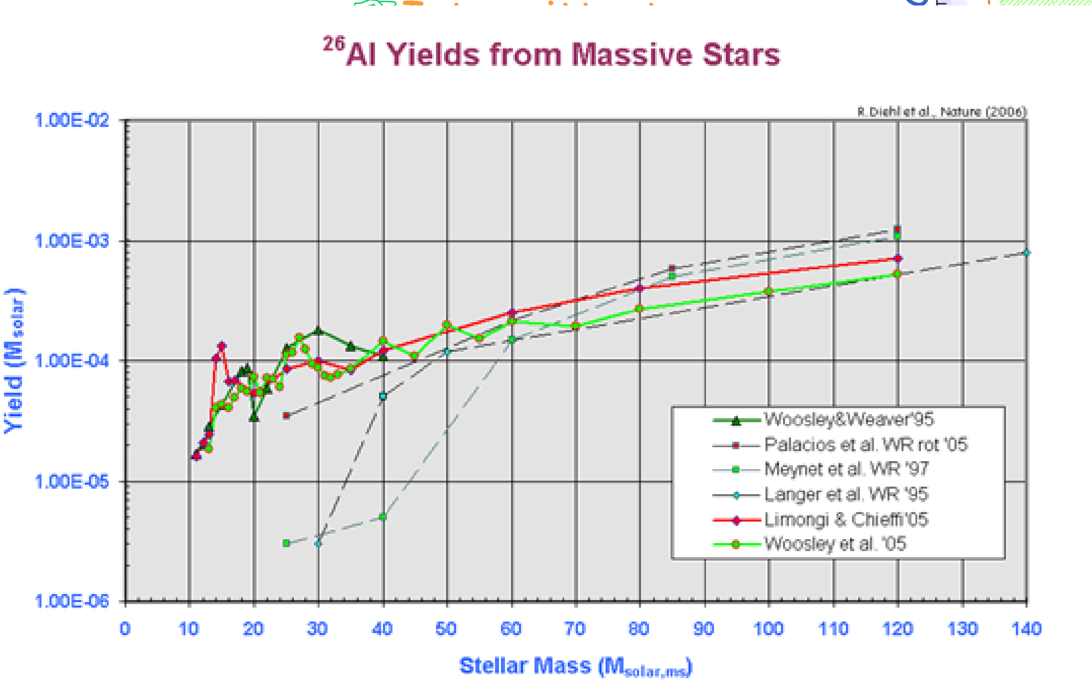

- ☆ ...a Physics
  - ☞ ...on Trigger
  - ☞ Shock Structure and Mixing

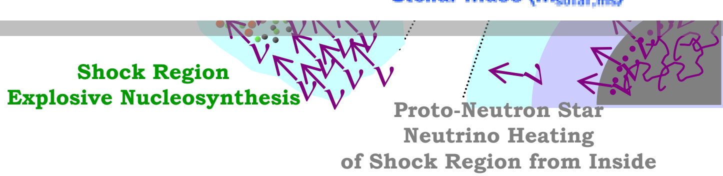

^{26}Al in the Galaxy: Massive-Stars… and more

1.04 10^6y	$^{26}Al \rightarrow ^{26}Mg^* + e^+$	1809

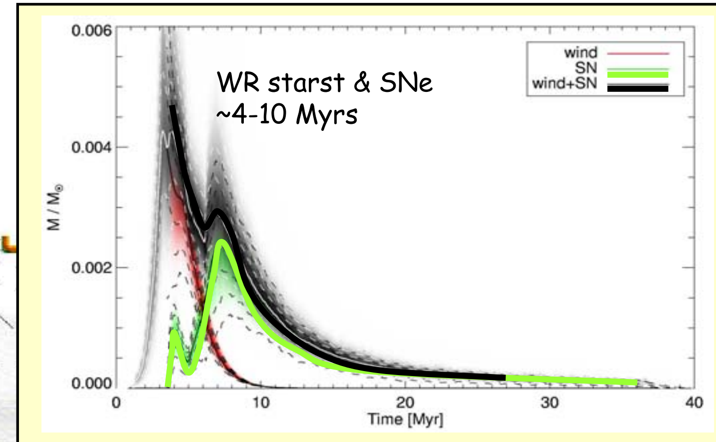

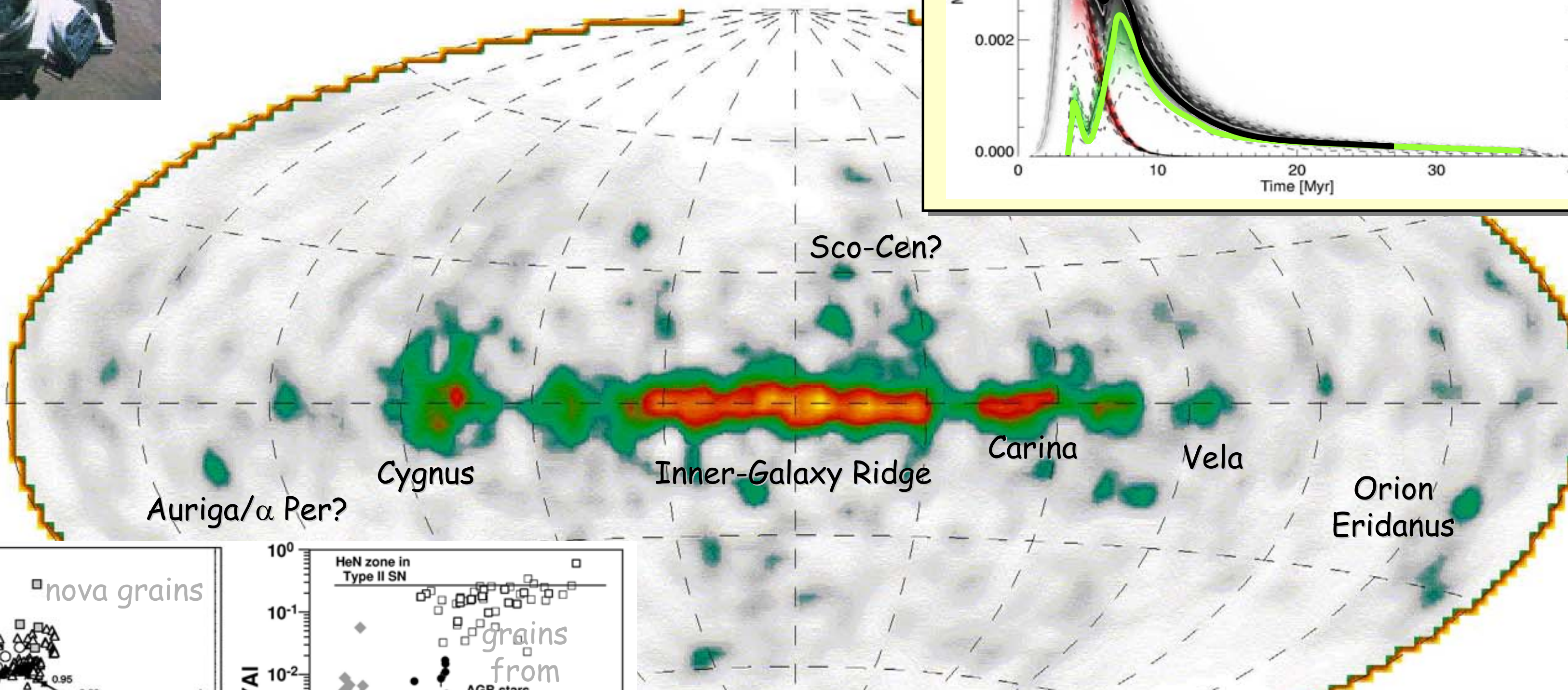

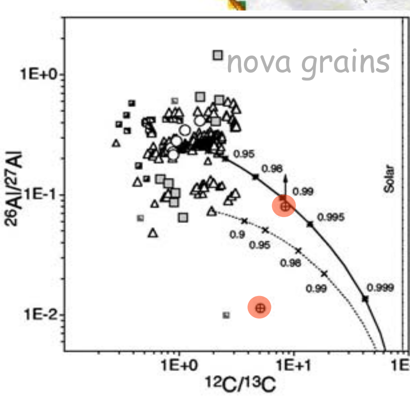

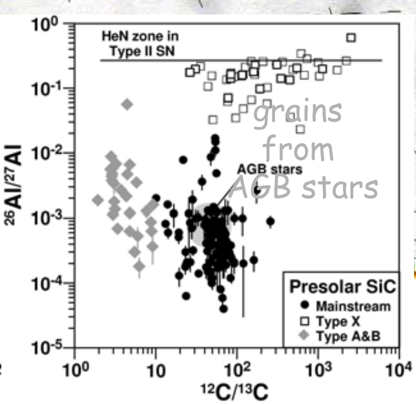

Complete CGRO Mission 1991-2000

(Plüschke et al. 2001)

Ge Spectroscopy of ^{26}Al Line with SPI/INTEGRAL

since Oct 2002

- ☆ ^{26}Al Glow of Inner Galaxy Confirmed, at ~Known Flux Level
- ☆ Line is Resolved, and not as broad as suggested (by GRIS)
  - ☞ *Diehl et al., Astron. & Astroph. (2006)*

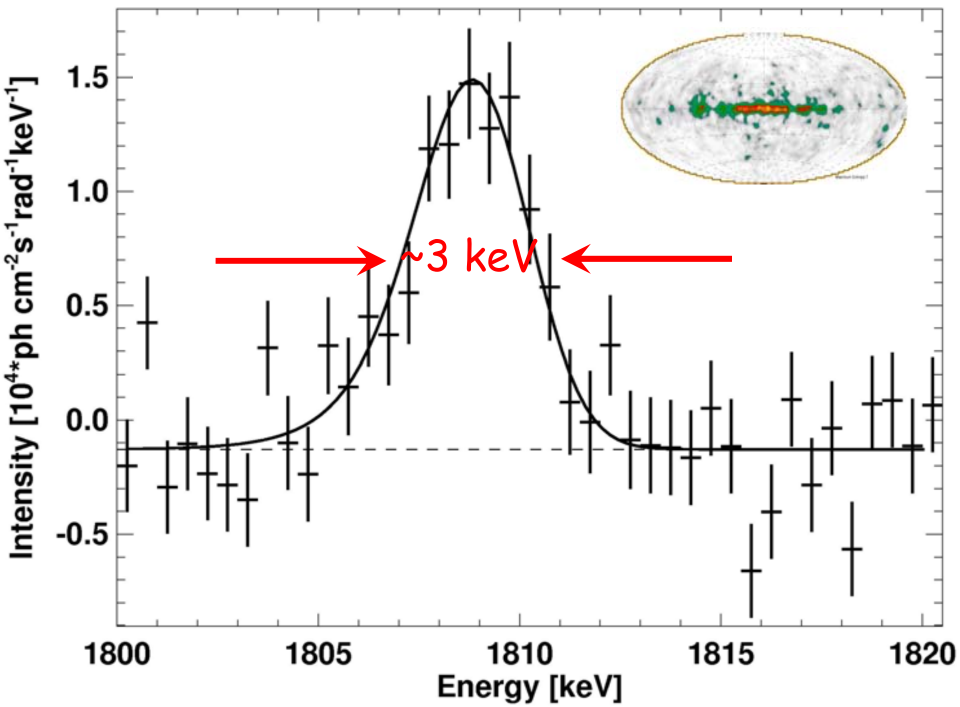

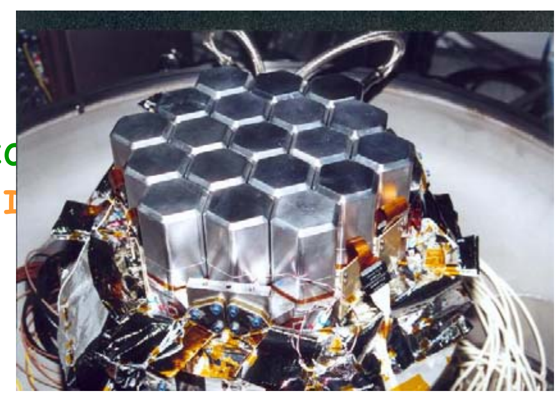

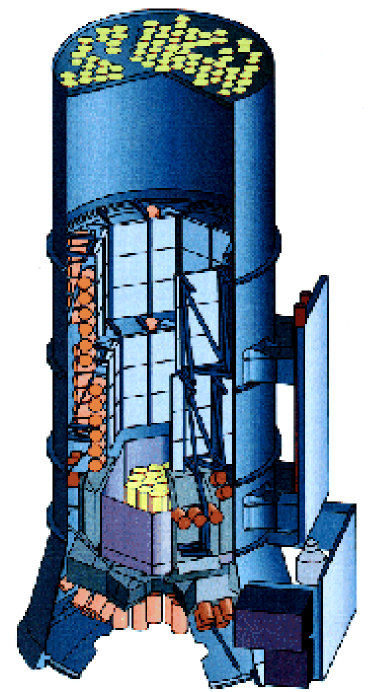

Using the ^{26}Al Line to Characterize the Galaxy

-> Diehl et al., Nature 2006

- ☆ Measured Gamma-Ray Flux
- ☆ Galaxy Geometry

} ➢ ^{26}Al Mass in Galaxy = 2.8 (±0.8) $M_{\odot}$

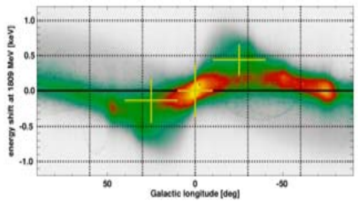

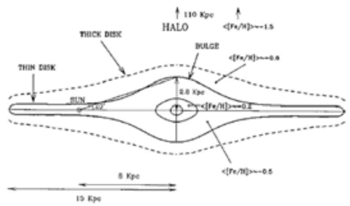

- ☆ ^{26}Al Yields per Star
- ☆ Stellar Mass Distribution

} ✓ cc-SN Rate = 1.9 (± 1.1) per Century

✓ Star Formation Rate = 3.8 $M_{\odot}$/yr

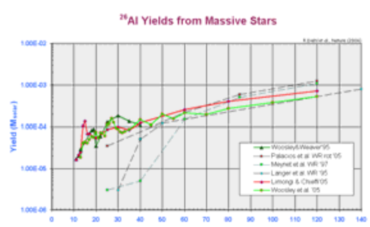

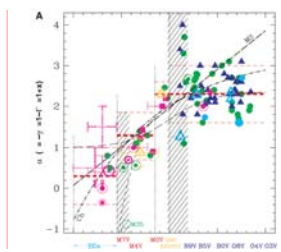

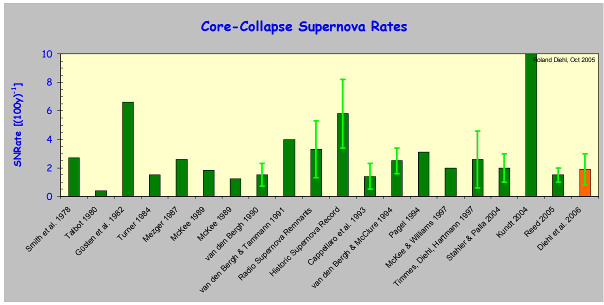

- ☆ Gas Mass in Galaxy

} ✓ Al Isotopic Ratio = 8.4 10^{-6}

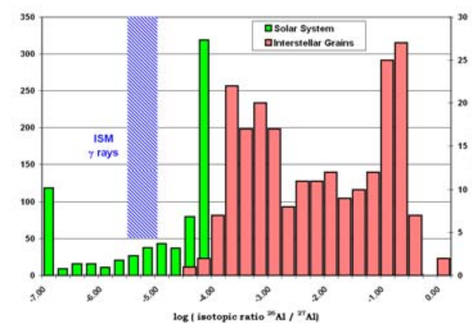

High-Resolution Gamma-Ray Spectroscopy Maintained in Space: SPI on INTEGRAL

- Cosmic-Ray Irradiation -> Degradation of Charge Collection
  - ☆ ~2% per Orbit, ~20% in 6 Months (@1 MeV)
- Annealing
  - ☞ ~100-200 hrs at 105°C, few hrs at 90K

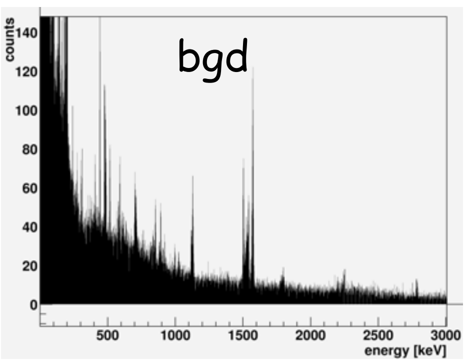

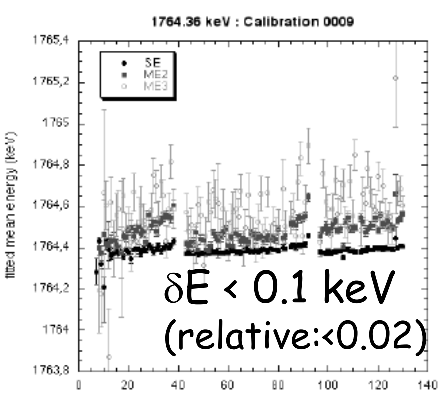

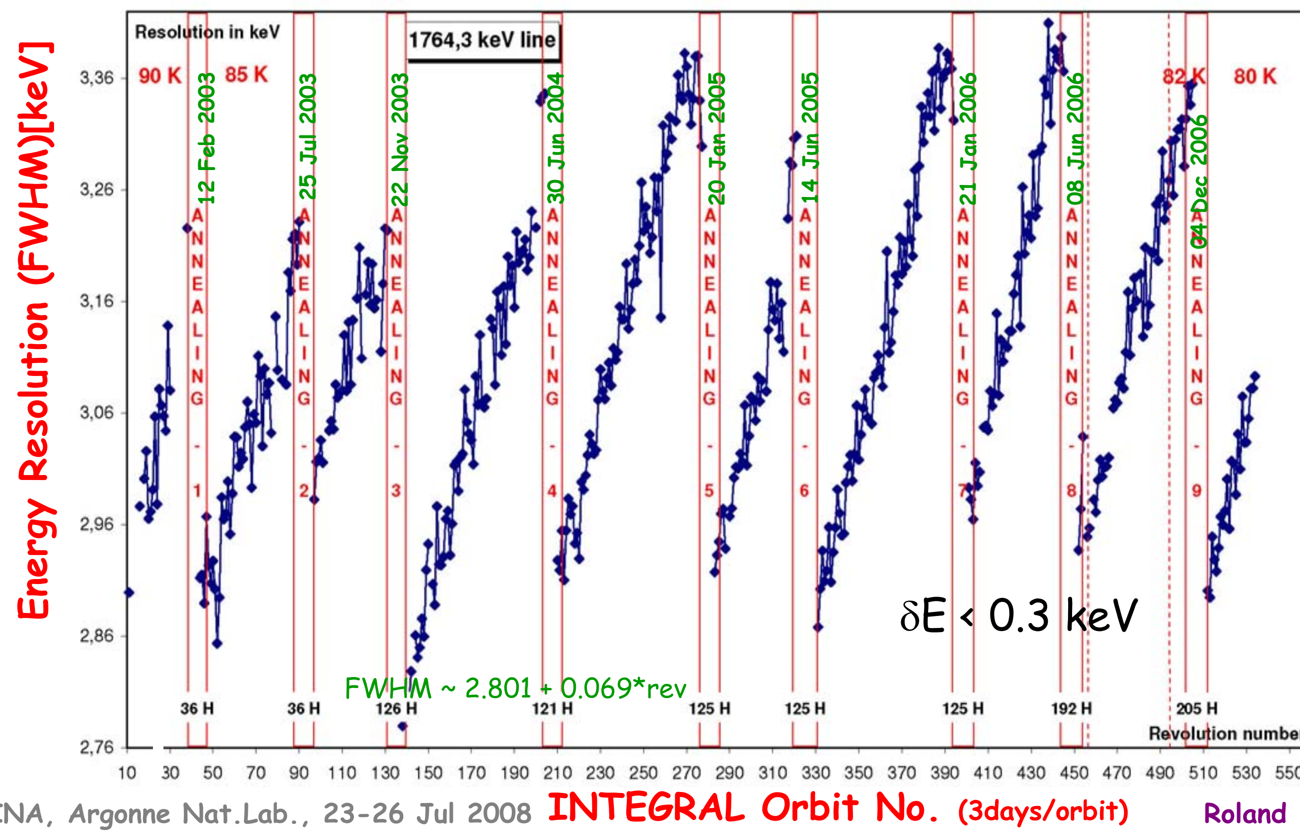

How Wide is the Celestial ^{26}Al Line?

- ☆ SPI Response * Celestial Line -> Actually-Observed Line Feature
- ☆ Fit Expected Spectral Signature to the Sky&Bgd-Fitted Spectral Signal
- ☆ Perform Statistical Uncertainty Analysis (Monte Carlo Markov Chain)

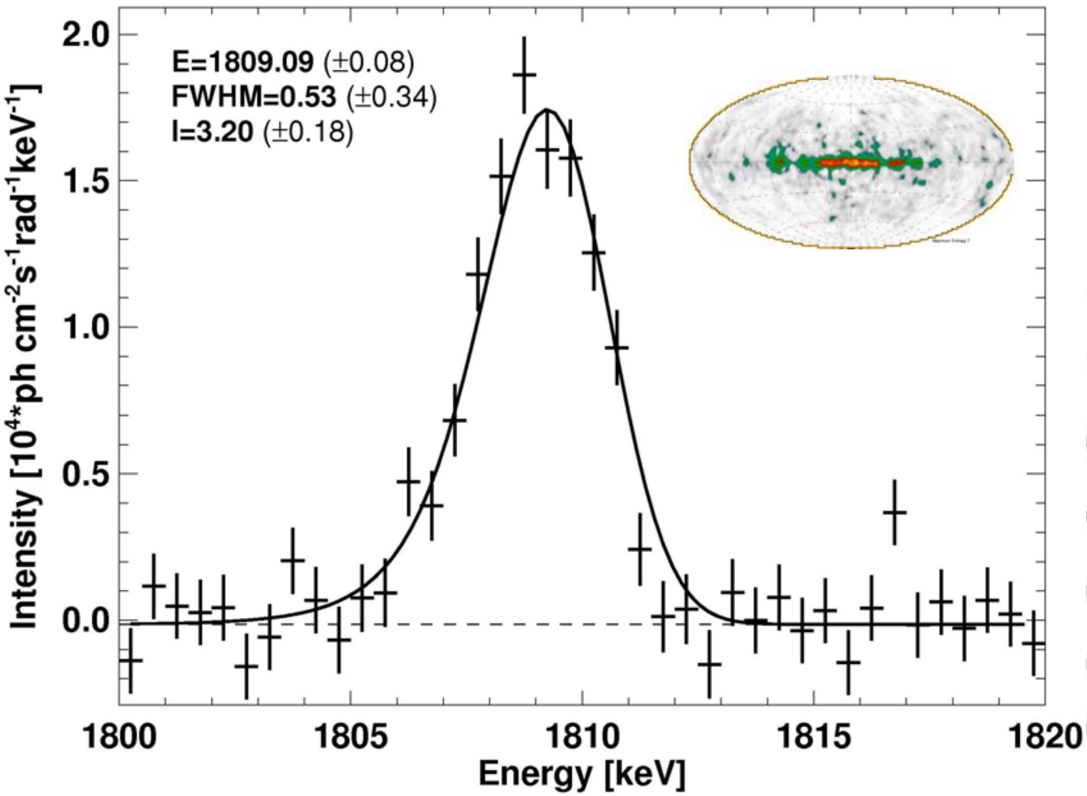

Celestial Line Width Constraint

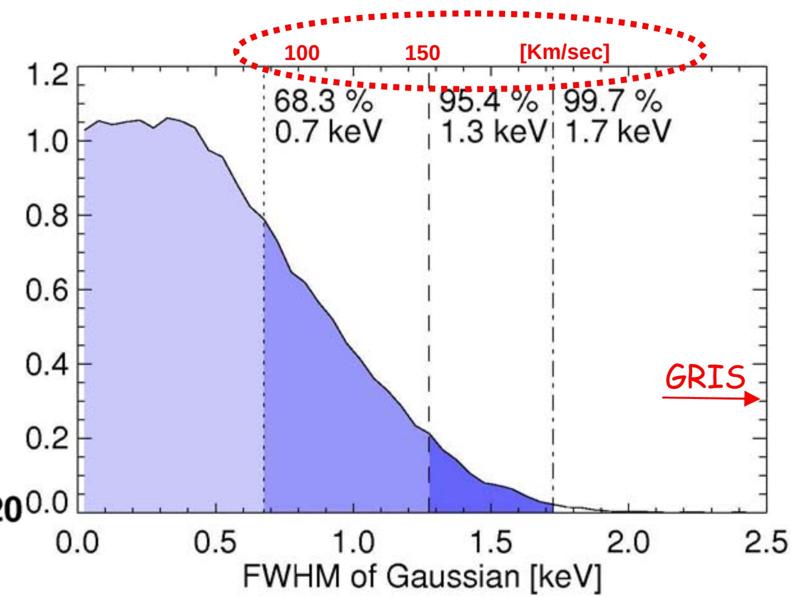

-> Data up to mid 2006; W.Wang et al., in prep.
Line Width Probability Distribution by K.Kretschmer

Massive Stars and the Interstellar Medium

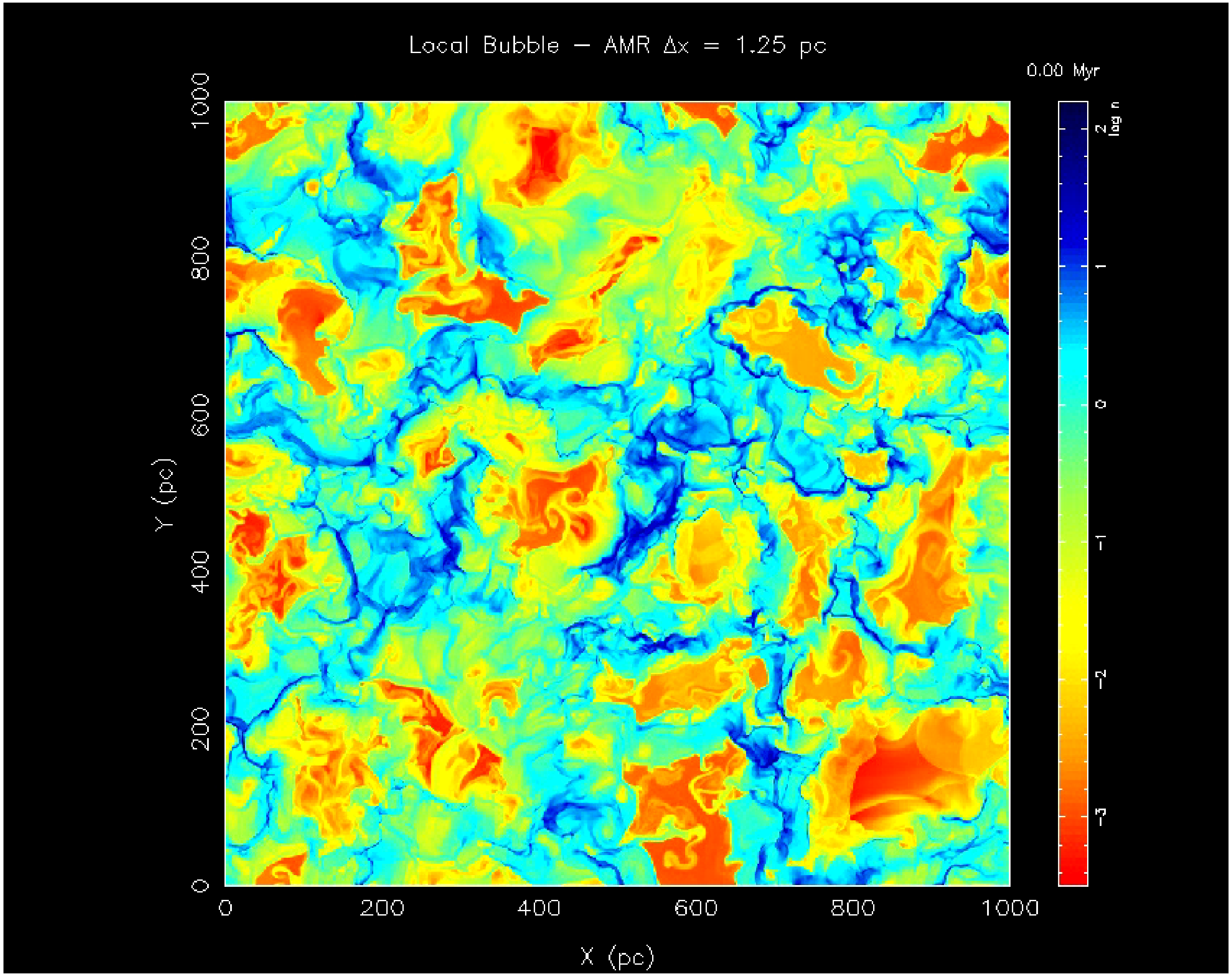

☆ The ISM is a Dynamic, Evolving Medium (≠ Multi-Phase Pressure Equilibrium)

☞ *D. Breitschwerdt & Miguel Avillez 2003*

cmp gadget sim Springel

^{26}Al Sources as a Probe of Galactic Structure?

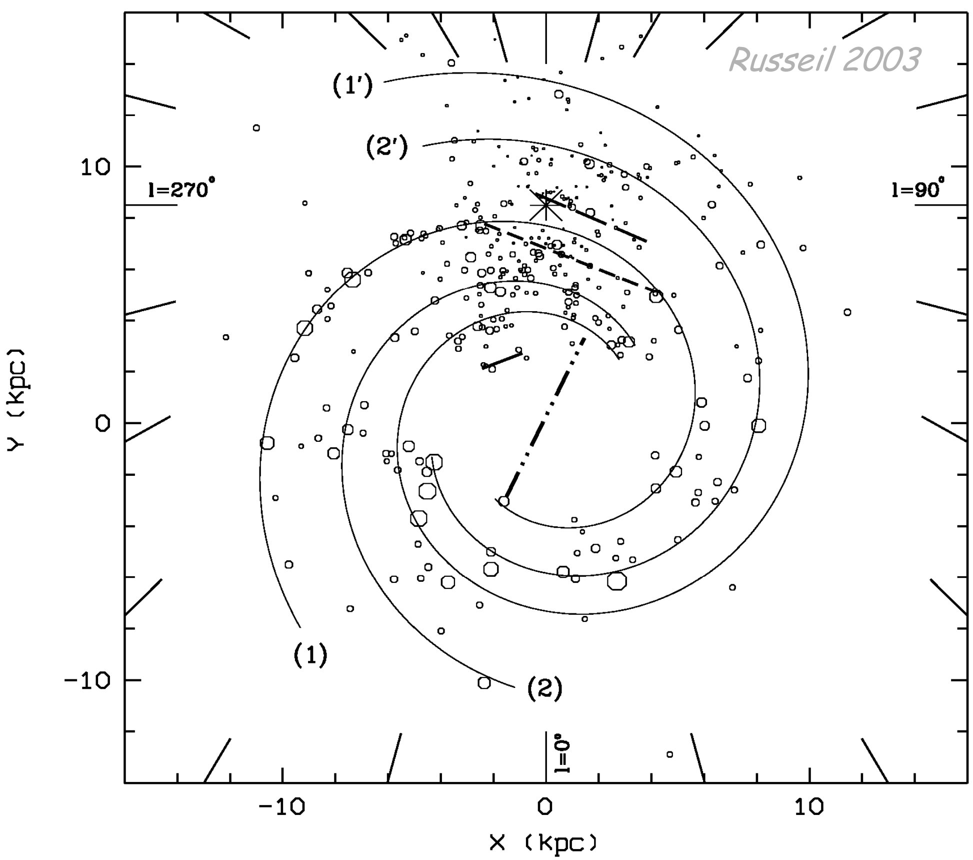

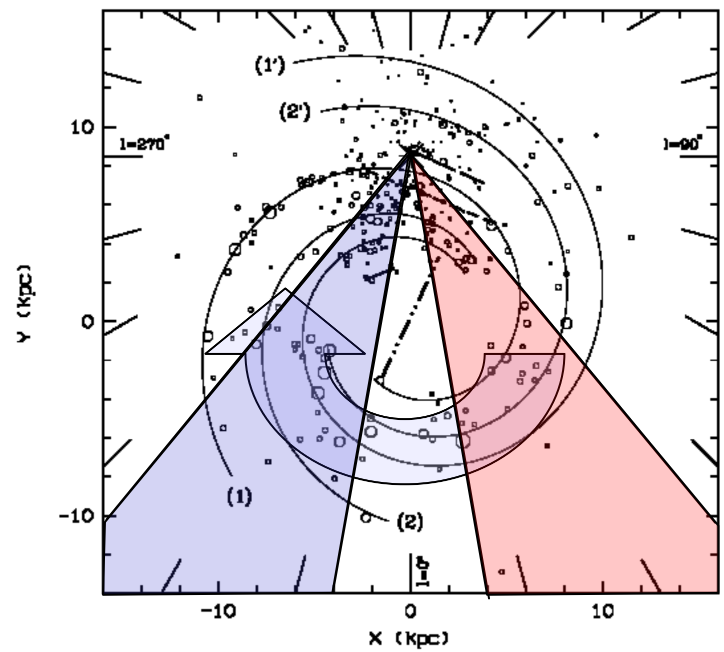

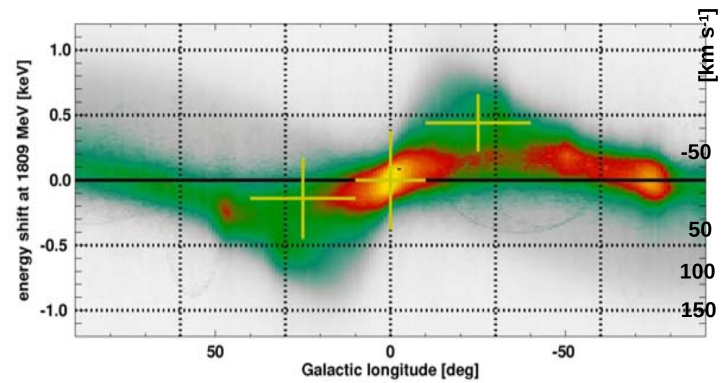

☞ *We Have Begun to Extend This Early Work with Finer Imaging Resolution*

Roland Diehl

Next Step: Spatial Resolution along Plane

- ☆ Does the Line Vary for Different Star-Forming Regions?
  - ☞ Age of SFR?
  - ☞ Dynamic State of ISM?
  - ☞ Bulk Motion of Hot ISM?

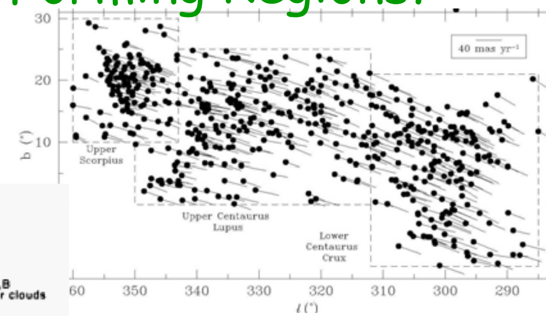

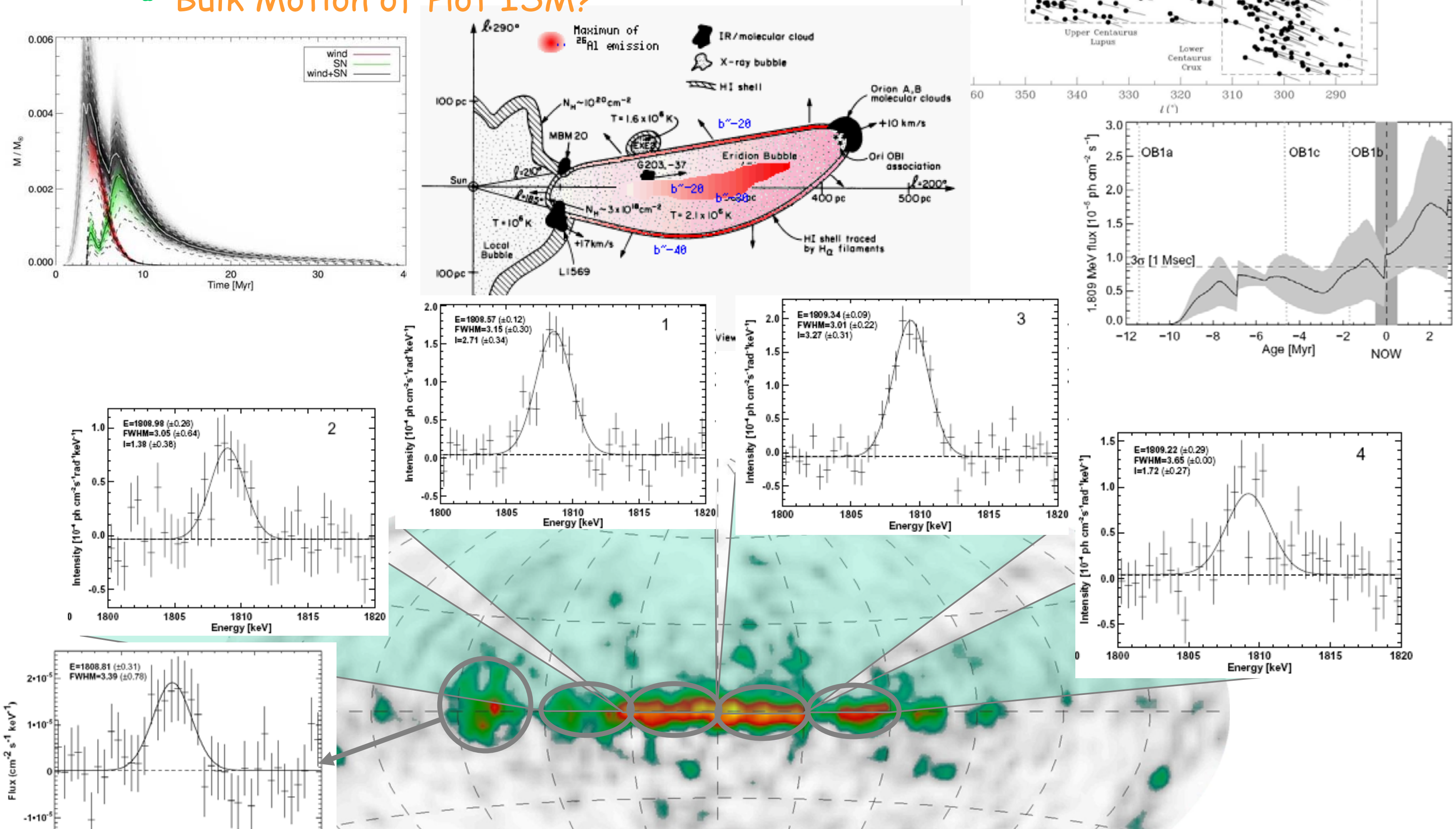

Recent Activity in the Upper Sco Region

Preibisch et al. 1999

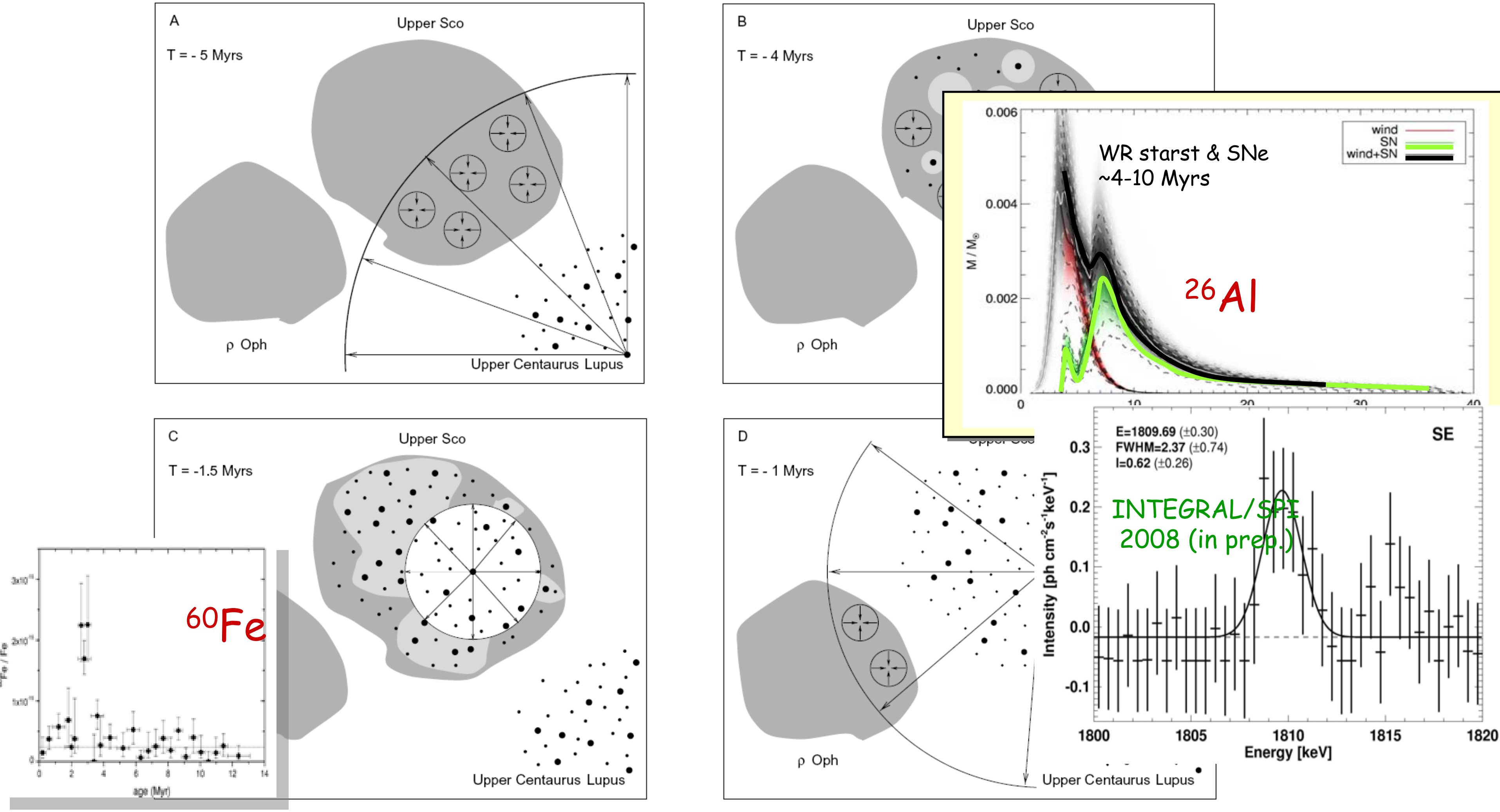

☆ Triggered Star Formation!!?!

- ☞ UCL Massive-Star Action Triggers SF in USco ~5 Myrs ago
- ☞ ρ Oph Molecular Cloud Hit by USco Massive-Star Action ~1 Myrs ago

Science Questions around ^{26}Al γ-rays

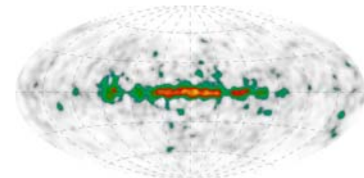

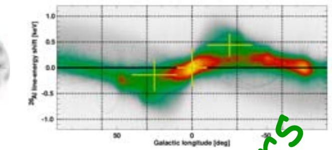

- ☆ How Much ^{26}Al is Produced?
  - ☞ In Steady State (Galaxy, other Galaxies)
  - ☞ By Specific Objects (SN, WR stars, AGB stars, Novae)
- ☆ Where is ^{26}Al Produced?
  - ☞ Star-forming Regions: Active, Young/Older
- ☆ Where does ^{26}Al Decay?
  - ☞ In hot/warm/cold ISM Phase, on Grains?

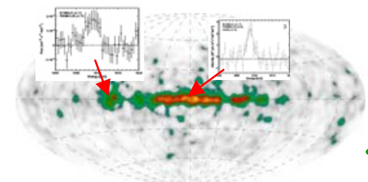

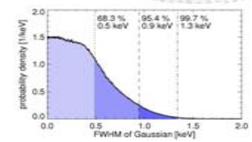

We Have First Answers

Next: Precision Answers

- ☆ Where can ^{26}Al Help to Understand Other Astrophysical Issues
  - ☞ Are our Models of Massive-Star Evolution Consistent with ^{26}Al Data?
  - ☞ What is the Number of Massive Stars in the Galaxy?
  - ☞ What is the Age of Star-Forming Groups?
  - ☞ Where are Otherwise-unseen (embedded) Star Formation Regions?
  - ☞ How Fast are Molecular Clouds Destroyed?
  - ☞ What is the ISM State around Massive-Star Groups?
  - ☞ How Effective are Groups of Massive Stars (Ionization, Heat, Shells)?

^{60}Fe Emission is Seen from the Galaxy

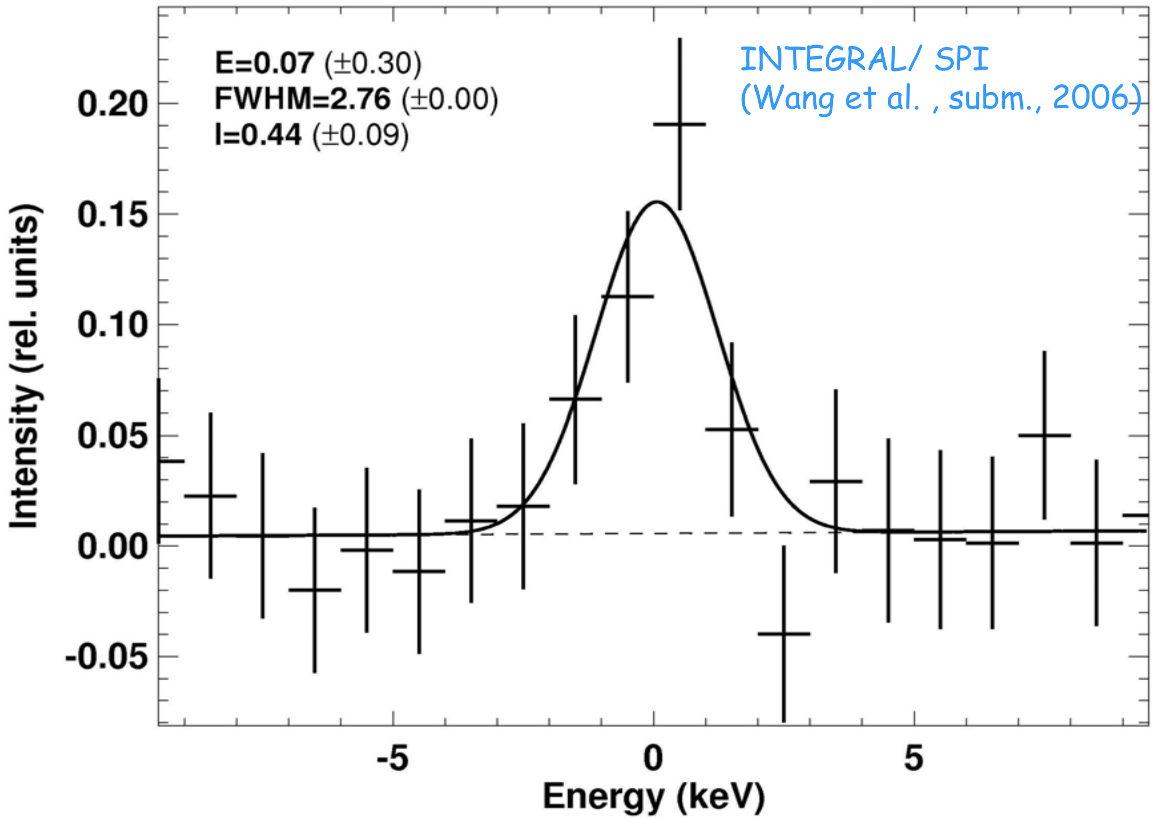

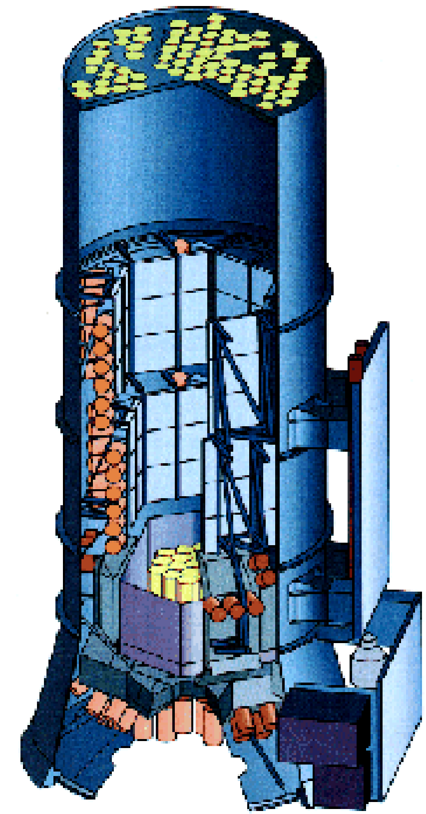

☆ Gamma-ray Signal Now Beyond 'Hints'/'Limits' (5σ)

☞ ^{60}Fe/^{26}Al Emission Ratio ~15%

^{60}Fe: Why is it Interesting?

2.0 10^6y	$^{60}Fe \rightarrow ^{60}Co^* \rightarrow ^{60}Ni^*$	59, 1173, 1332

- ☆ ^{60}Fe is Produced through Successive Neutron Captures
  - ☞ r-Process Astrophysics...

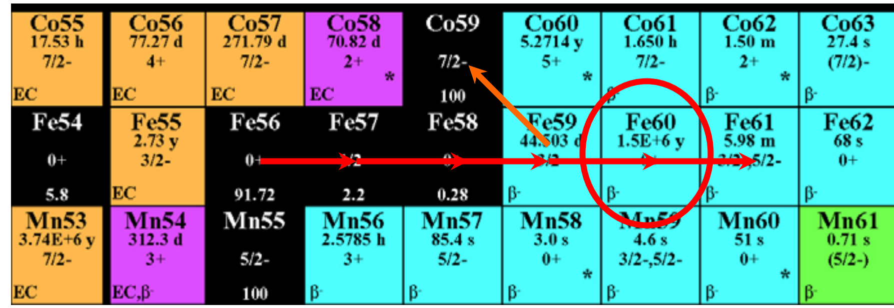

- ☆ ^{60}Fe has been Detected in Pacific Ocean Crust
  - ☞ Nearby SN ~2 My ago?

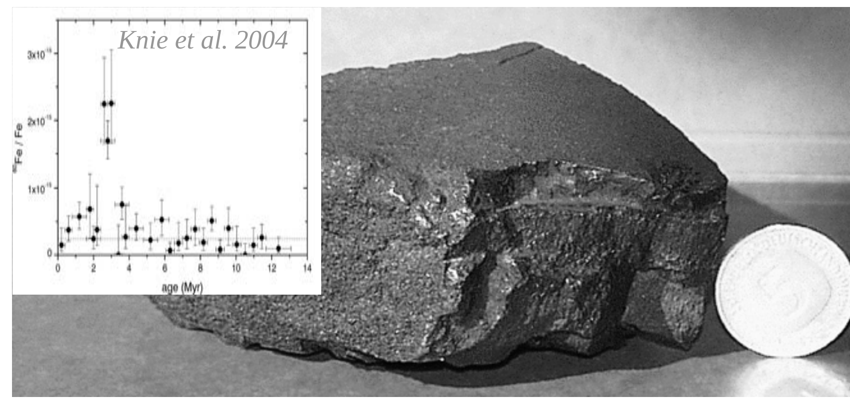

- ☆ Massive Stars are Likely Sources of ^{60}Fe
  - ☞ Observable in the Galaxy (as ^{26}Al is)?
  - ☞ **Compare Two Isotopes from Same Sources!**

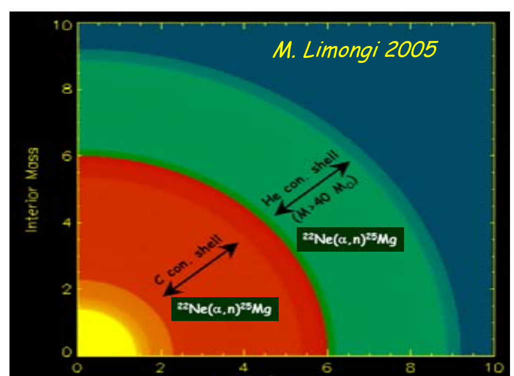

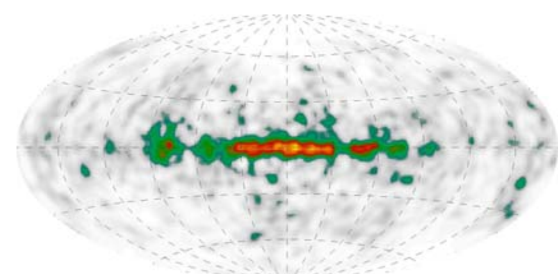

^{60}Fe Production in Stars

2.0 10^6y	$^{60}Fe \rightarrow ^{60}Co^* \rightarrow ^{60}Ni^*$	59, 1173, 1332

☆ No Production during ANY Central-Burning Phase

☆ Need Convection plus n Source

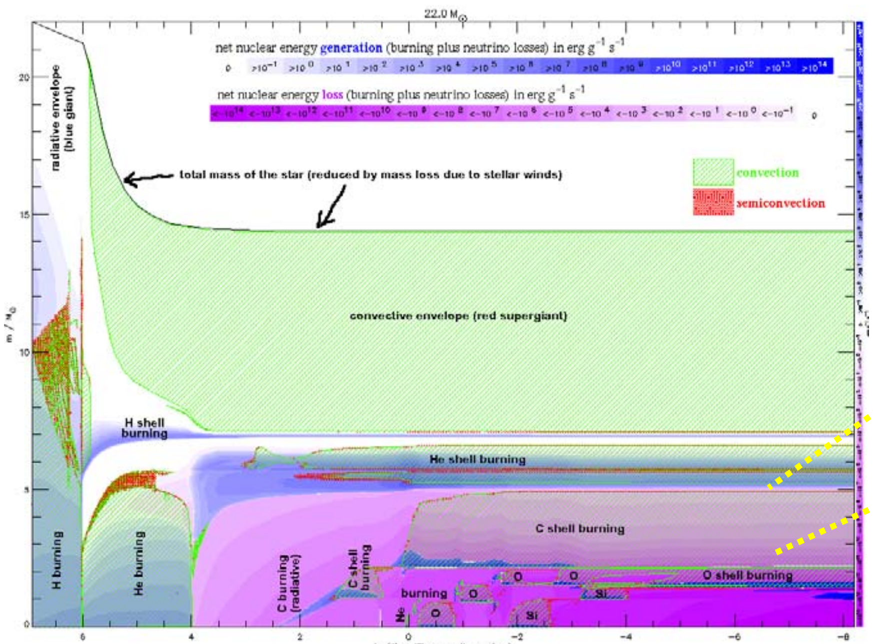

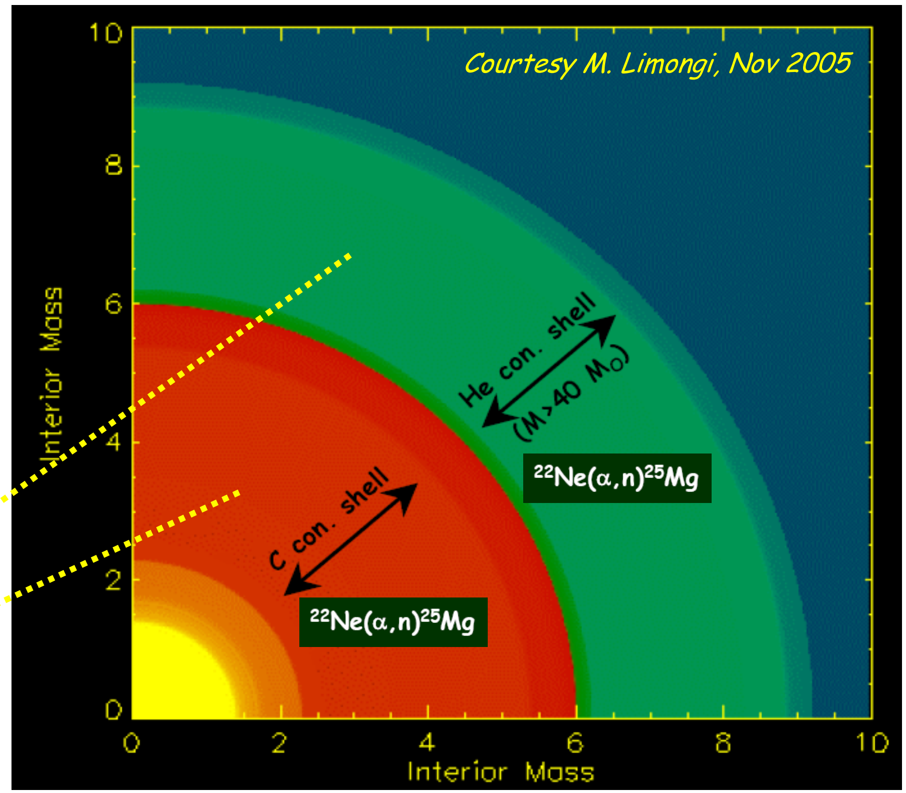

Negligable

☆ Ejection by Supernova Explosion

^{60}Fe from Massive Stars: Observations vs. Theory

2.0 10^6y	^{60}Fe → ^{60}Co* → ^{60}Ni*	59, 1173, 1332

- ☆ Current Model Agrees (again) with Data on ^{60}Fe/^{26}Al γ-Ray Intensity Ratio
  - ☞ But: Uncertainties are Large:
    - ☞ Ratio <0.3; Massive Stars?
    - ☞ Revised Yields Had Led to Higher Predicted Ratios ~1.0
    - ☞ Revised Stellar Models Again Reduced Predicted Ratios

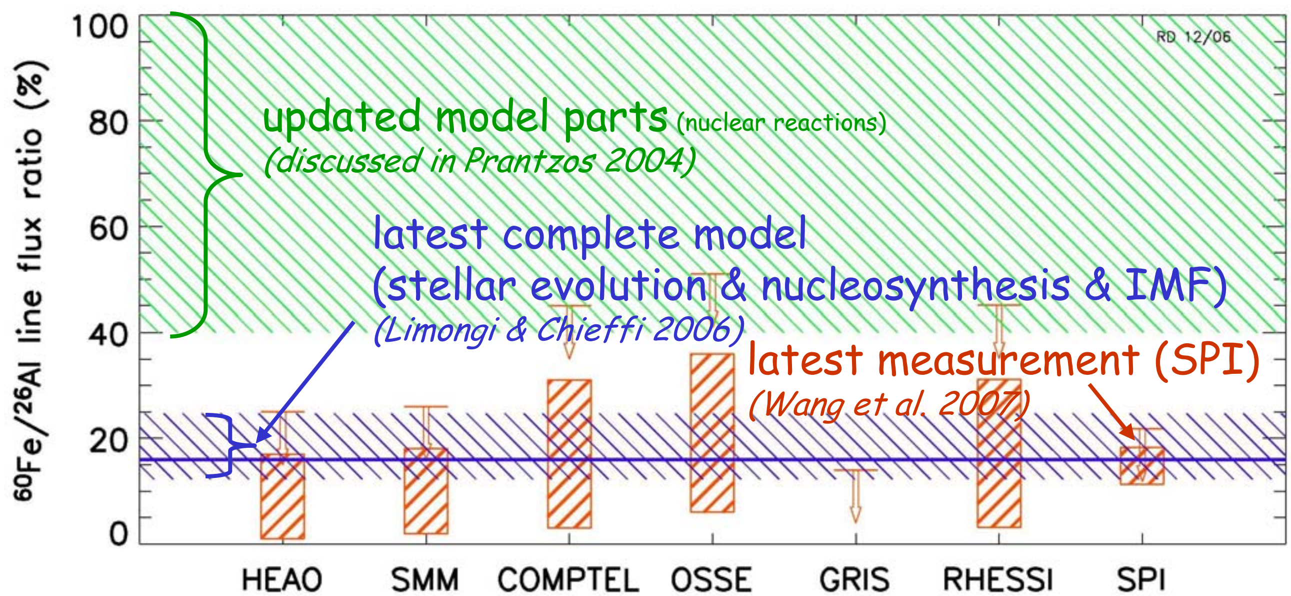

- ☆ Assessments Needed:
  - ☞ Stellar Models?
  - ☞ Nuclear Physics?
  - ☞ Gamma-Ray ^{60}Fe Signal Origin?
- ☆ Recent ^{60}Fe Lifetime Re-Determination *(Rugel et al.)*-> Significantly Longer!

Annihilation of Positrons in the Galaxy

…. 10^5y	$e^+ + e^- \rightarrow Ps \rightarrow \gamma\gamma$..	511, <511

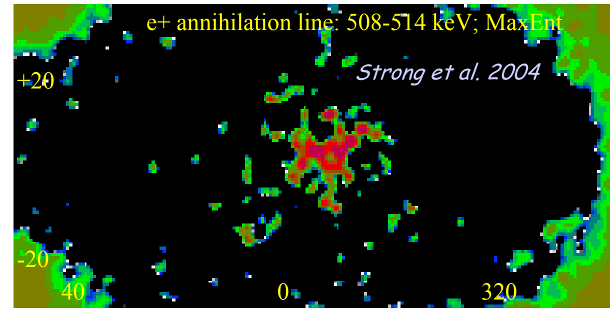

Imaging (511 keV Line, Cont.) with SPI:

- Extended, ~bulge-like Emission (δl~8°,δb~8°)
- Weak Disk Emission Seen; No "Fountain"

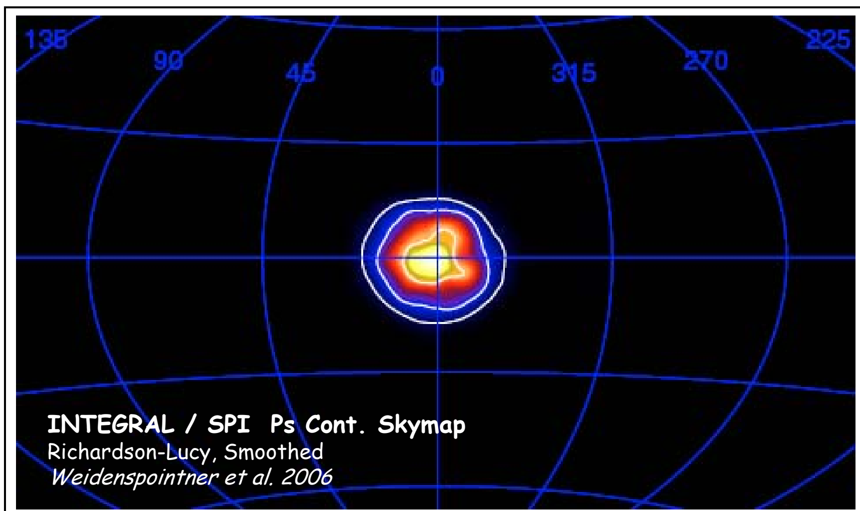

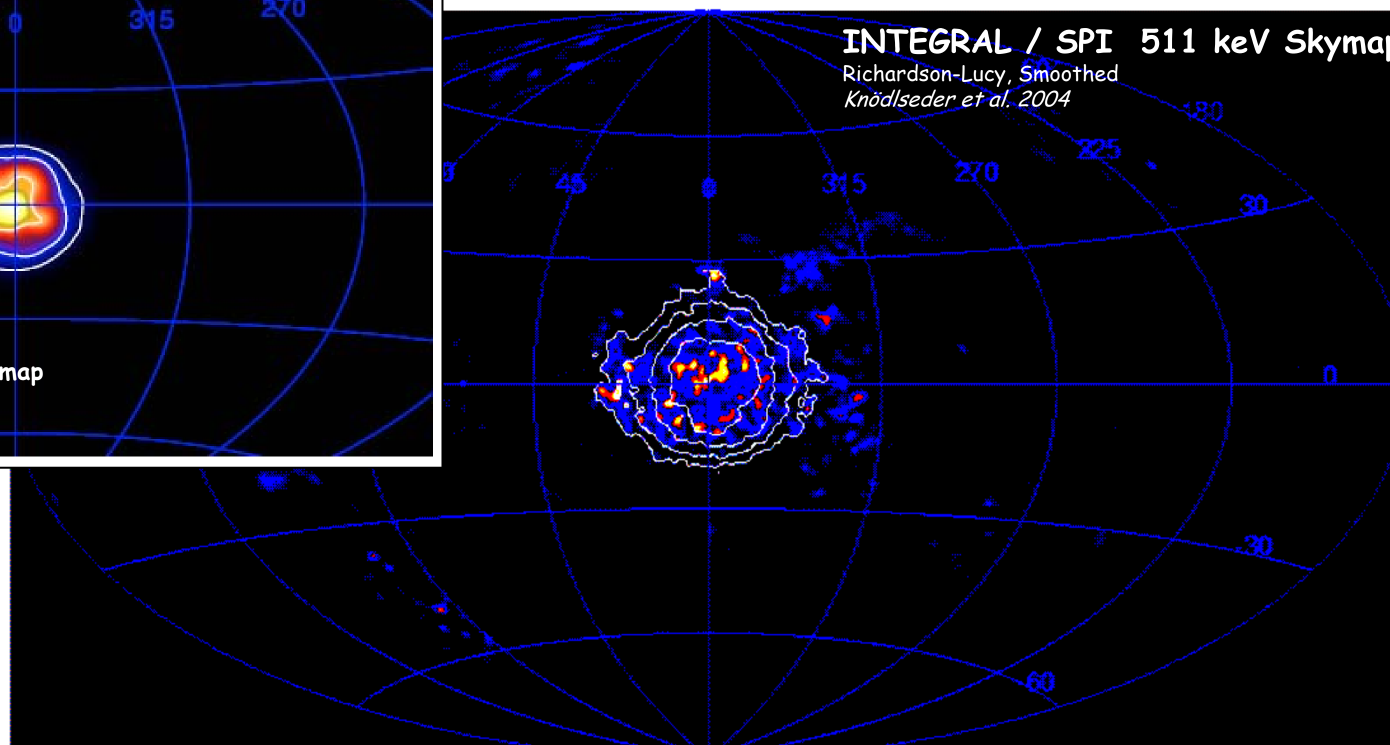

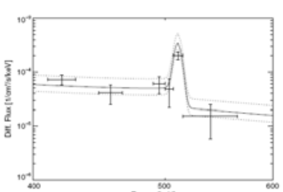

What are the Positron Sources??

- ☆ Identify Each of the KNOWN Types of Sources
  - ☞ Individual Sources?
  - ☞ Morphology of Galactic-Disk Emission
  - ☞ Assemble a Sky Model for the Known Integrated Emission, e.g.:

- Positron Annihilation

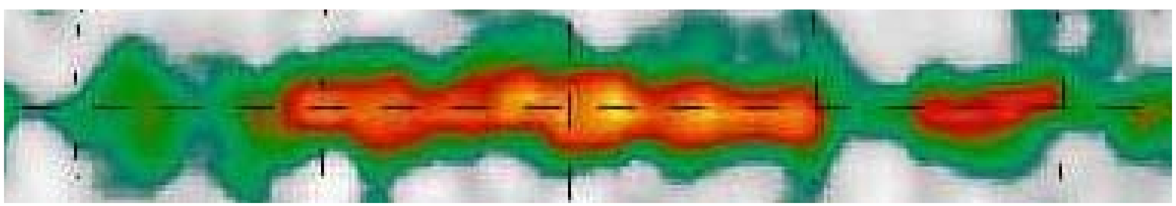

- ^{26}Al Radioactivity

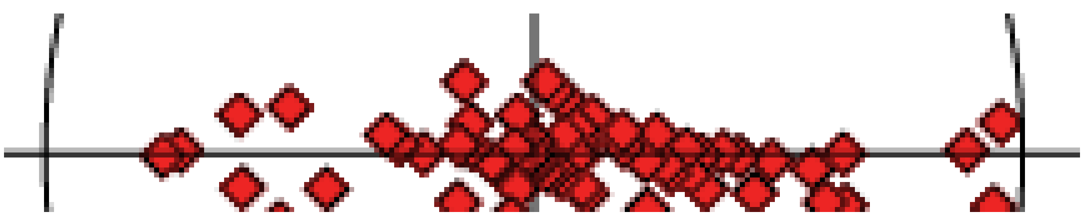

- Binary Systems (LMXBs)

- ☆ See if Significant Residual (bulge) Emission Remains
- ☆ An Unexpected / New Type of Sources? (e.g. DM?)

Instrumental Sensitivities around Nuclear Energies

☞ next steps: advances by factor ~3...10

☞ Continue with INTEGRAL until Next Mission is in Place

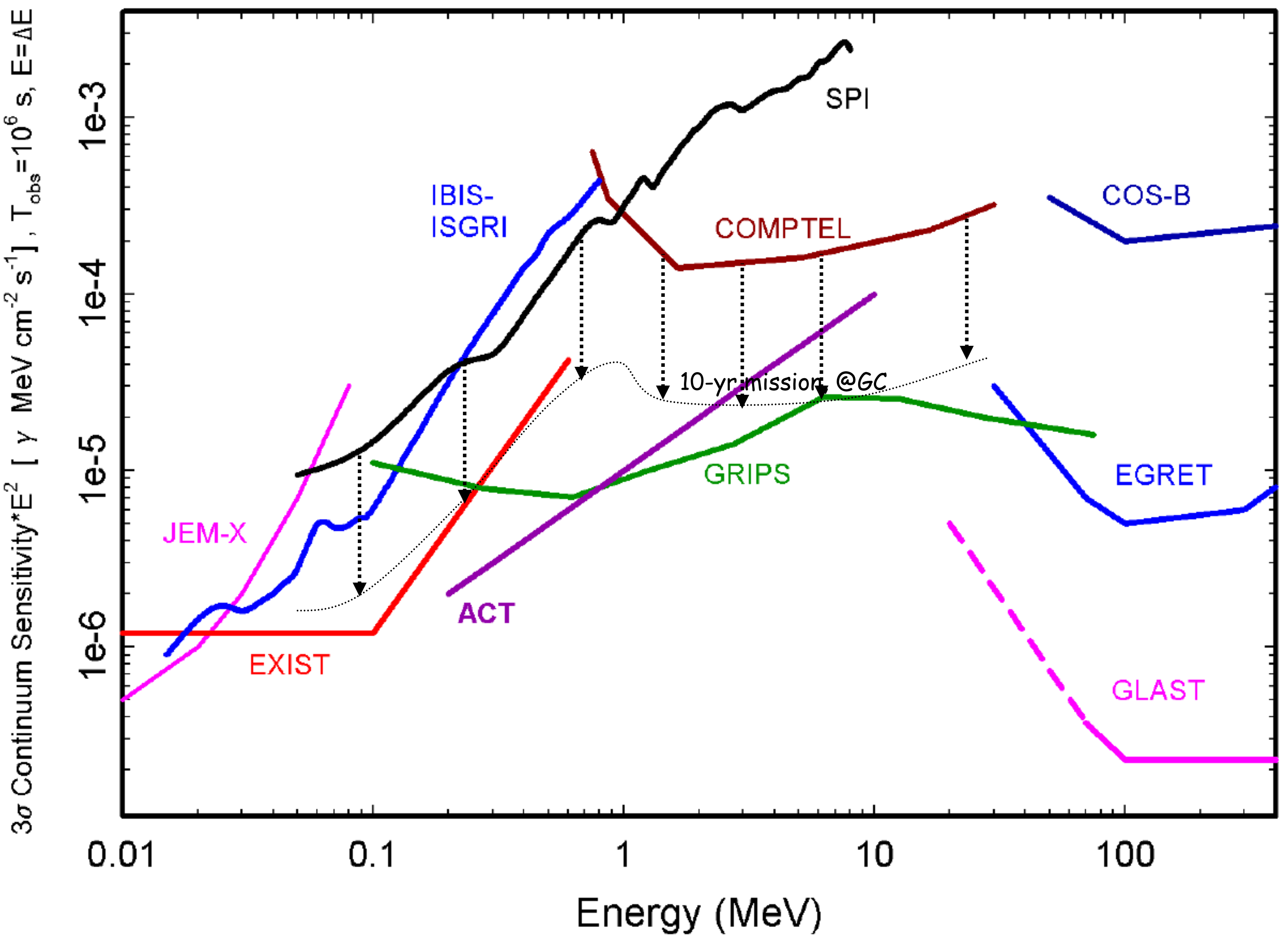

The GRIPS Perspective (2015+?): From All-Sky to Specific-Source Studies

- ☆ Current Gamma-Ray Line Surveys Can Only See Brightest Emission:

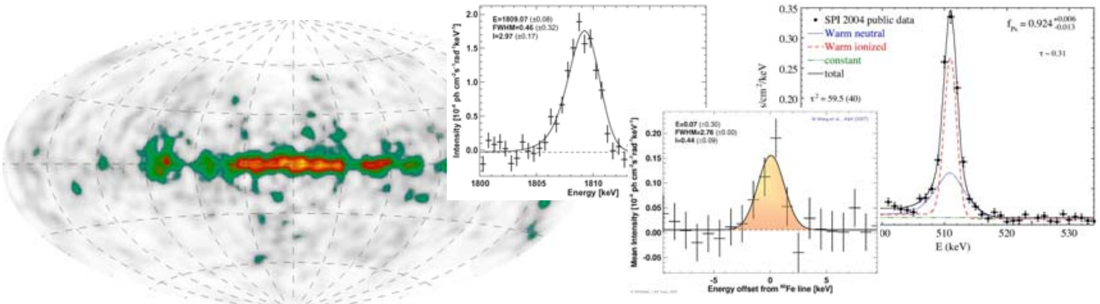

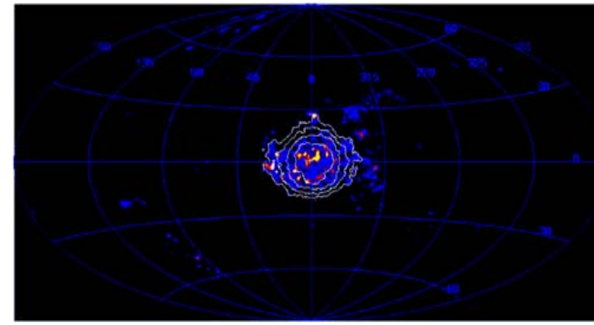

- ☆ GRIPS Will Provide Localized Results:

All-sky image in the ^{26}Al line after five years

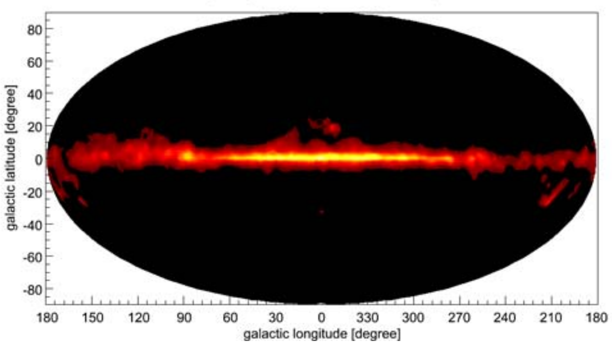

All-sky image in the ^{60}Fe lines after five years

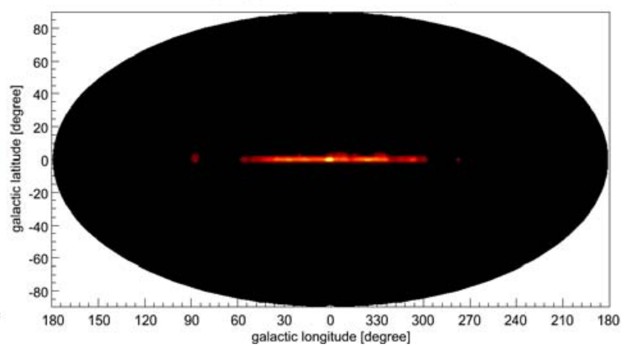

All-sky image in the 511 keV annihilation line after five years

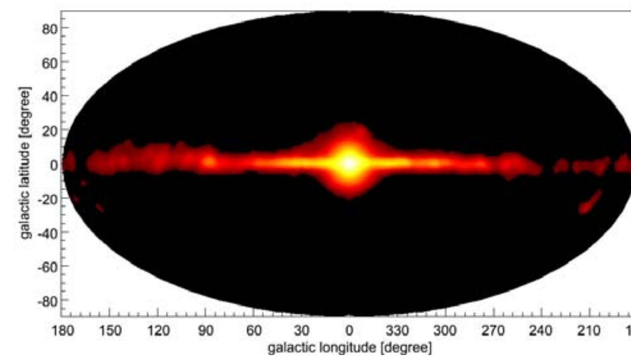

- ☞ ^{26}Al to ^{60}Fe to Positron Yields per Massive-Star Group

- ☞ We Know ~ 500 Star-Forming Complexes; Gamma-Rays will also see Embedded SFR's →

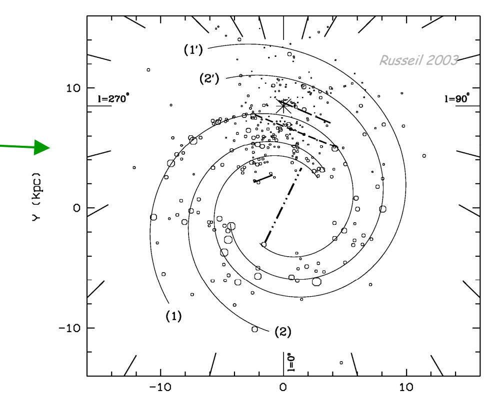

- ☆ From All-Sky to Many Specific Sources
  → Study the Conditions for Pop I Star Evolution

Inferrence of Isotopic Abundances

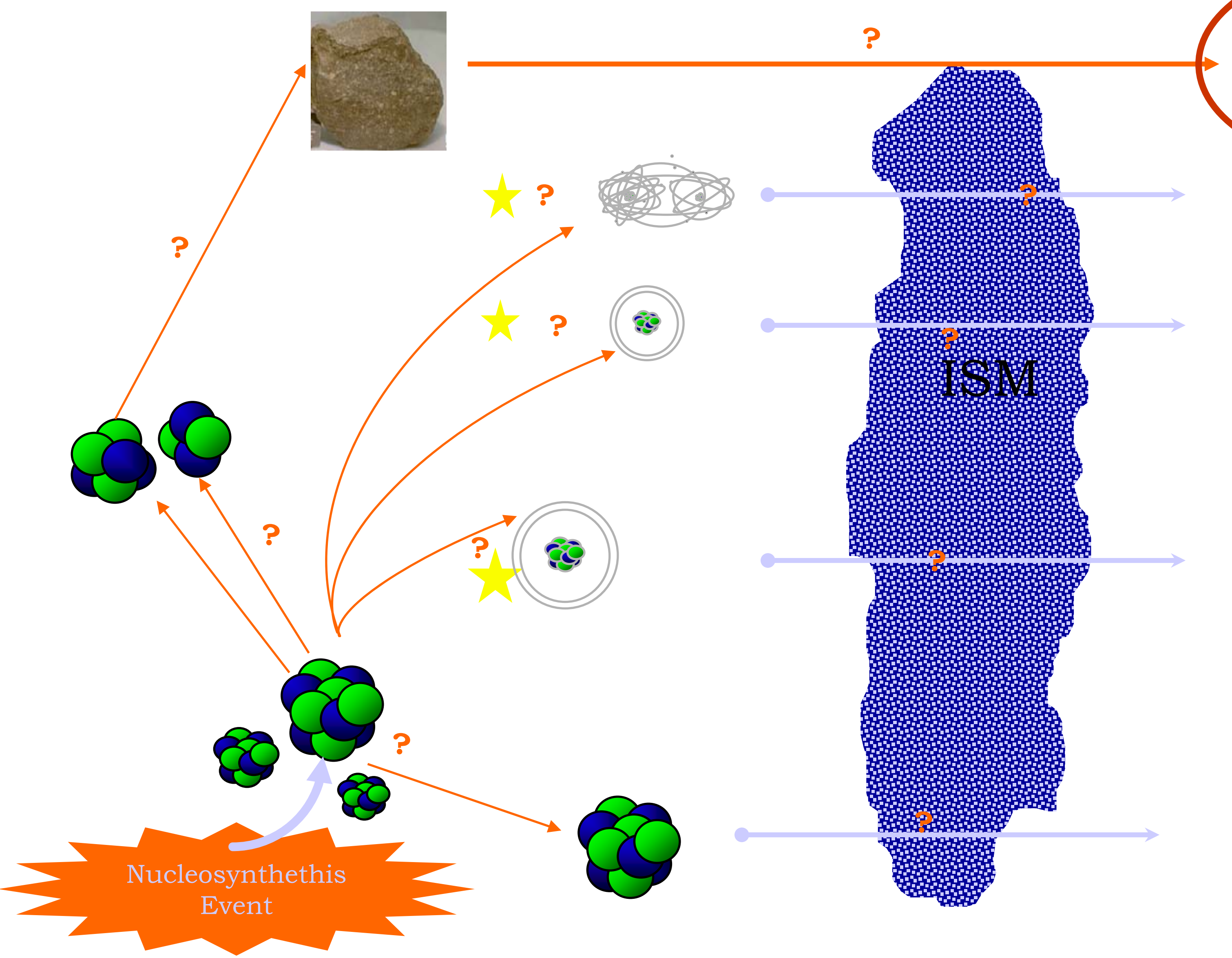

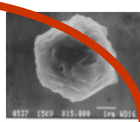

- Meteoritic Studies &
- Material Samples
- Molecular Absorption-lines (Radio,IR)
- Atomic Absorption-lines (opt,UV)
- Atomic Emissionlines (opt,UV,X)
- Gamma-Ray Lines from Radioactive Isotopes

Abundances from Meteorites & Grains

- Trajectories of Asteroid-Belt Bodies Hit Earth...

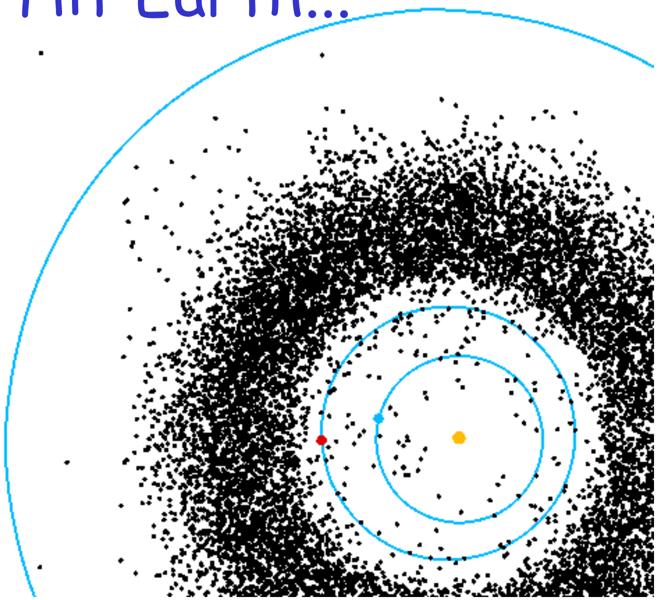

FIG. 1. Meteorite Baszkówka, side view. Size = ~30 × 18 cm. Photograph by M. Stepniewski.

Meteorites

- ☆ "Falls":
  - ☞ Meteorite is Observed While Falling
- ☆ Debris Scattered Over Trajectory

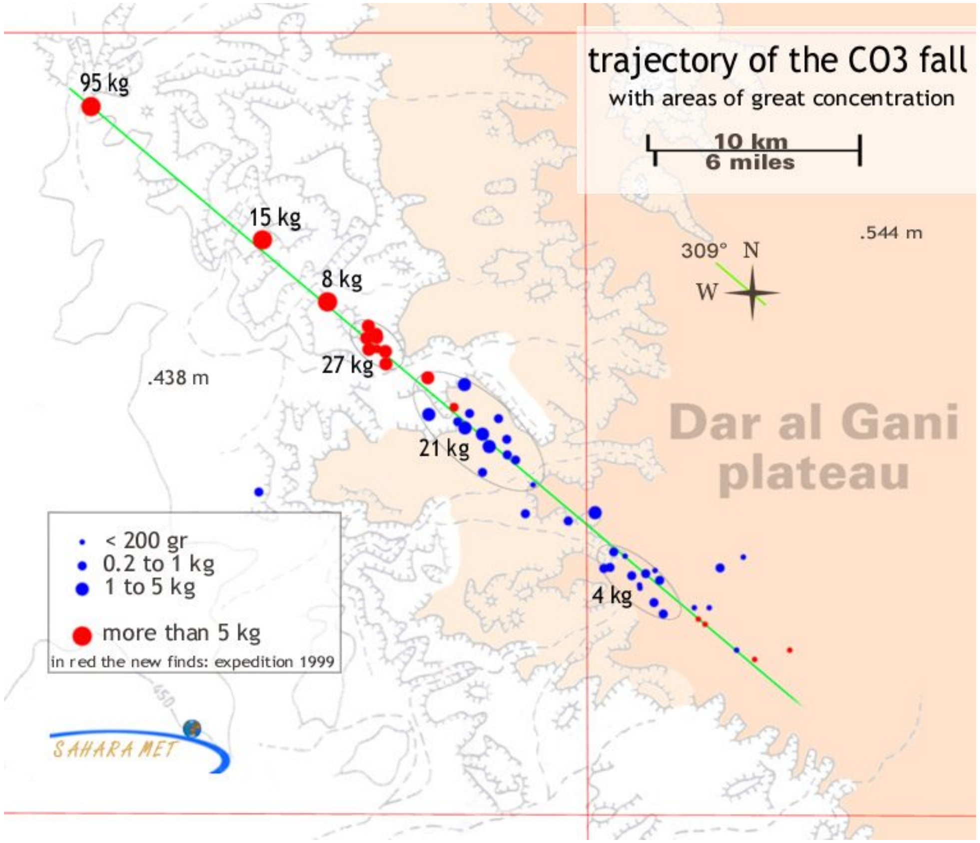

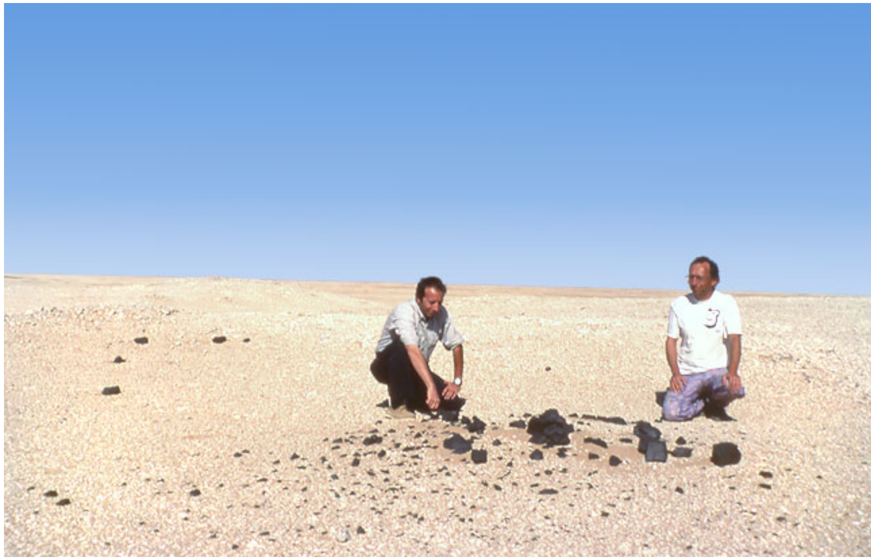

Condensation of Presolar Nebula

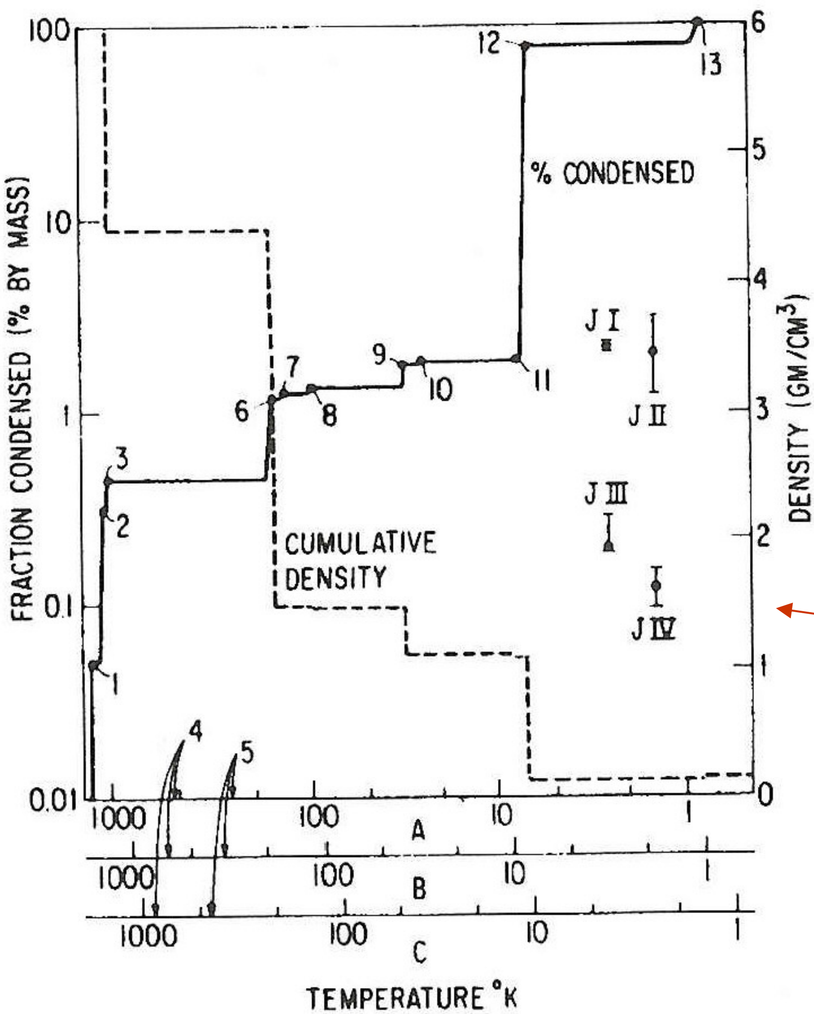

Step Number	Reaction
Equilibrium Condensation	
1	Condensation of Ca, Al, and Ti oxides
2	Condensation of Fe-Ni alloy
3	Condensation of enstatite ($MgSiO_3$)
	Condensation of (Na,K)$AlSi_3O_8$
4	Fe-Ni alloy + $H_2S(g) \rightarrow FeS(s)$ and $NiS(s)$
5	$CO(g) + 3H_2(g) \rightarrow CH_4(g) + H_2O(g)$
	Calcium silicates + $H_2O(g) \rightarrow$ tremolite
6	Fe metal + $H_2O(g) \rightarrow FeO(s) + H_2(g)$
7	Enstatite + $H_2O(g) \rightarrow$ serpentine
8	$N_2(g) + 3H_2(g) \rightarrow 2NH_3(g)$
9	$H_2O(g) \rightarrow H_2O(s)$
10	$NH_3(g) + H_2O(s) \rightarrow NH_3 \cdot H_2O(s)$
11	$CH_4(g) + 8H_2O(s) \rightarrow CH_4 \cdot 8H_2O(s)$
12	$CH_4(g) \rightarrow CH_4(s)$
13	$Ar(g) \rightarrow Ar(s)$
14	$Ne(g) \rightarrow Ne(s)$
15	$H_2(g) \rightarrow H_2(s)$
16	$He(g) \rightarrow He(s)$
Disequilibrium Condensation	
1	Condensation of Ca, Al, and Ti oxides
2	Condensation of Fe-Ni alloy
3	Condensation of enstatite ($MgSiO_3$)
4	$CO(g) + 3H_2(g) \rightarrow CH_4(g) + H_2O(g)$
5	$N_2(g) + 3H_2(g) \rightarrow 2NH_3(g)$
6	$H_2O(g) \rightarrow H_2O(s)$
7	$NH_3(g) + H_2S(g) \rightarrow NH_4SH(s)$
8	$NH_3(g) \rightarrow NH_3(s)$
9	$CH_4(g) \rightarrow CH_4(s)$
10	$Ar(g) \rightarrow Ar(s)$
11	$Ne(g) \rightarrow Ne(s)$
12	$H_2(g) \rightarrow H_2(s)$
13	$He(g) \rightarrow He(s)$

- ☆ Model Condensation Sequences
  - ☞ Dense, Tightly-Bound Material Condenses First

Laboratory Technologies for Isotopic-Composition Analyses

- ☆ Physical & Chemical Preparation of Meteorite
  - ☞ Dissolve Meteoritic Matrix through Acids
    -> Hardest Component (most refractory, oldest)

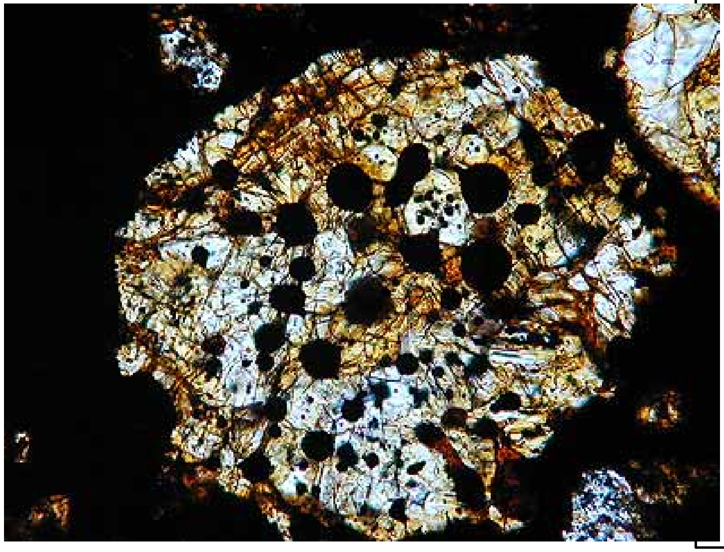

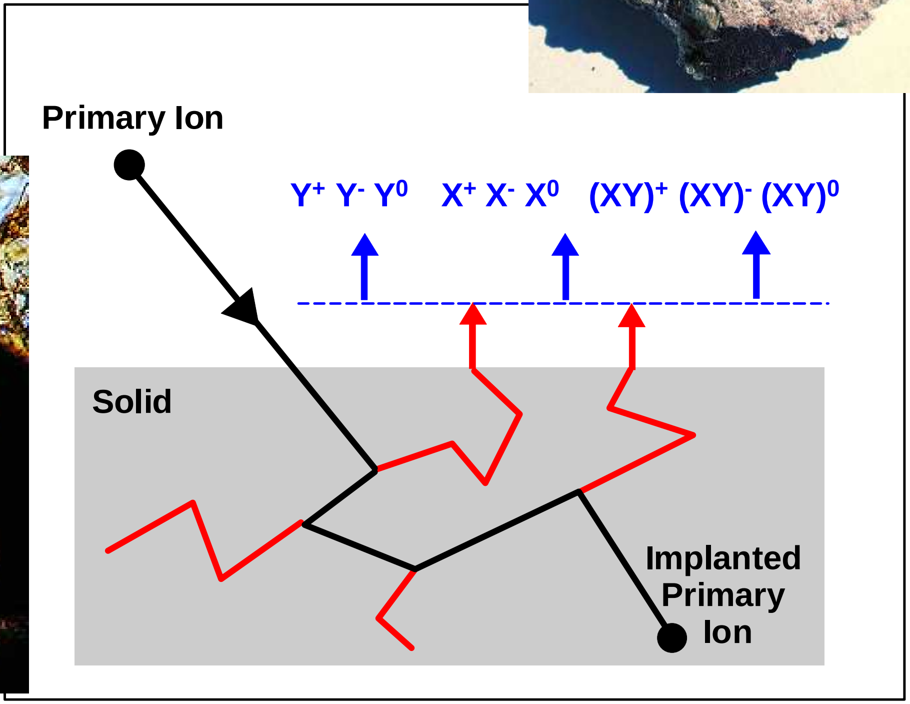

- ☆ Secondary-Ion Analysis
  - ☞ Secondary-Ion Mass Spectroscopy
    - » nanoSIMS with Ion Microprobes
    - » TOF-SIMS
    - » Resonant IMS (RIMS)

nanoSIMS

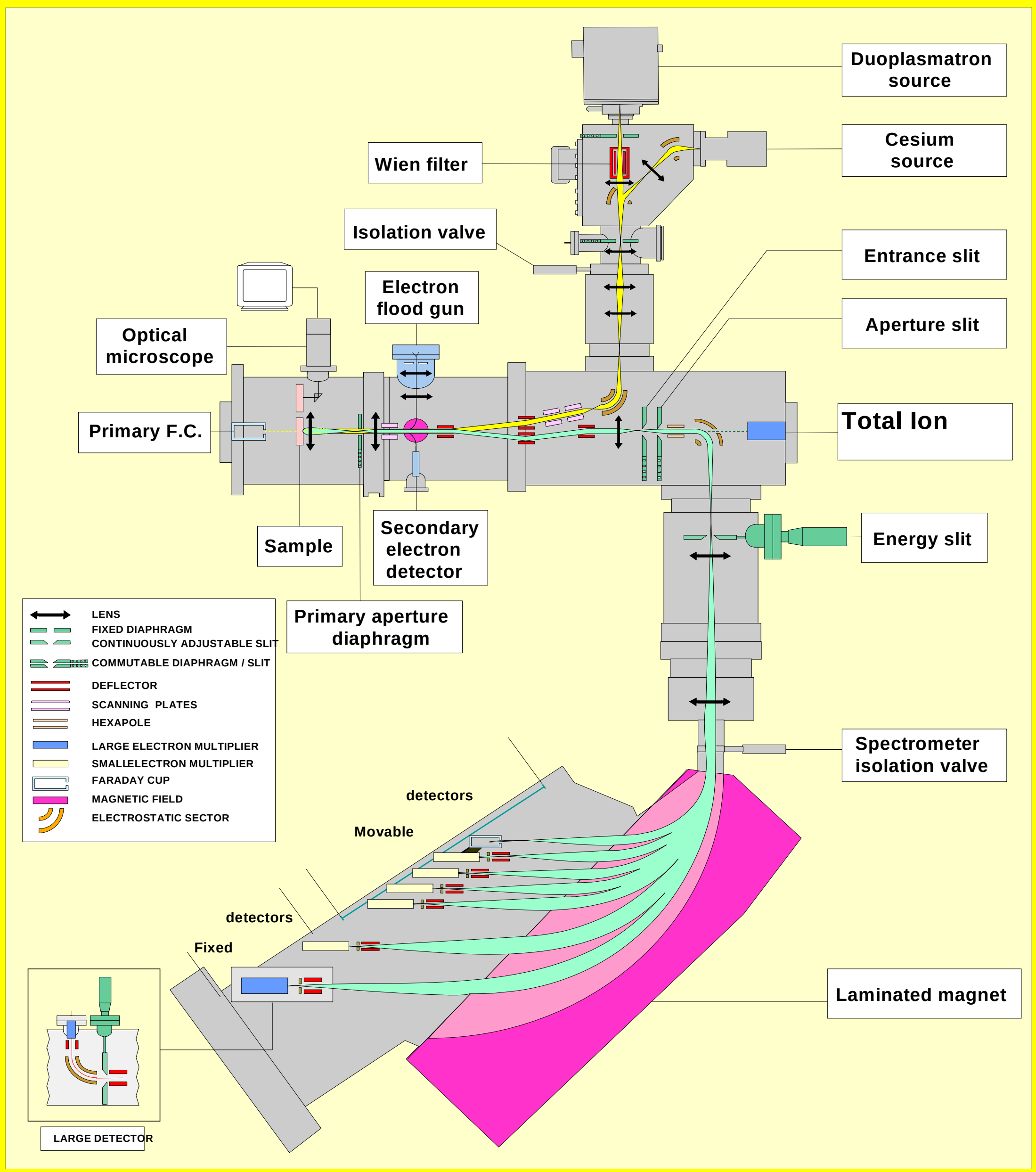

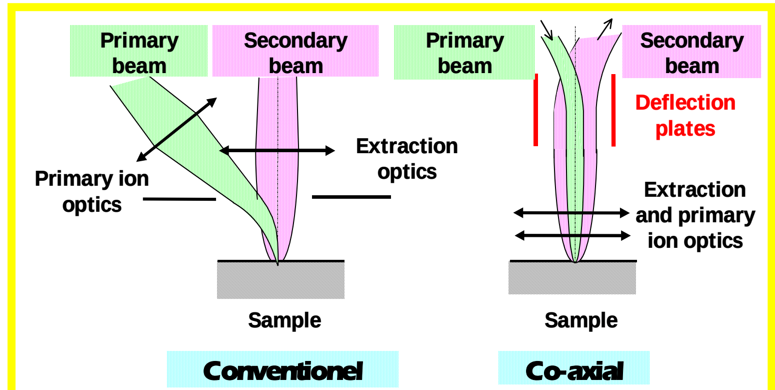

☆ Key Features:

- High Lateral Resolution ~50nm)
- High Secondary-Ion Detection Efficiency
- Up to 6 Ion Detection Channels
- "CAMECA, St.Louis/ Mainz >2000

^{60}Fe in Solar-System Meteorites

- ☆ ^{60}Ni Excesses wrt. Ni Isotopes Detected in Meteorites
  - ☞ ^{60}Fe/^{56}Fe ~ 3 10^{-7} ... 1 10^{-6}

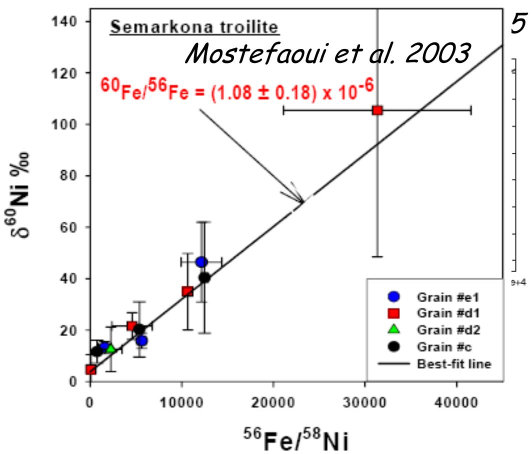

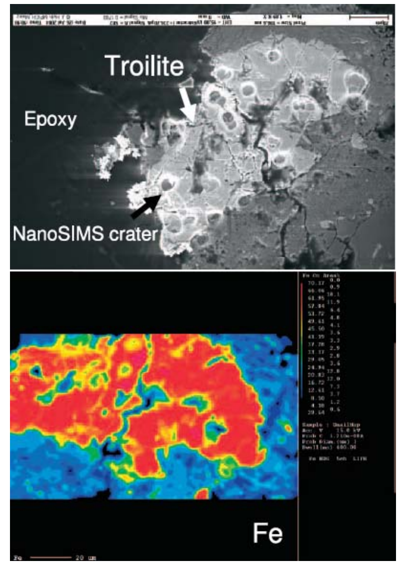

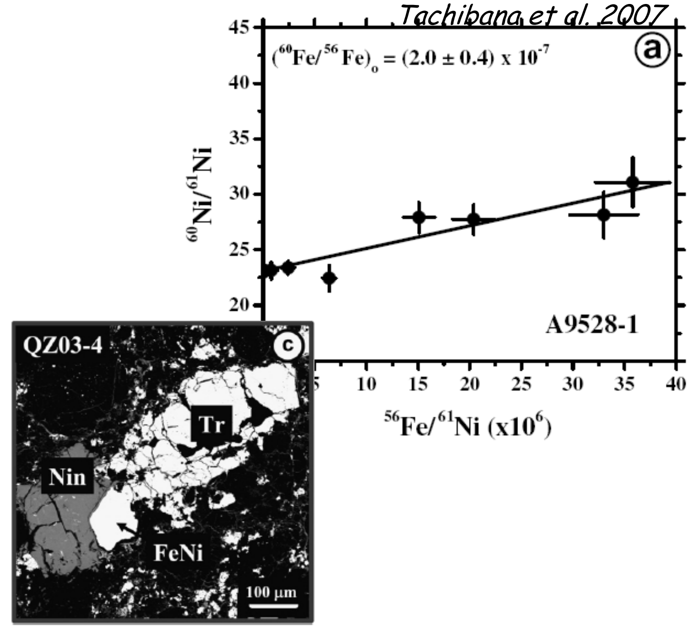

- ☆ ISM Abundance Ratio?
  - ☞ ^{26}Al & ^{60}Fe from ISM γ's & SAD ^{27}Al,^{56}Fe -> ~ 1.4 10^{-7}
- ☆ The "Disk Area" of a Newly-Formed Stellar System is ~10 My
- ☆ Chondrules are Formed ~Myrs *after* Decoupling of SolarSys from ISM
  - ☞ When, Exactly, Does Chondrule Formation Occur?
  - ☞ Was ^{60}Fe a Significant Heat Source of Chondrules?
  - ☞ Has there been 'late' SN Enrichment?

Detection of Presolar Grains

- ☆ Huge (compared to solar-sample variances) Isotopic Abundance Anomalies
  - ☞ C or O Isotopes
    - – Solar Variation ~10%
    - – Total Range ~10^5

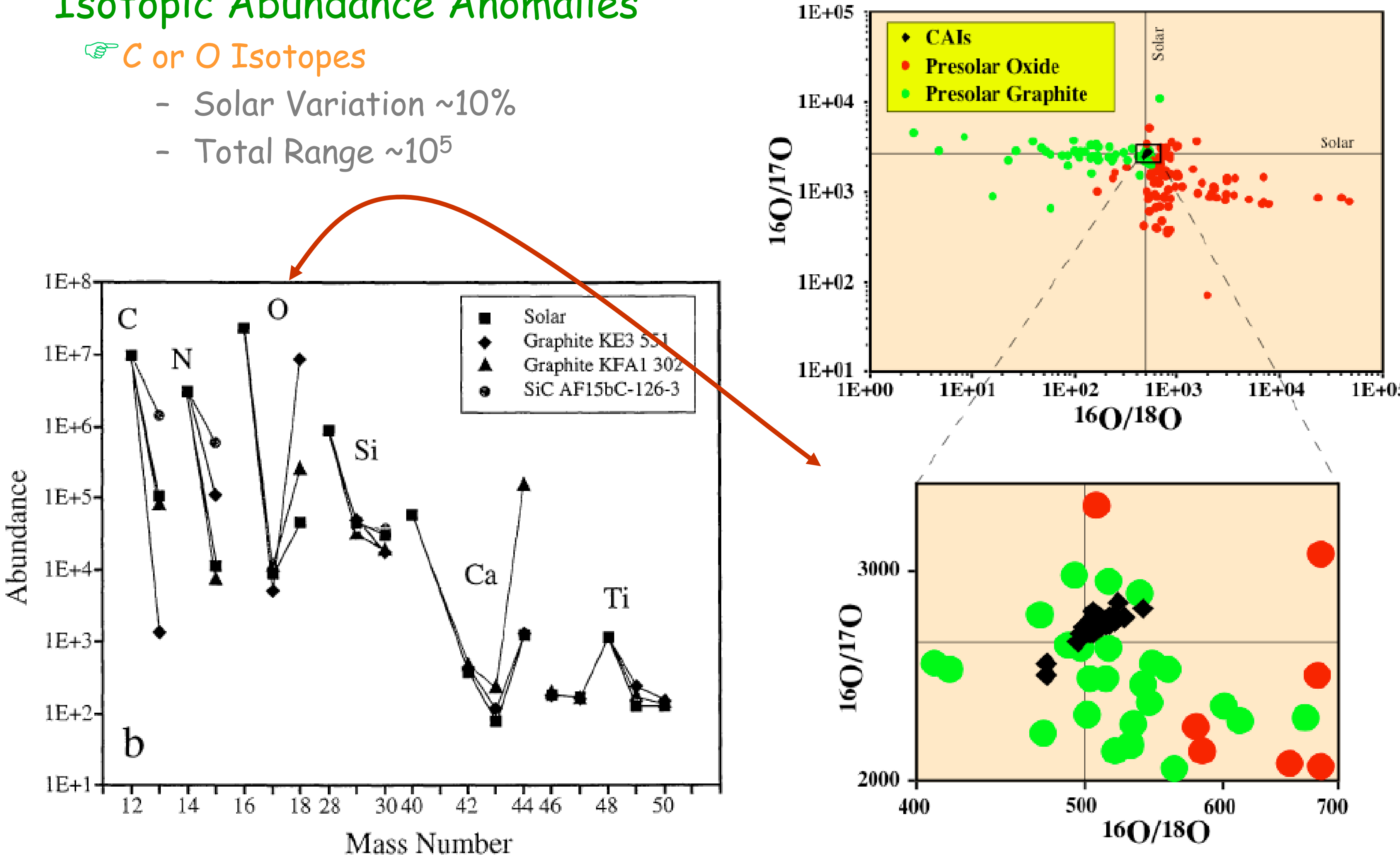

Presolar-Grain Types

Zinner 1998

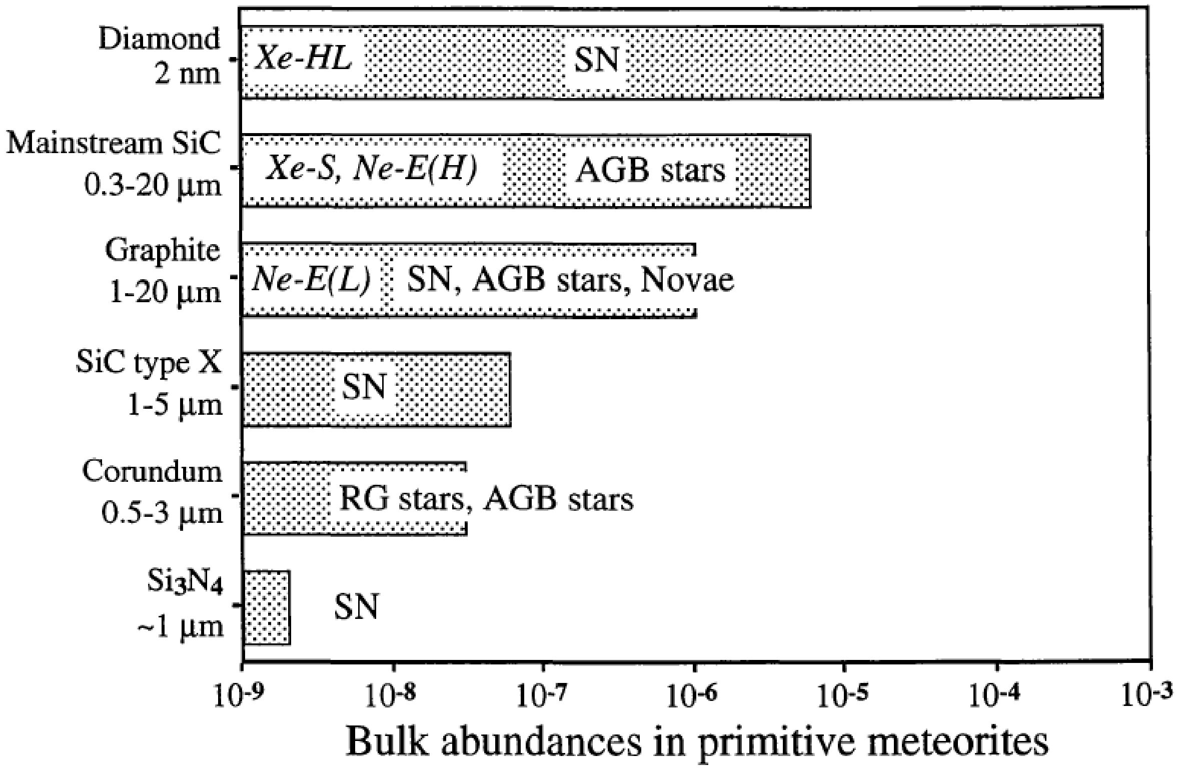

FIG. 1. Types of presolar grains discovered to date in primitive meteorites. Given are their relative abundances (mass fractions), sizes, likely stellar sources and the exotic noble gas components carried by some of them. Silicon carbide and graphite grains contain tiny subgrains of Ti-, Zr- and Mo-carbides.

☆ Driven by Detection Method

Nuclear Burning in AGB Stars: Cool-Bottom Burning?

- ☆ AGB Stars Eject Products from H Shell Burning
  - ☞ Convective Envelope
  - ☞ He Burning Products Ingested by Shell Instabilities
  - ☞ AGB Stars are Copious Dust Grain Producers

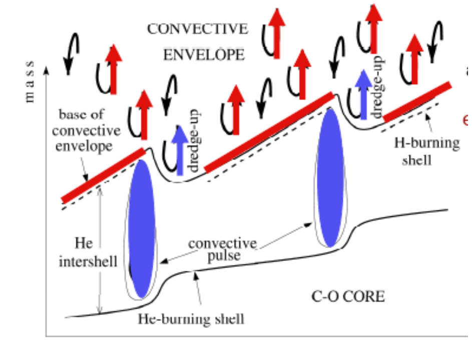

- ☆ Isotopic Ratio Measurements vs. Stellar Model Calculations
  - ☞ 'Normal' AGB H Shell Burning Cannot Reproduce Observed High $^{26}Al/^{27}Al$
  - ☞ Cool-Bottom Burning as Alternative? *(Nolett et al. 2003; Zinner et al. 2006)*

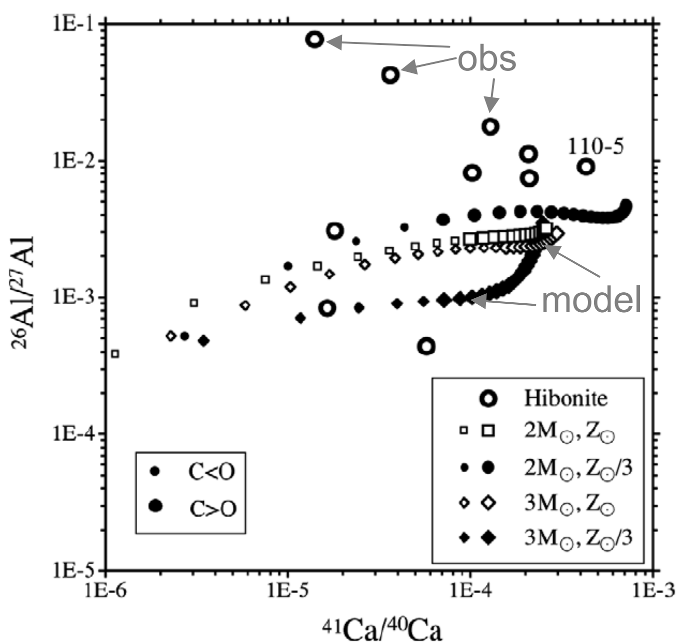

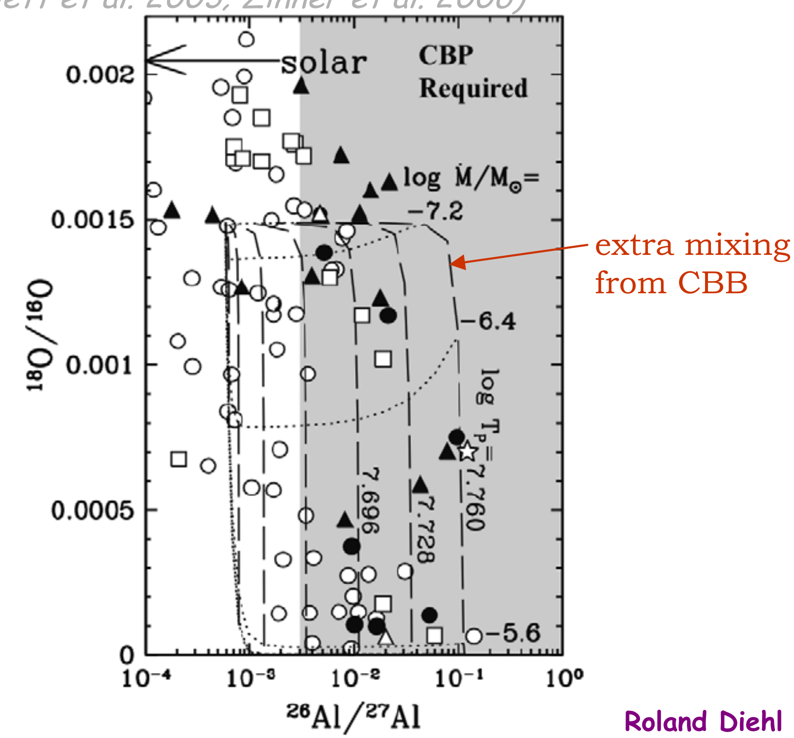

Roland Diehl

Stardust: Presolar "X" Grains

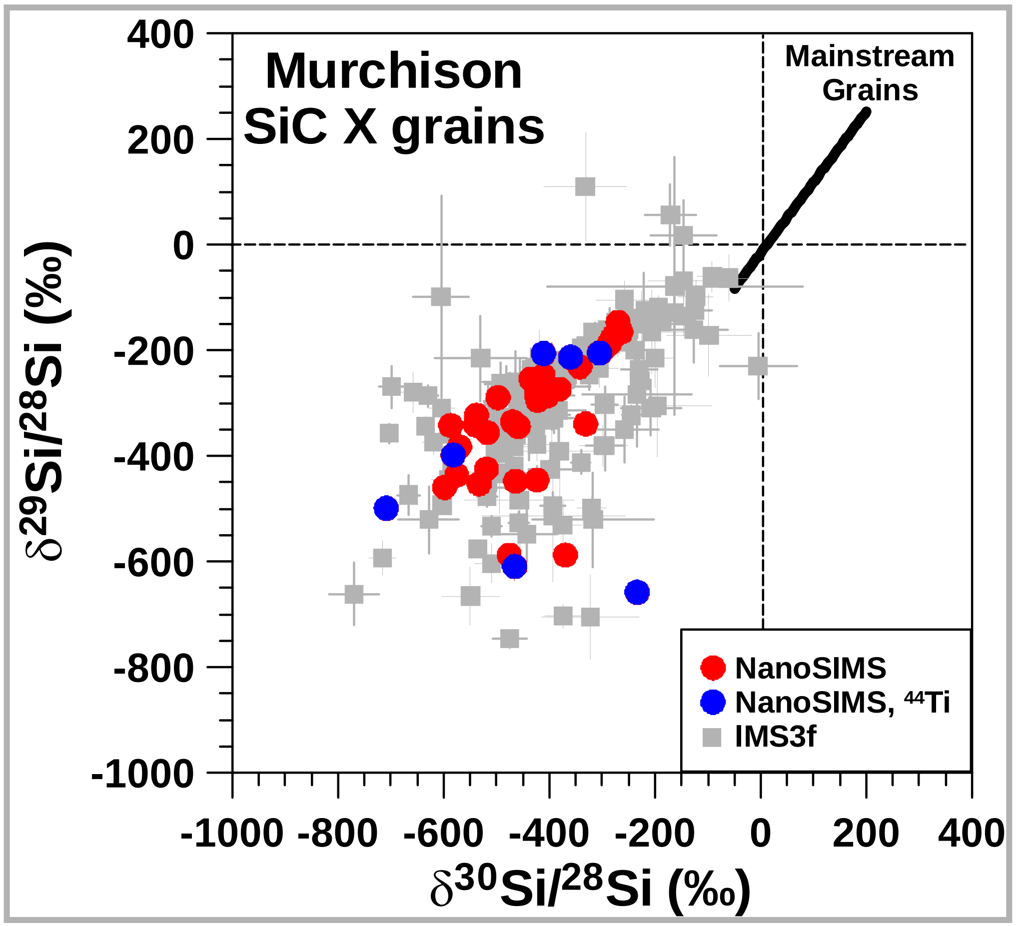

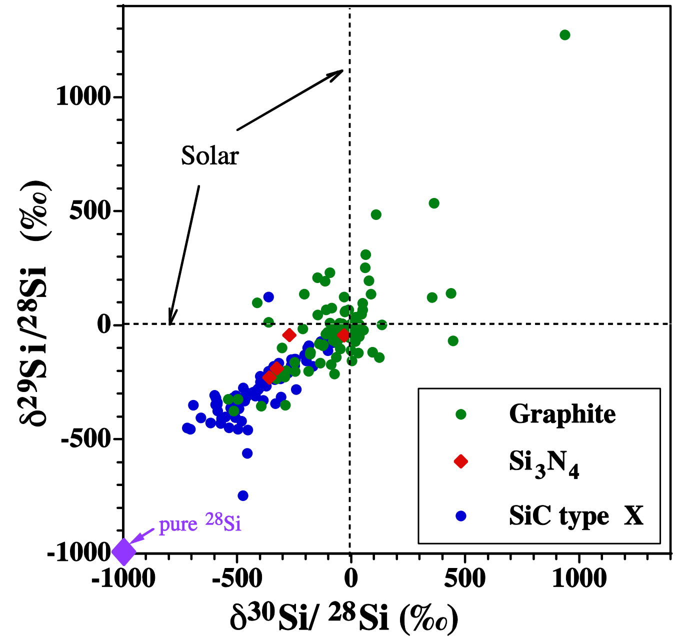

$\delta^{i}Si/^{28}Si$ (‰) = $((^{i}Si/^{28}Si)_{Grain}/(^{i}Si/^{28}Si)_{Solar} - 1)\times 1000$

- "Mainstream" SiC Grains from C-rich Stars -> AGB Stars
- SiC X grains are a rare type of presolar SiC
- Isotopic signatures: Excesses in ^{12}C (most grains), ^{15}N, and ^{28}Si, large amounts of ^{26}Al and presence of ^{44}Ti (some grains)
- cc SN are the most likely stellar sources

Roland Diehl

Stardust Mission: Collecting Interplanetary Dust

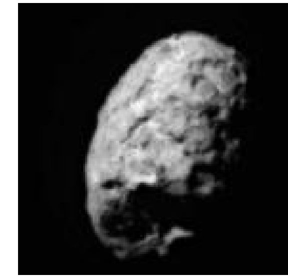

- ☆ Aerogel Layers Deposited in Interplanetary Space
- ☆ Sample Return for Analysis in Terrestrial Laboratory
  - ☞ "Stardust" Mission: Sample Return from Comet Wild
  - ☞ launched Feb 7, 1999; sample return Jan 16, 2006

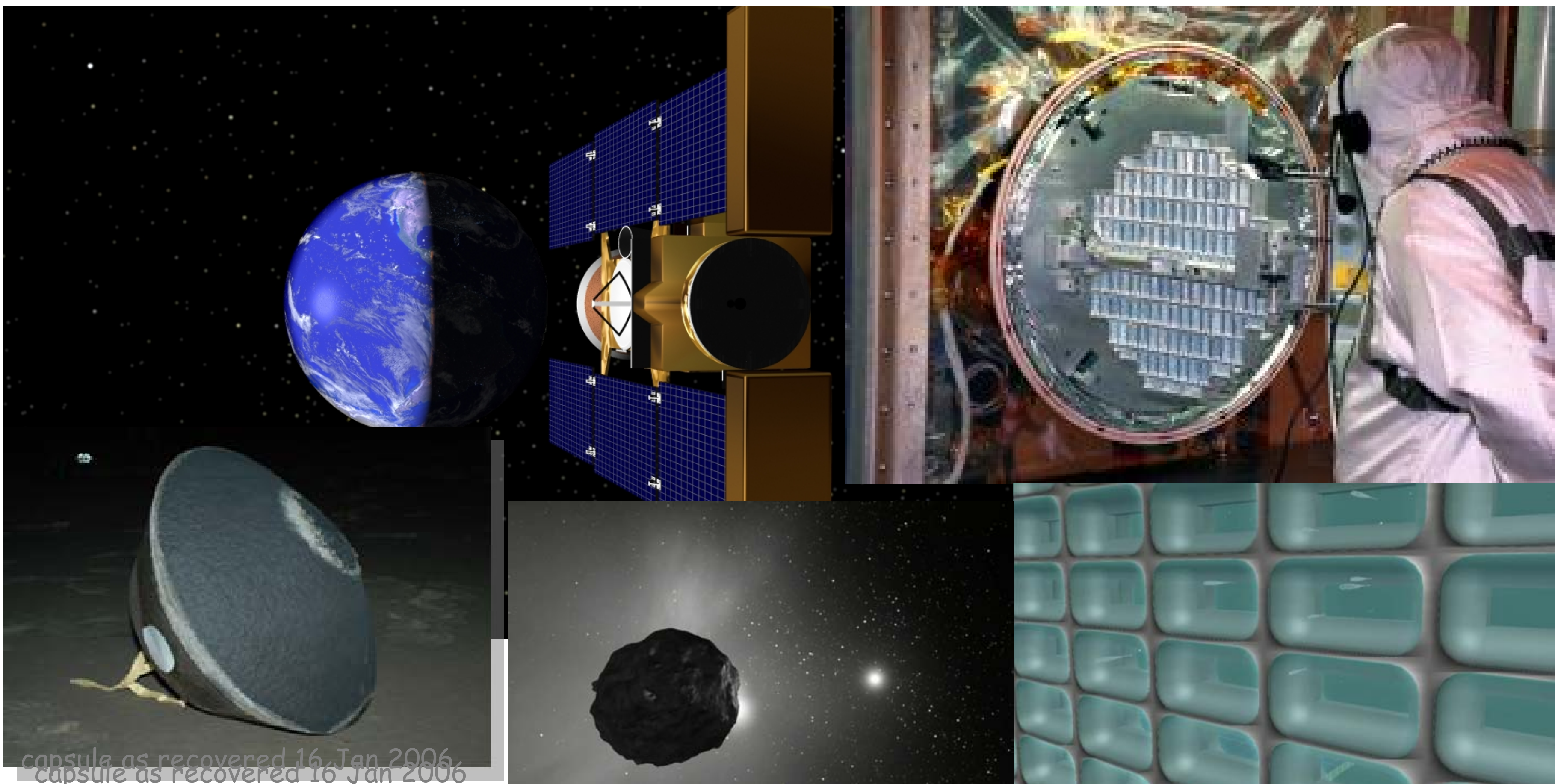

Interplanetary Cosmic-Ray Measurements

- ☆ ACE/CRIS
  - ☞ Advanced Composition Explorer 1997+
  - ☞ Cosmic Ray Isotope Spectrometer
  - ☞ Mass and Charge Analysis through Si Solid State Detector
    - » measure energy deposit in SSS
    - » measure Q/E in hodoscope

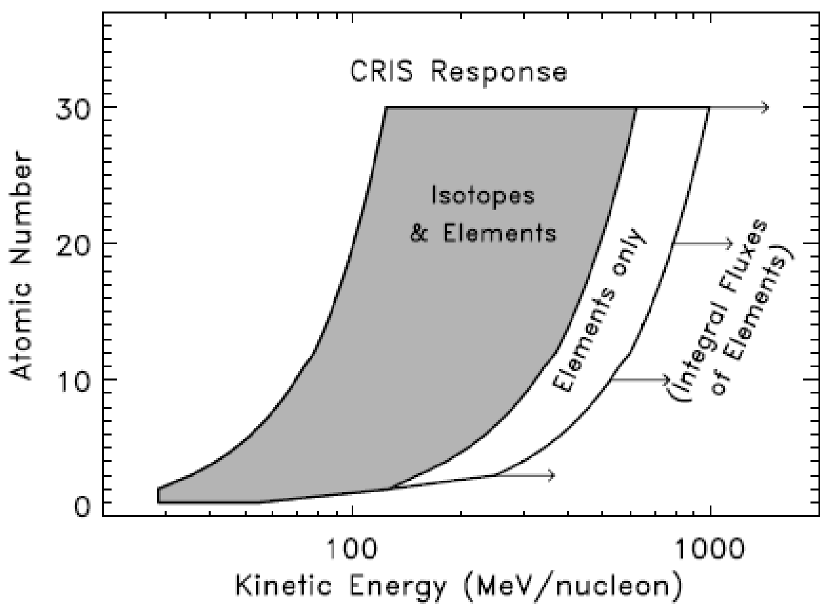

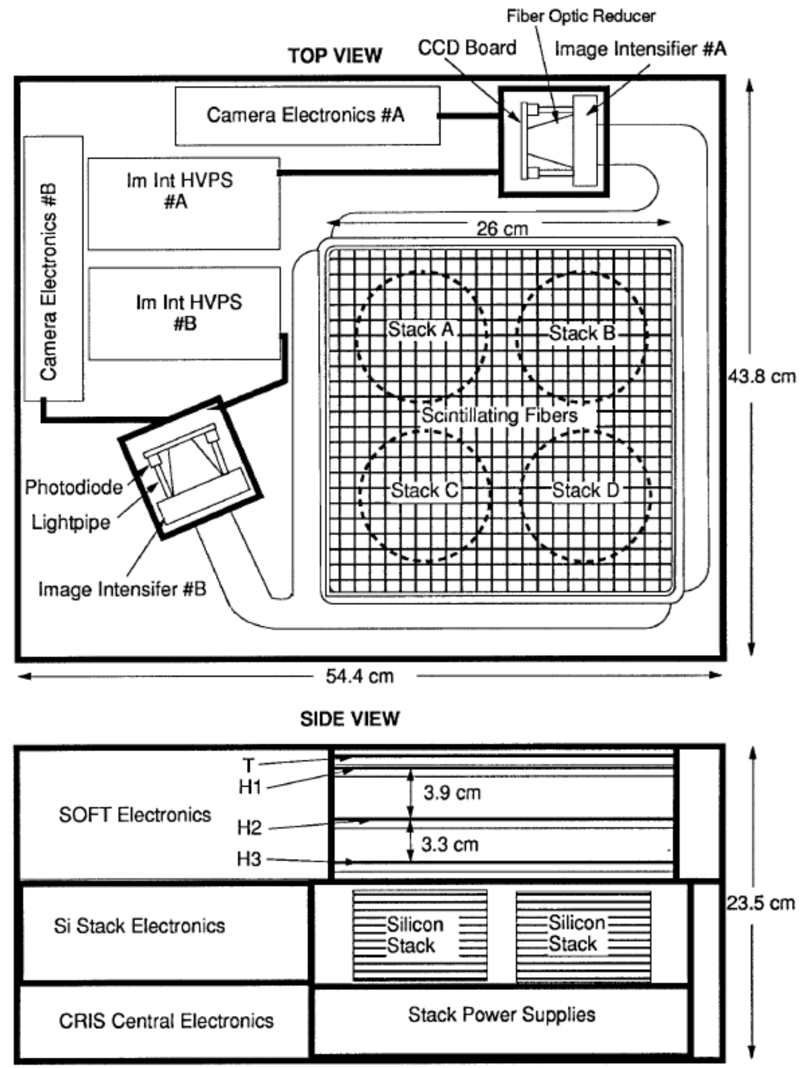

Radioactive-Isotope Constraints on Propagation of Cosmic Rays in Galaxy

- ☆ Spallation Reactions Produce Radioactive Isotopes When Cosmic-Rays Collide with Ambient ISM Gas
- ☆ Spallation Cross Sections are Determined from Lab Measurements
- ☆ Abundances of Unstable Isotopes -> CR Path Length in Galaxy
  - ☞ Compare Isotope Ratios to 'leaky-box' Models for CR Propagation:

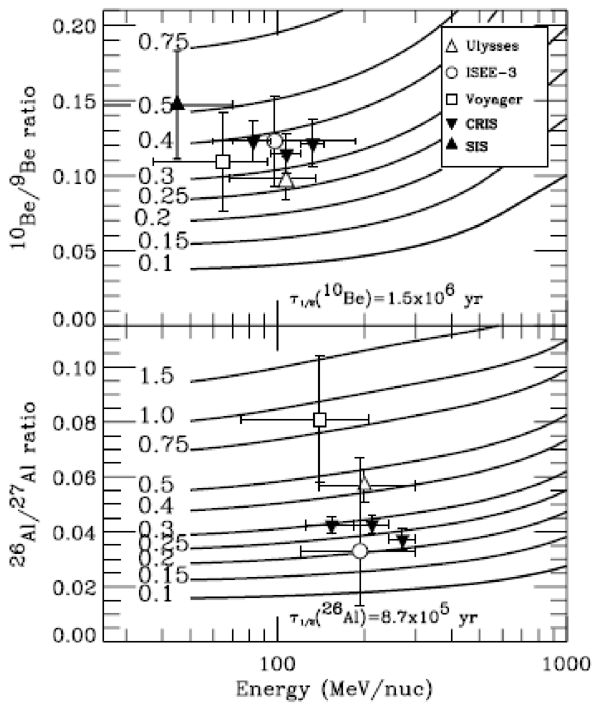

-> Density of Confinement Region [H atoms cm^{-3}]

- ☞ Size of Galactic-Disk Region 'Sampled' by Different Isotopes:

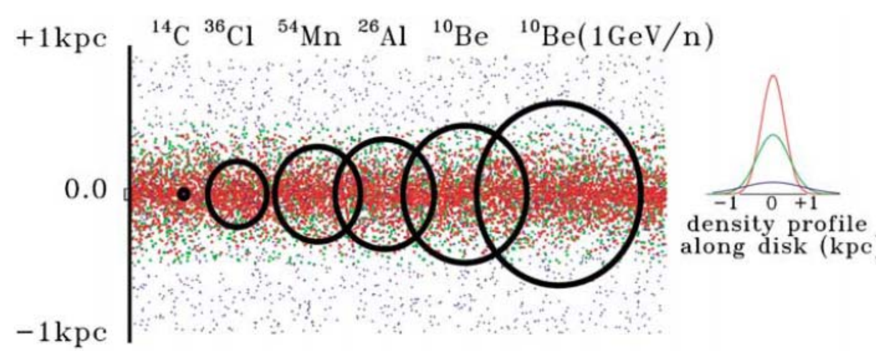

Roland Diehl

Radioactive Isotope Clocks

- ^{59}Ni and Acceleration Delay
  - ☆ ^{59}Ni Decay by e Capture Only
    - ☞ If Accelerated (=Ionized): No Decay
    - ☞ Before Acceleration: Decay
  - ☆ Decay Time ~10^5 y
    - ☞ Presence of ^{59}Ni in CR's
      = Immediate Acceleration
      ($<\tau=10^5$ y)
      of Freshly-Generated Material
    - ☞ Absence of ^{59}Ni and Presence of ^{59}Co
      = Decay Before Acceleration
      = Delay Between Production of CR
      Source Composition and its Acceleration

ACE/CRIS, *Wiedenbeck et al. 2001*

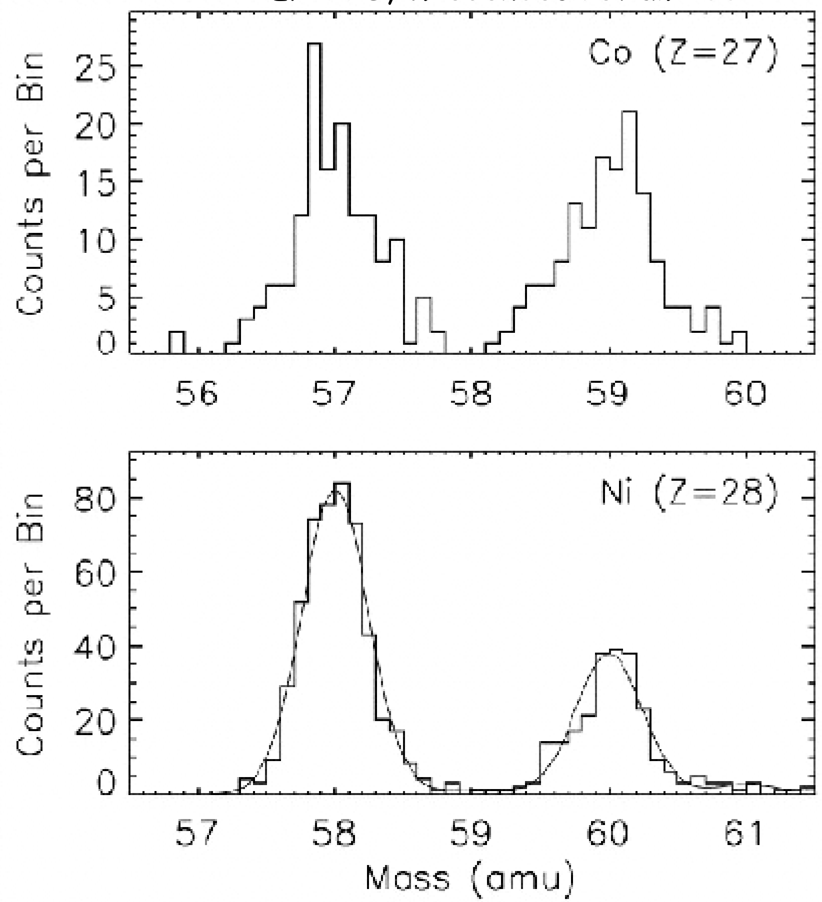

Air Shower Experiments

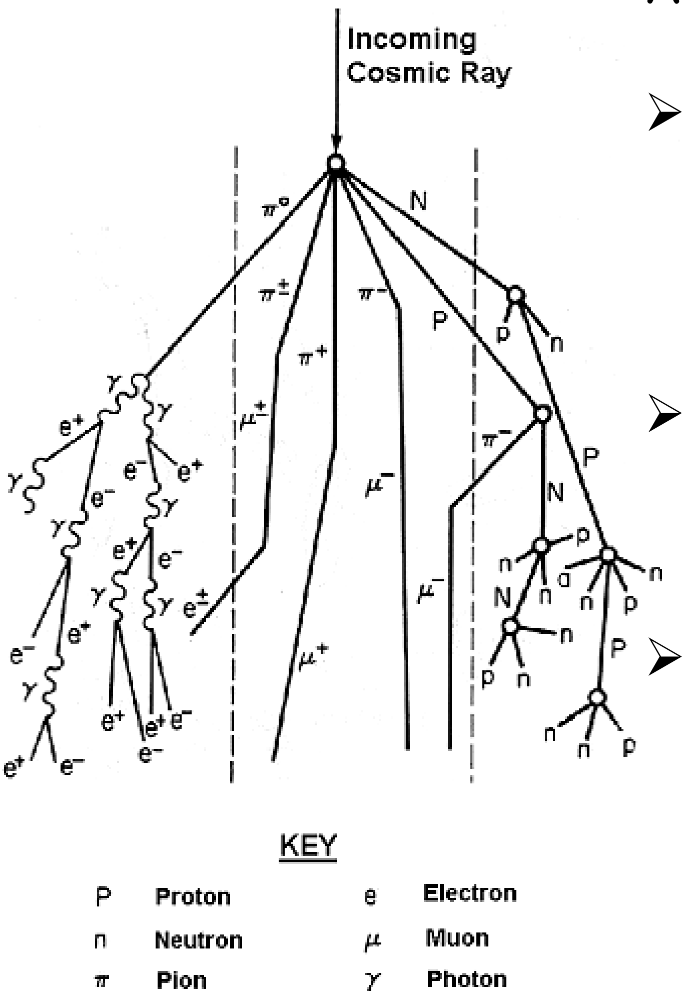

Air showers consist of 3 components:

- hadronic component
  primary proton scatters off atmospheric nuclei, thereby producing protons, neutrons, pions, kaons, ...
- myonic component
  the decay of charged pions and kaons generates myons
- electromagnetic component
  the decay of neutral pions generates γ\`s, which initiate electromagnetic cascade through pair creation and bremsstrahlung

The Cosmic-Ray Composition...

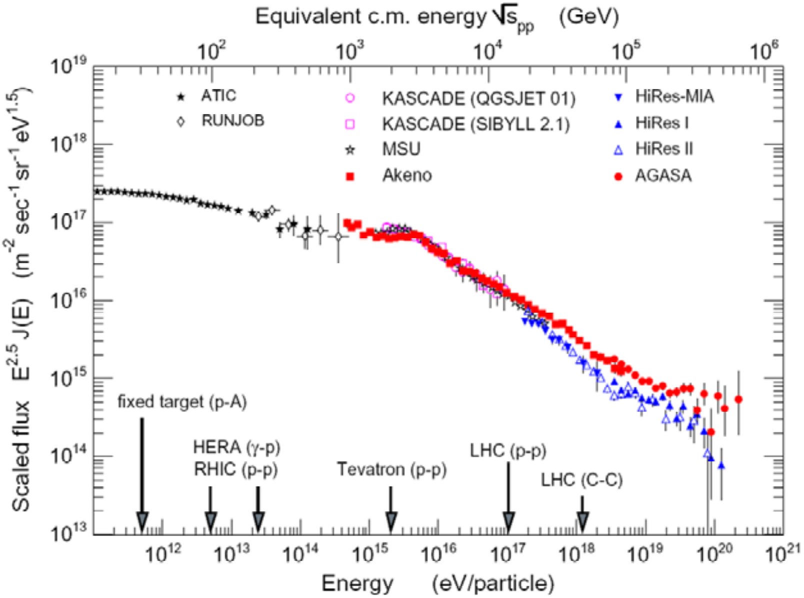

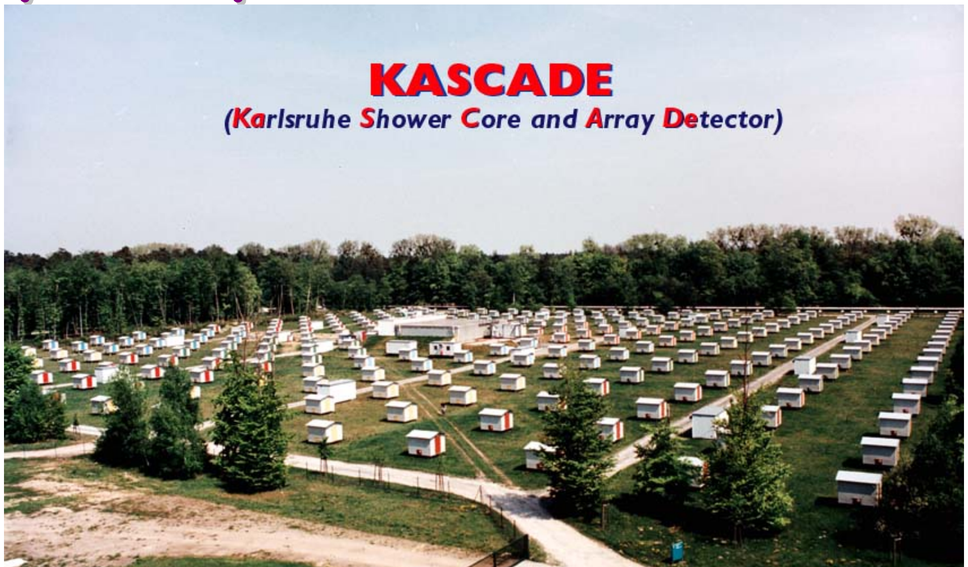

- ☆ Comparison of Observed Shower Patterns with MC Simulations
  - ☞ "Knee" = Steepening of Light-Element Spectrum
  - ☞ Around ~10^{18} eV, the composition changes from heavy-nuclei-dominated to (pure) protons

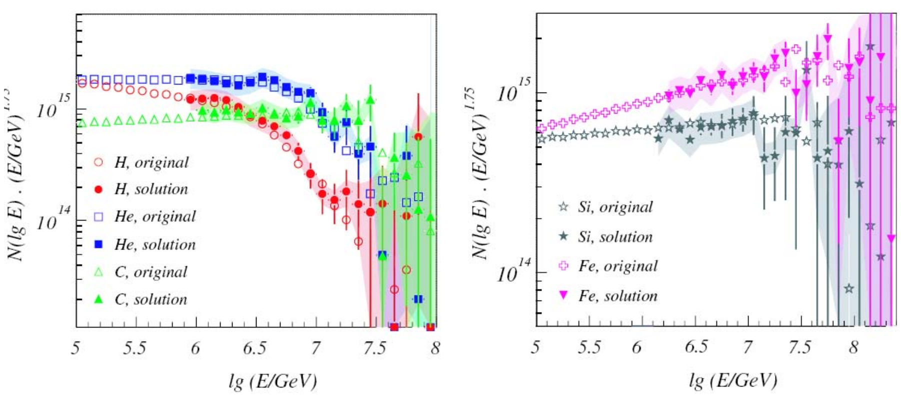

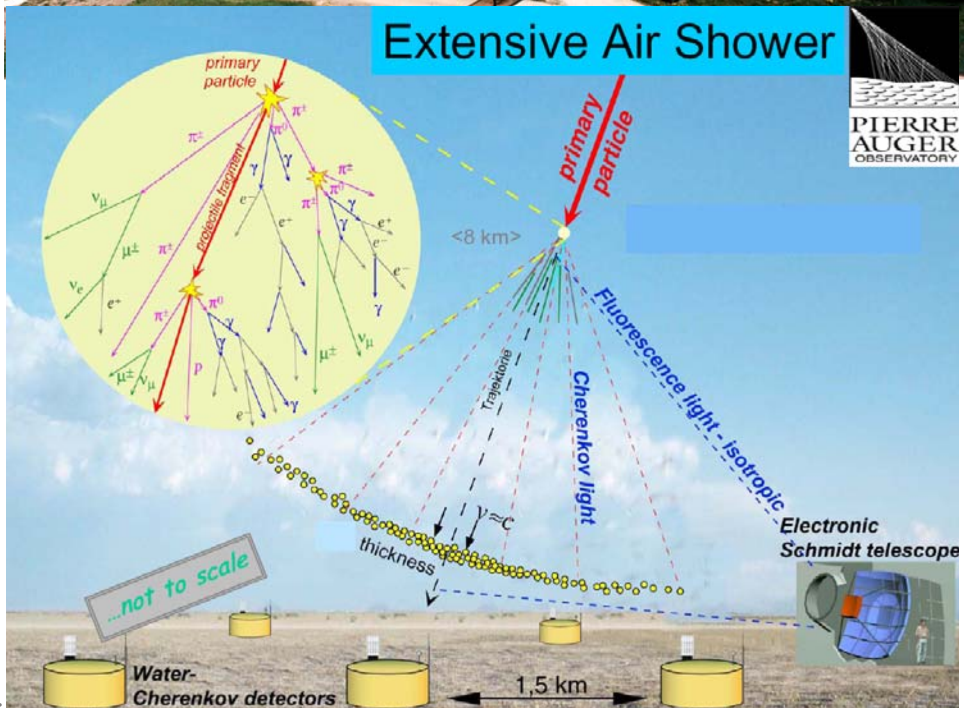

Inferrence of Isotopic Abundances

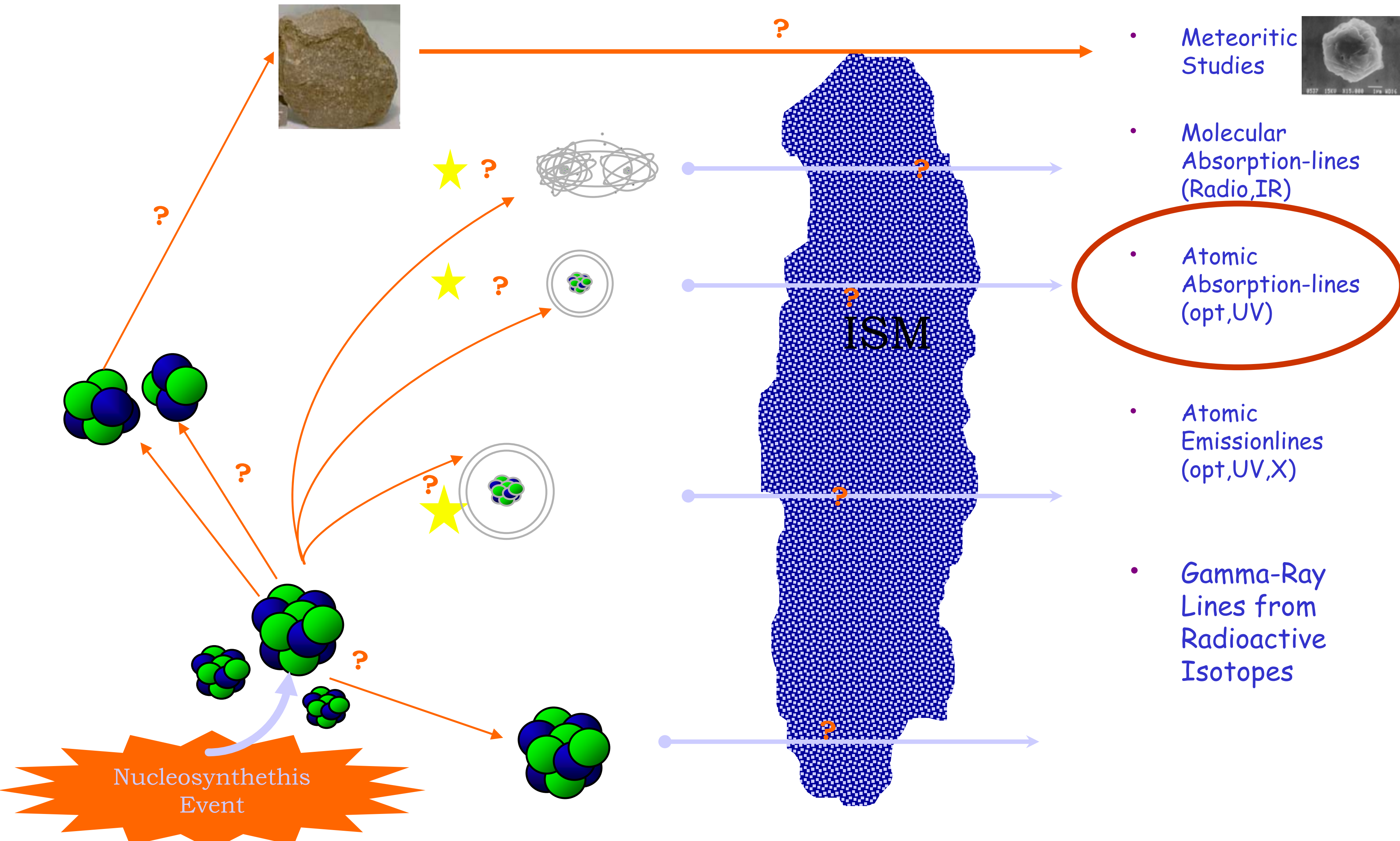

Stellar Classification and Radiation Origin

- Spectral Classification Encodes Temperature
- Plasma Radiation Mechanism Depends on Temperature
  - ☞Molecules and Dust
  - ☞Neutral Atoms
  - ☞Ionized Atoms

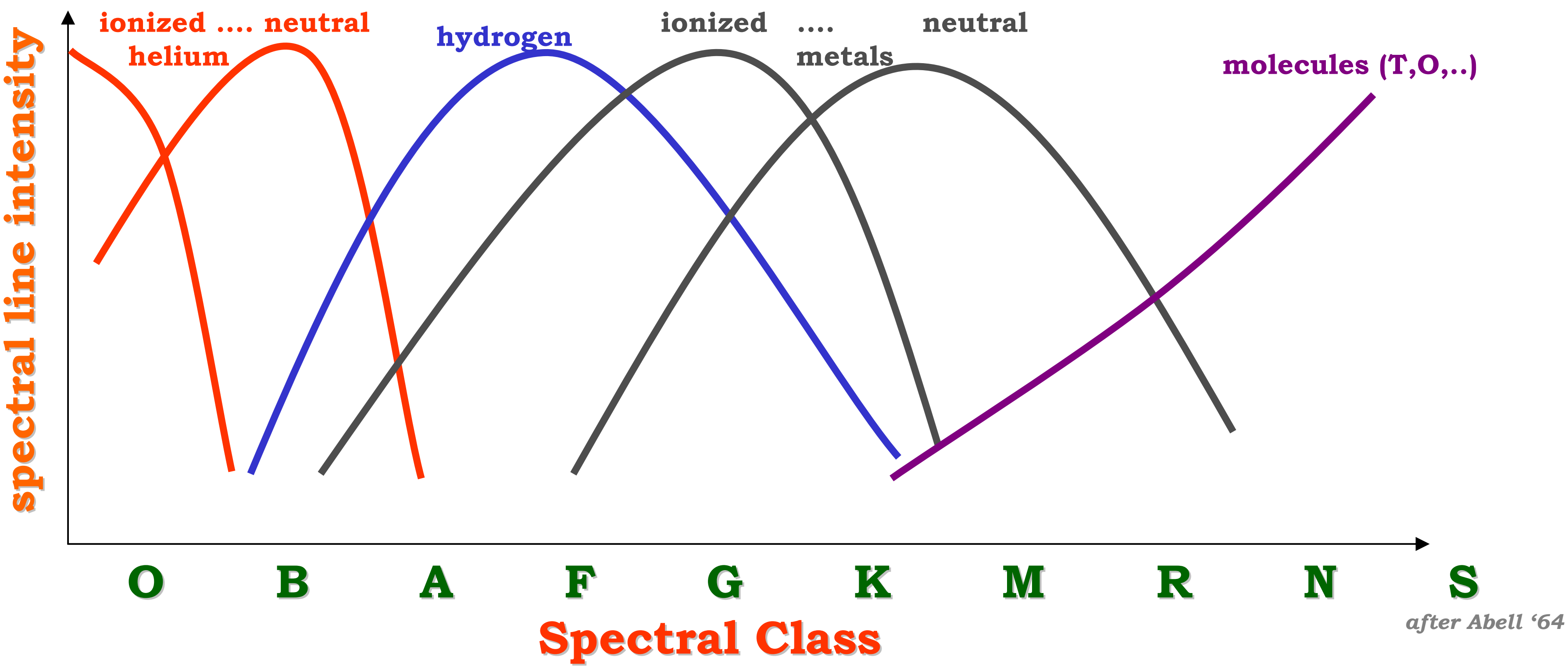

Roland Diehl

Spectroscopy Measurements and their Analysis

How do you extract elemental abundances from these lines?

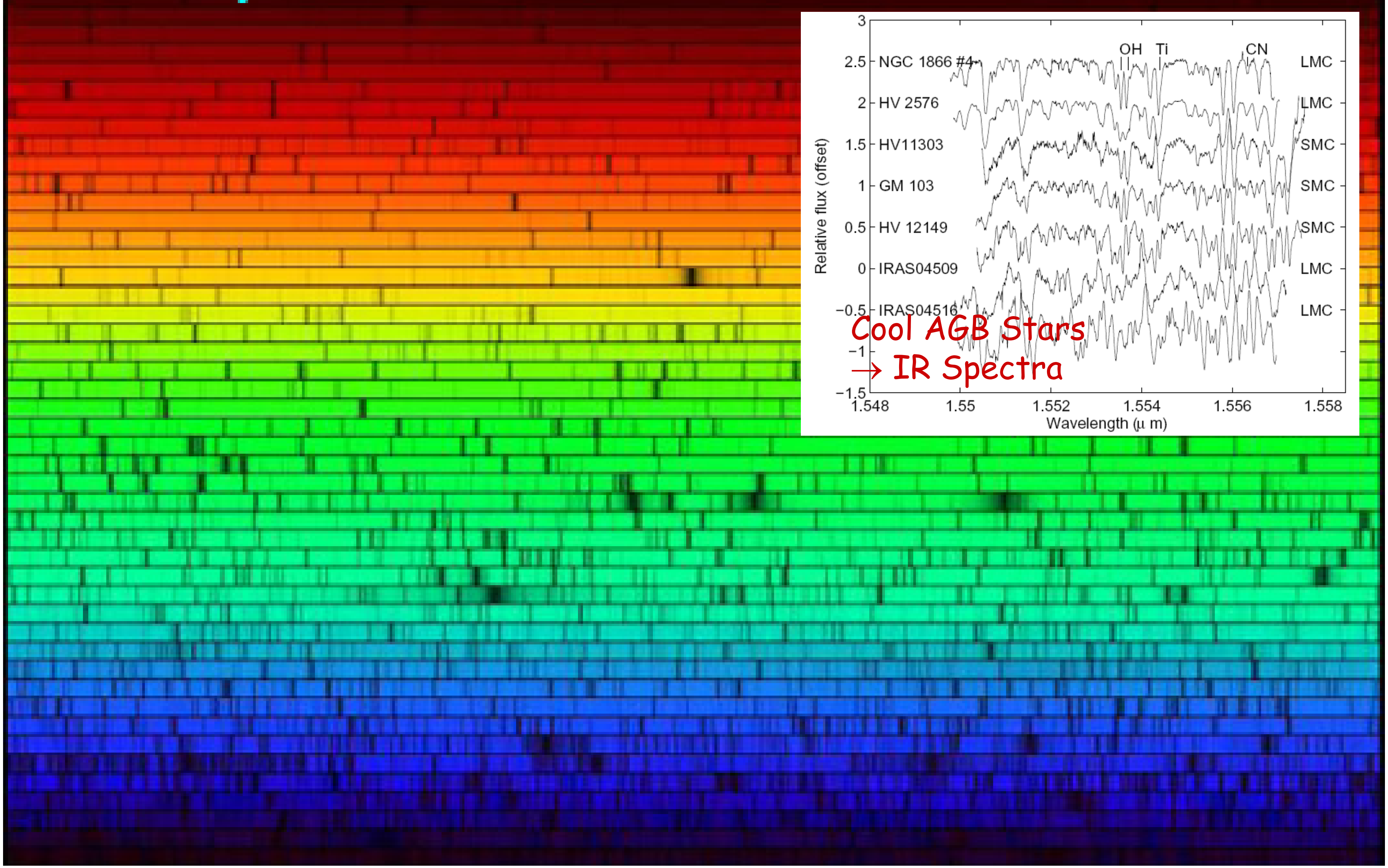

Determination of Abundances from Absorption Lines

- ☆ Line Absorption Depth -> Abundance
  - ☞ Optically Thin Lines
    - – Use "Equivalent Width"

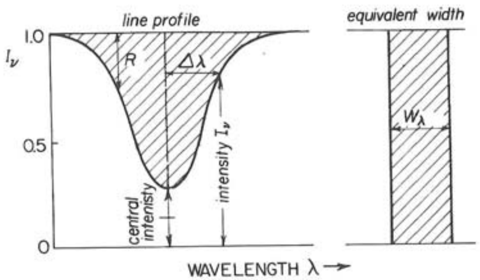

  - ☞ Impact of Atmospheric Depths:
    - – "Curve of Growth"
      - » Stellar Continuum Passes Through Photosphere, Being Absorbed -> Exponential Law
      - » Corrections: Doppler Broadening and Line Wing Treatment -> Deviations from Exponential Law
      - » *see e.g. Pagel 1997*
      - » *Superseded by Full-Spectra Modelling...*

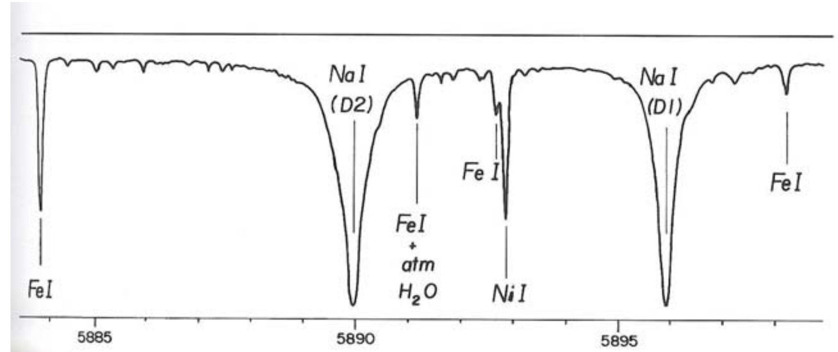

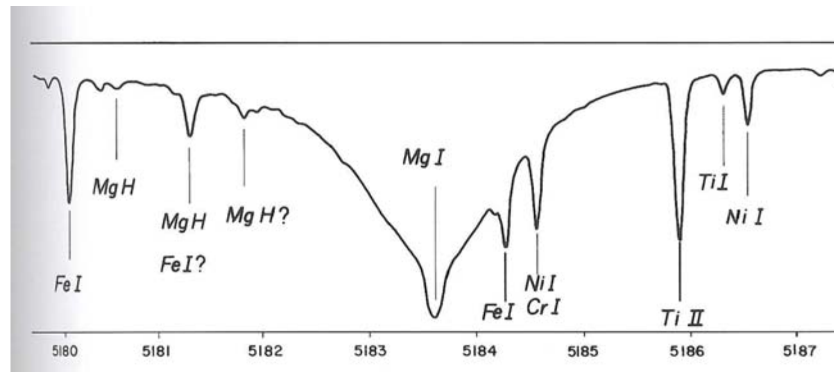

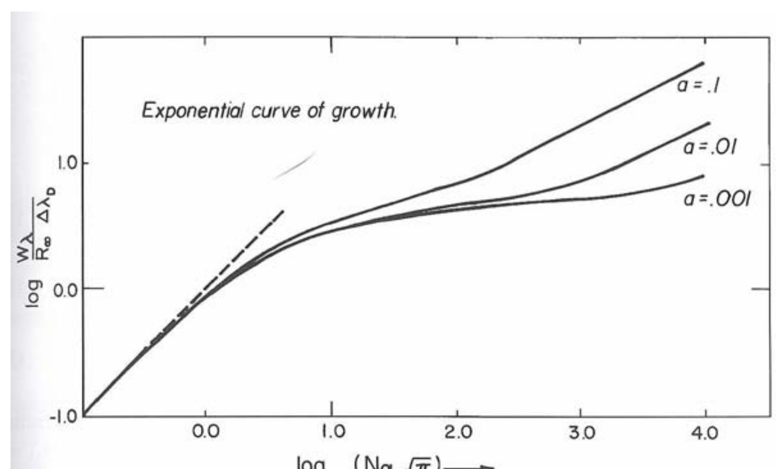

Modelling a Stellar Spectrum

- Ingredients: Stellar Parameters
  - ☆ Temperature $L = 4\pi R^2 \sigma \cdot T_{eff}^4$
    - ☞ Determine 'effective' Temperature (equivalent BB)
      - using calibrations between relative bandpass intensities and standard spectra
  - ☆ Distance
    - ☞ from Parallaxes, ...
    - ☞ Yields L, R from T_{eff}
  - ☆ Mass $g = \frac{GM}{R^2}$
    - ☞ Determine Surface Gravity
      - from pressure-broadened lines (i.e. line profiles)
  - ☆ Metallicity
    - ☞ Determine global metallicity, Using SAD
    - ☞ Determine Pivot Element Abundance (Fe Lines)

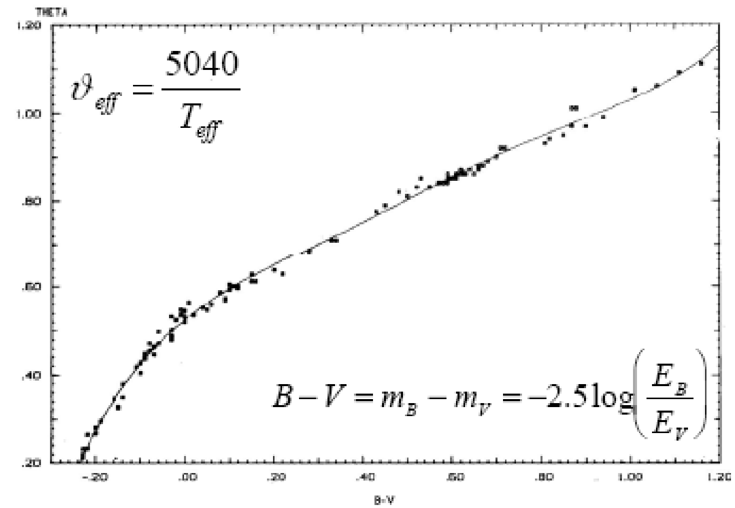

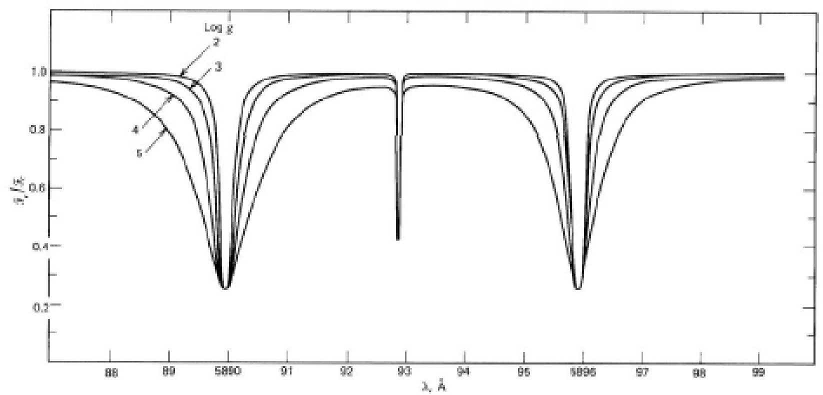

Iterative Determination of Abundances

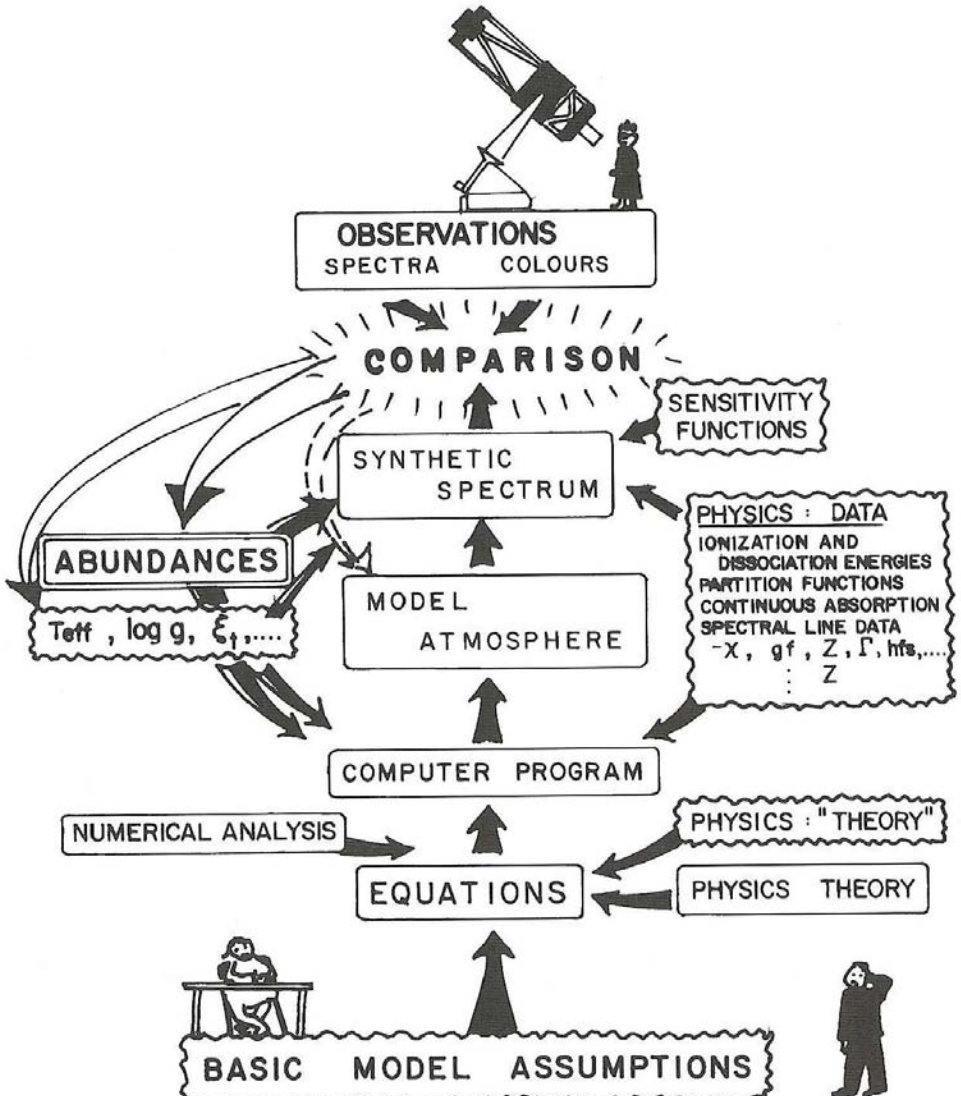

from Pagel (1997)

Example: C,N in a Metal-Poor Star

- ☆ CN Line System with Band Head at 3883 A
- ☆ Varying the N Abundance

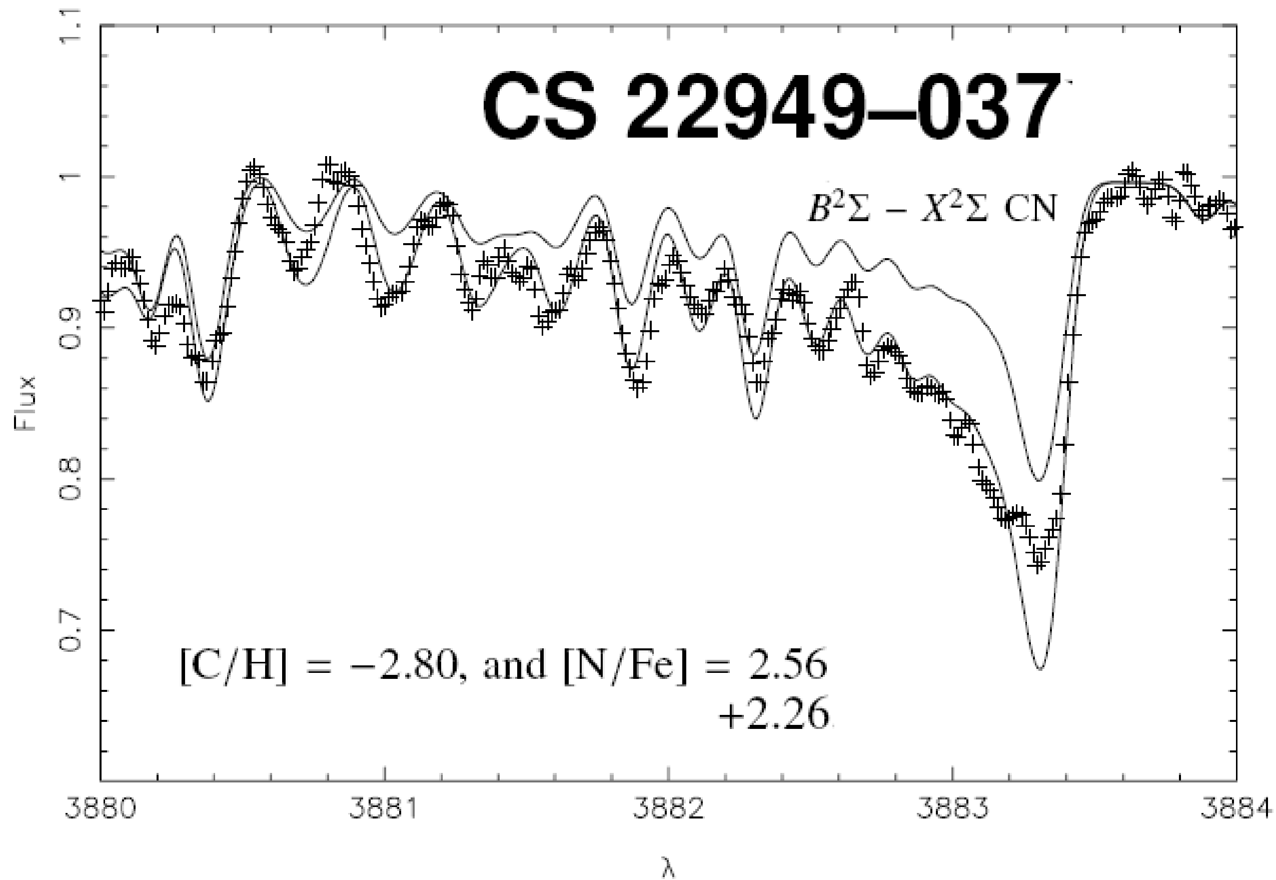

☞ *Depagne et al. 2002*

Isotopes: Spectra for Cooler Types of Stars

- Photospheric Temperature Determines Absorbing Species
  - ☆ Giants, AGB Stars:
    - ☞ Molecules Become Important
    - ☞ High-Resolution Spectroscopy Identifies Isotopic Features

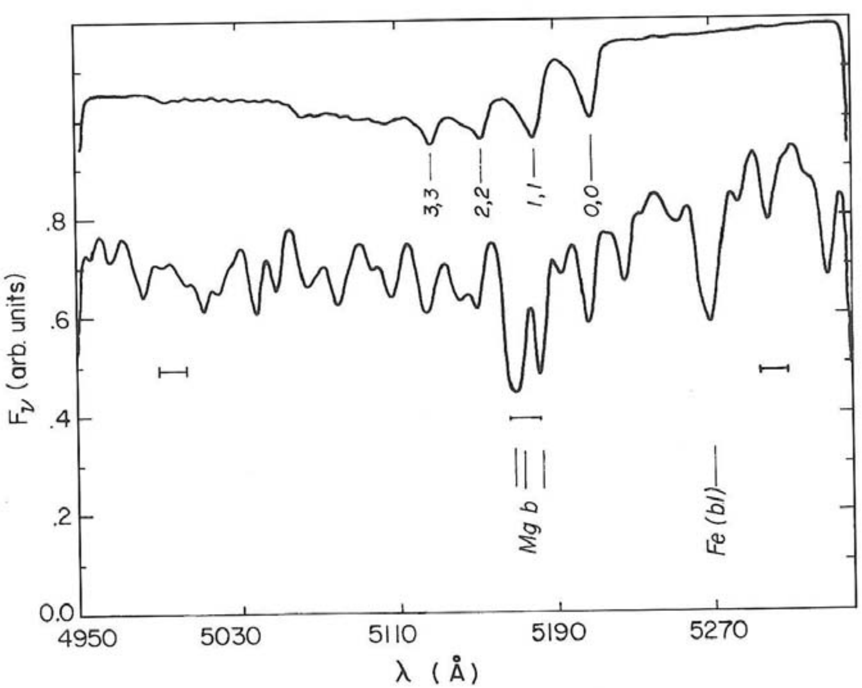

Fig. 3.17. Synthetic spectrum of a red giant, $T_{\rm eff}$ = 4500 K, log g = 2.25 in the region of the strong Mg I b lines (cf. Fig. 3.9). The upper spectrum is the same with atomic lines 'switched off' and shows molecular bands of MgH. Adapted from Mould (1978).

Young et al. 2003

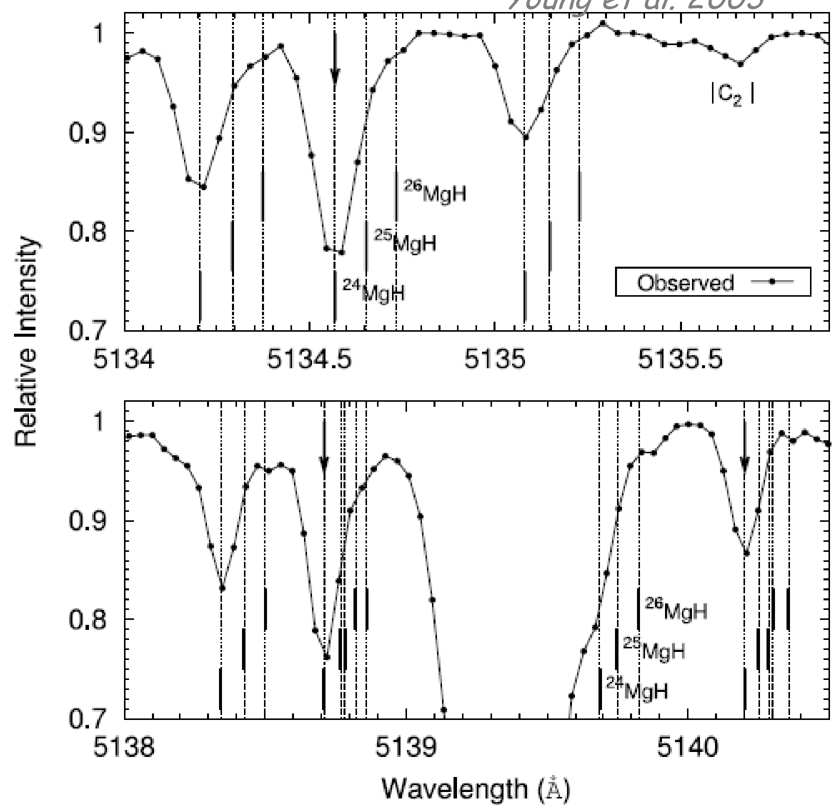

FIG. 3.—Spectrum of G 17-25 from 5134 to 5136 Å (*top*) and from 5138 to 5140.5 Å (*bottom*). The positions of the ^{24}MgH, ^{25}MgH, and ^{26}MgH lines are shown. The lines used in the isotopic analysis to derive the ratios are marked by arrows.

Current-State-of-the-Art Example: C Isotopes

- ☆ Optimize Spectral Resolution in Observations
  - ☞ Very Large Telescope (VLT), UVEchelle Spectrograph (UVES)

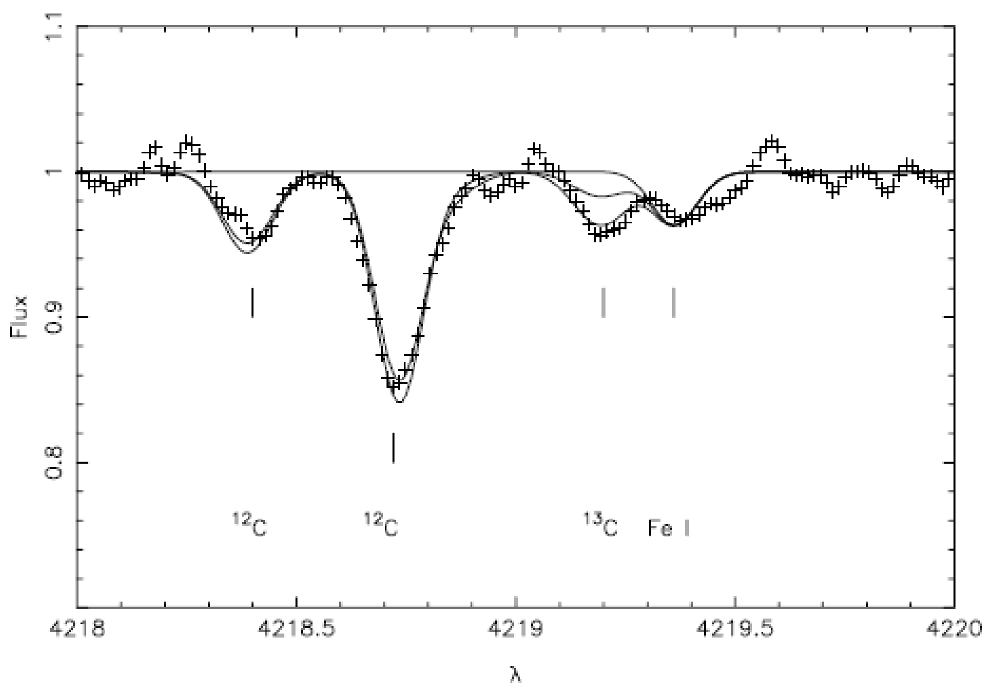

Fig. 3. Comparison of the observed spectrum (crosses) and synthetic profiles (thin lines) for $A^2\Delta - X^2\Pi$ ^{12}CH and ^{13}CH lines computed for $^{12}C/^{13}C = 4$ and 10, and with no ^{13}C.

Impact of Atomic-Level Transitions

- ☆ Hyperfine-Structure Transitions or Isotopic Shifts Become Significant for Lanthanides
- ☆ Often Not (Yet) Measured in Laboratory

- ☆ Abundance Errors from Inadequate HFS Inclusion up to Factor 5

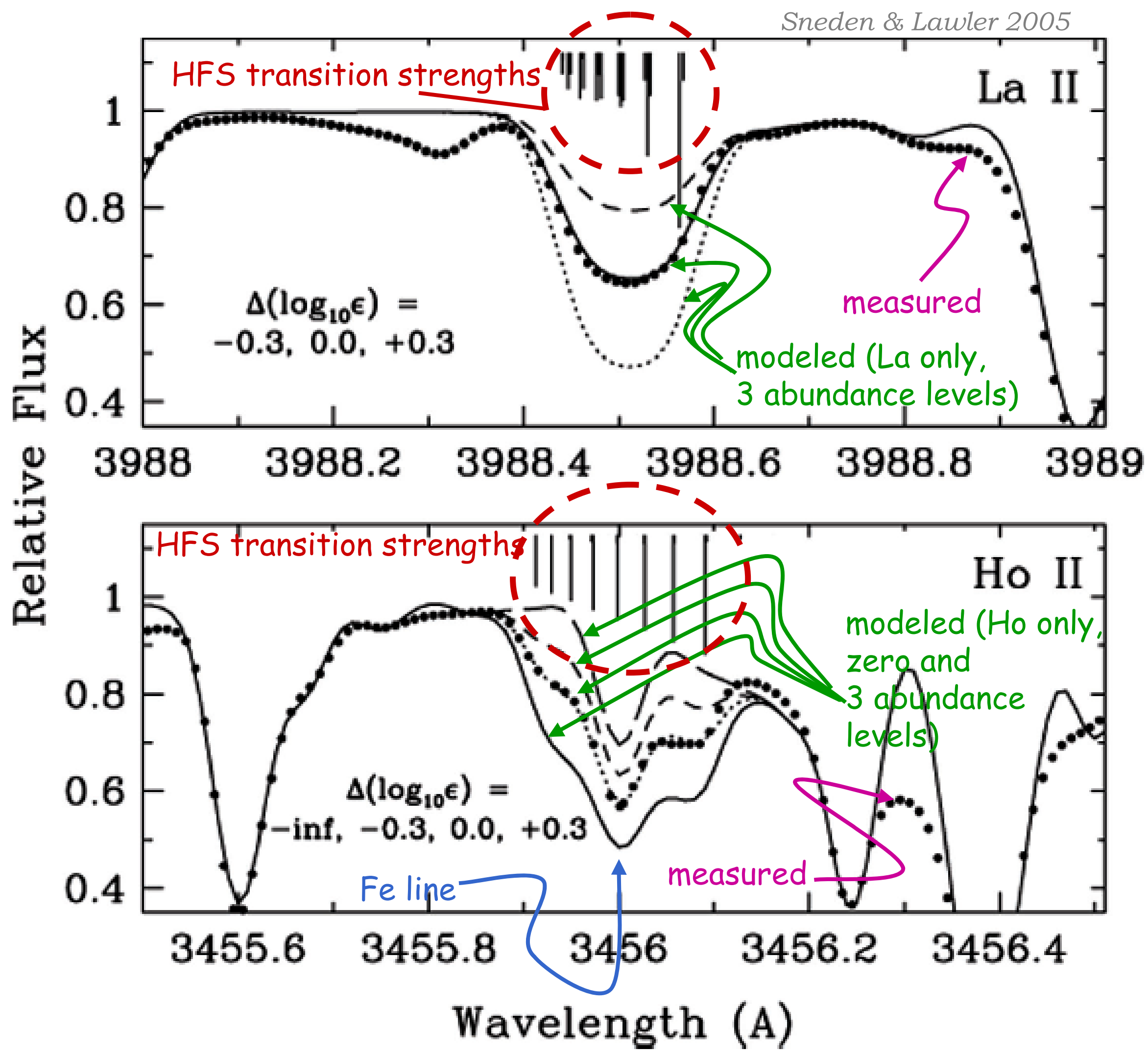

... more spectroscopy measurement methods...

- ☆ background-lit interstellar gas

- ☆ gas emission in different states

Abundances in Diffuse ISM

Diffuse Interstellar Medium:

- ☆ Observe Absorption Lines of Background Star Spectra (A_V<2)
- ☆ Characteristic Densities: 1 cm^{-3} < n_H < 1000 cm^{-3}, Characteristic Temperatures: 50K < T < 150K

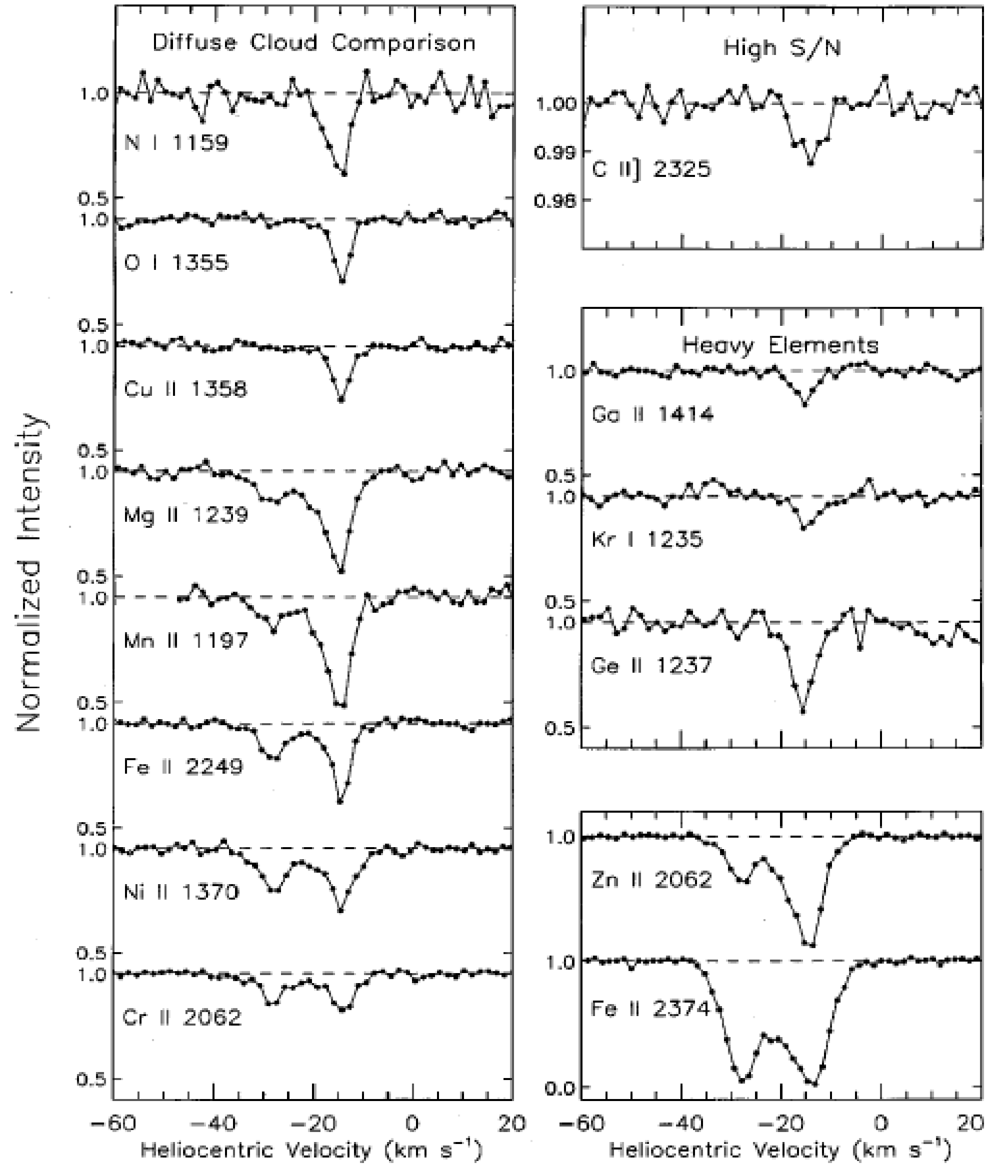

Figure 3 Continuum normalized profiles for selected interstellar lines in the direction of ζ Oph.

Abundances in Interstellar Gas

- Differences to Stellar Photospheric Abundances:
  - ☆ Selective Condensation of Elements onto Dust Grains
  - ☆ Formation of Specific Molecules

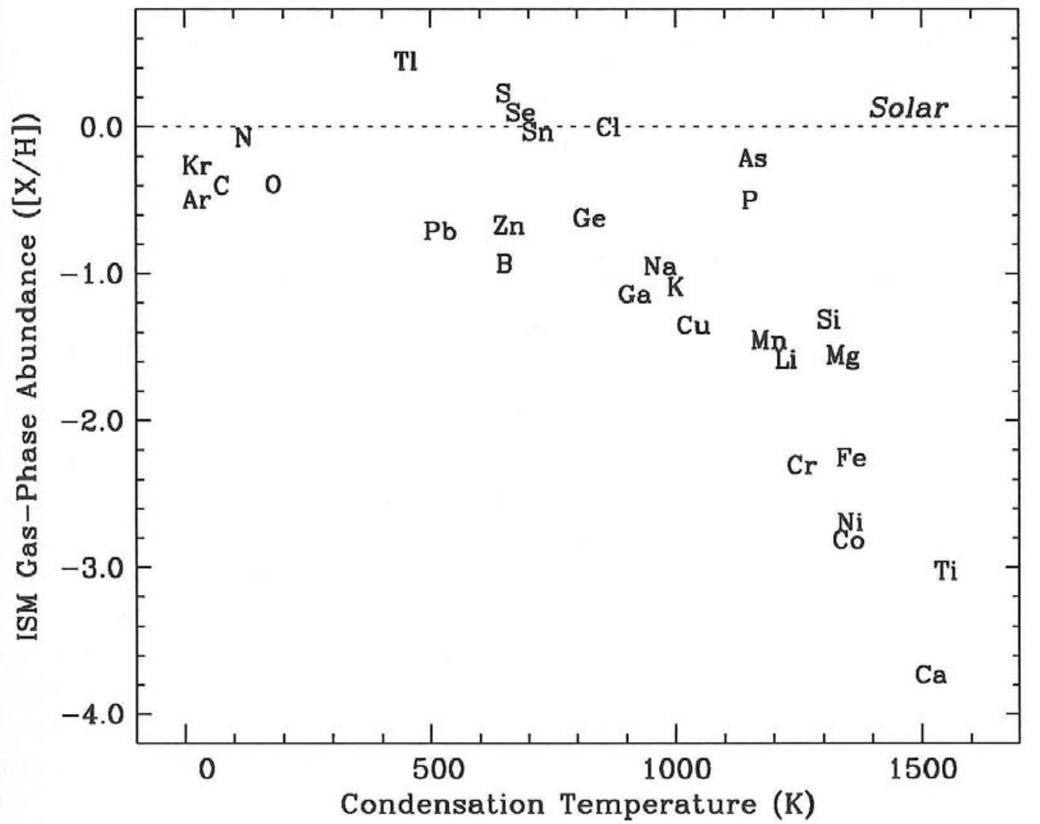

Fig. 1. Interstellar gas-phase abundances toward the star ζ Oph as a function of the elemental condensation temperature (Savage and Sembach 1996). These abundances are expressed in logarithmic form relative to those of the solar system.

Quasar Absorption Line Spectroscopy

- ☆ Quasar:
  - ☞ Bright, Distant Light Source
  - ☞ Emission Line Spectrum
- ☆ Less-Distant Gas Clouds & Galaxies:
  - ☞ Absorption Lines
  - ☞ Lower Redshift
  - ☞ Absorption Line Pattern (shifted)
    - » "Ly α forest"
    - – DLA: $N_H > 10^{20} cm^{-3}$
  - ☞
    - » Extract Absorption-Line Pattern Attributed to Specific/One Galaxy/Cloud
    - » Evaluate Relative Abundances

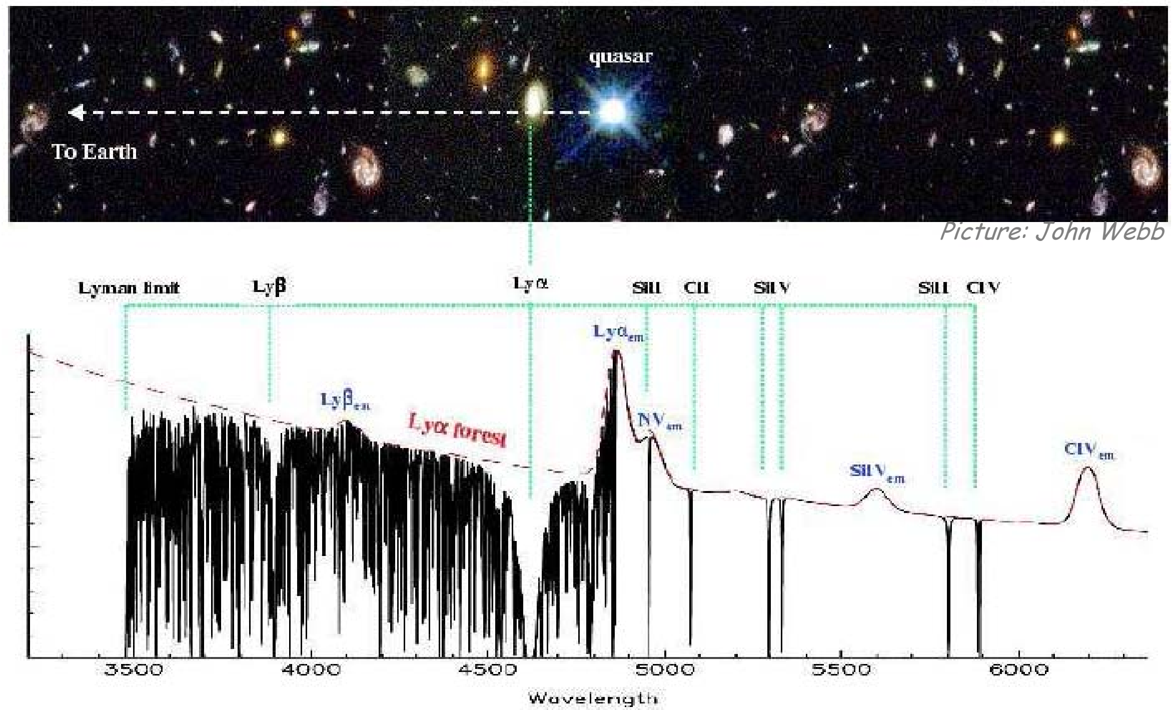

Picture: John Webb

Redshift	Lookback Time (Gyr)	Lookback time (t/t_∞)
0	0	0
0.5	5.4	0.37
1	8.3	0.57
2	11.0	0.76
3	12.2	0.84
4	12.9	0.89
5	13.3	0.92
6	13.5	0.93
10	14.0	0.97
∞	14.5	1.00

Absorption from Atomic Nuclei: a Perspective?

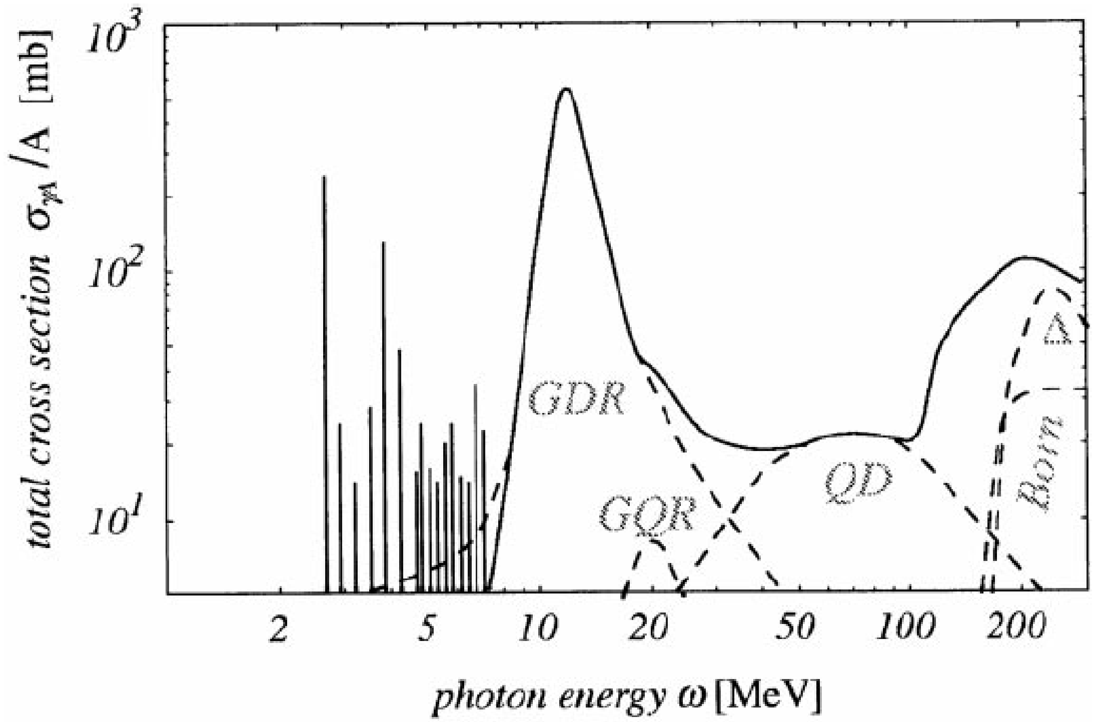

- ☆ We See Effects of **(with increasing energy)**:
  - ☞ Excitation of Single Nucleons in Nucleus Potential ("Nuclear Lines")
    - $h\nu = E_{nucl}$
  - ☞ Collective Excitations of Nucleon Groups ("Pygmi/Giant Resonances")
    - giant resonances: protons versus neutrons
    - quasi-deuteron resonances: a pair of proton and neutron
    - each of these occur in all multipole orders
  - ☞ Excitations of Single Nucleons ("Delta Resonance")
  - ☞ ...-> Hadron/Quark Phase Transitions

Emission Line from Neutral Gas: H Abundance!

- ☆ Nomenclature: "HI"
- ☆ E.M.Radiation from H Transition = Hyperfine-Structure (e^- spin ↑↓ ↔ ↑↑)
  - ☞ Line at 1420.4 MHz = 21.1 cm

$$\tau_{collision} << \tau_{transition}$$

  - ☞ Thermal Population

$$\frac{h\nu}{k_B} = 7 \cdot 10^{-2} K << T_{gas} \rightarrow \frac{N_2}{N_1} = 3$$

» known level populations

$$I = \frac{3}{16\pi} A h \nu_0 \int N_H dl$$

  - ☞ I -> Measurement of Total Column Density

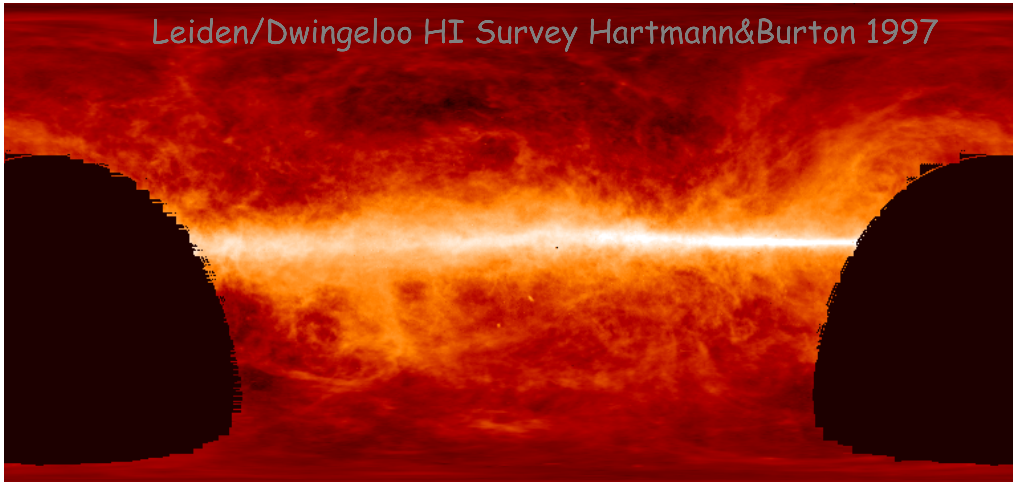

Molecular-Gas Line Emission:
Dense (star-forming) Clouds

- ☆ Radiation from
  - ☞ Electronic Transitions ~2 eV optical
  - ☞ Vibrational Transitions ~0.2 eV NIR
  - ☞ Rotational Transitions 10^{-16} eV Radio
- ☆ Optical Depth $\tau_{radio} << \tau_{optical}$ (from dust absorption)
  - ☞ Mostly Radio Measurements

$$\nu = \frac{j\hbar}{2\pi\mu r_0^2}$$

» e.g.: CO m=6.859 amu, r_o=1.128 10^{-8} cm ,

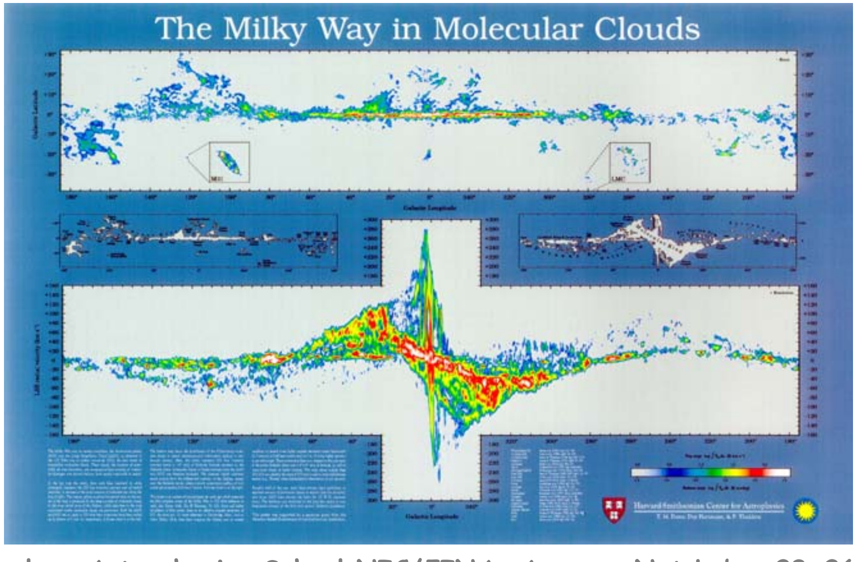

rotational transitions =>

j=1->j=0:	115 GHz	2.61 mm
	230	1.3
	345	0.87

equidistant levels

Recombination Lines from Ionized Gas

- ☆ Recombination Transitions
  - » e.g. Balmer Series Ha 656.3 nm n=1
    Hb 466.1 nm n=2
    or $H_{Br\gamma}$ 2.1 μm
- ☆ Ionization of Gas by Central Source (HII Regions, Planetary Nebulae)
- ☆ Ionization/Recombination Dynamic Balance: (<-conservation of atoms)

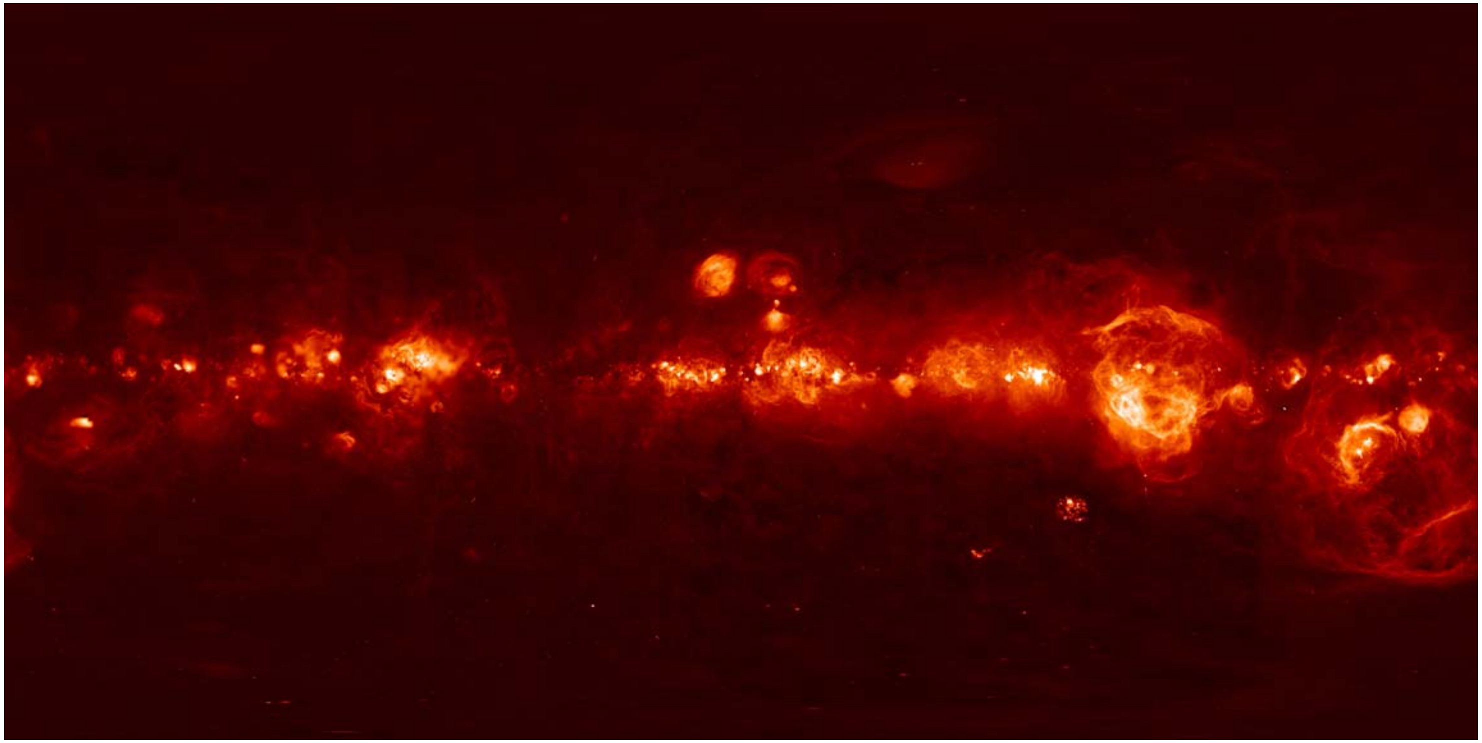

X-Ray Spectroscopic Images of Cas A

- Recombination Lines of Highly-Ionized Species

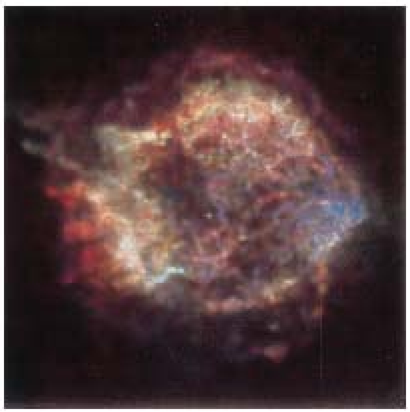

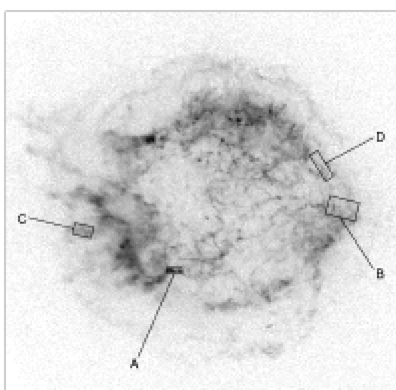

FIG. 2.—Broadband unsmoothed *Chandra* X-ray image of Cas A using a square-root intensity scaling. The spectral extraction regions in our study are indicated.

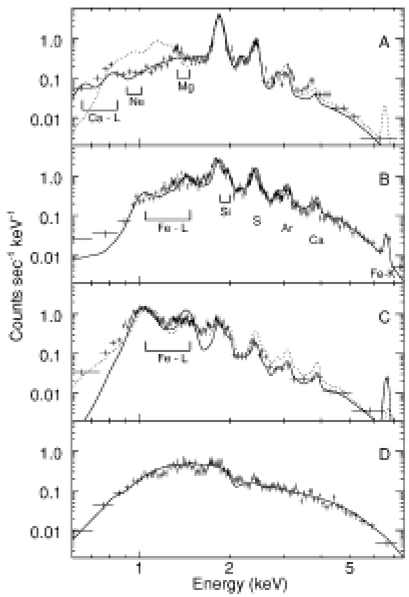

FIG. 3.—Energy spectra from several regions in Cas A as indicated in Fig. 2. The horizontal error bars show the widths of the energy bins, and the vertical ones indicate the statistical error on the measured event rate; systematic errors are not included. Superposed on the data points are smooth curves of simulated *Chandra* ACIS-S spectra. The simulations for regions A, B, and C are of a shock-heated plasma with NEI fractions absorbed by line-of-sight interstellar material. The dotted curves in regions A and C and the solid curve in region B assume abundances corresponding to explosive incomplete Si burning. A considerably better match for region A uses O-burning abundances (*solid curve*). The solid curve for region C is more Fe-rich; i.e., the Si, S, Ar, and Ca abundances are reduced by factors of 5 or more from their values in incomplete Si burning. The solid curves for regions A, B, and C have temperatures of 2.5, 2.5, and 2.8 keV, ionization timescales of 2.5 × 10[illegible], 7.0 × 10[illegible], and 7.0 × 10[illegible] cm⁻³ s, and column densities of 0.9 × 10[illegible], 2.3 × 10[illegible], and 1.5 × 10[illegible] atoms cm⁻², respectively. All the models for regions A, B, and C also include significant amounts of continuum emission from material with a lower atomic number. The solid curve for region D is an absorbed power-law model with a photon index of 2.6 and a column density of 1.3 × 10[illegible] atoms cm⁻².

- X-Ray Lines in Fe, Si, S, Ar, Ca Show Clumps with Large Enrichments
  => Ejecta(?)
- Fe Line Emission Features Outside Si,S,Ar,Ca Line Features
  => Mixing / Turbulence During Explosion(?)

->Hughes et al., ApJ 528, 2000;
Hwang et al., ApJ 537, 2000

- *Issues: ...NEI? (i.e., $T_e=T_{ion}$?)*

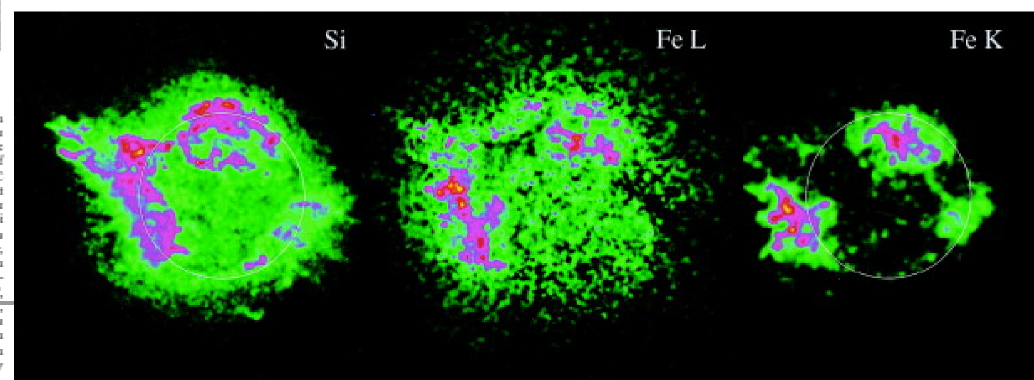

What did we Learn?

How Do Nucleosynthetis Sources Enrich the Galaxy with Heavy Elements?

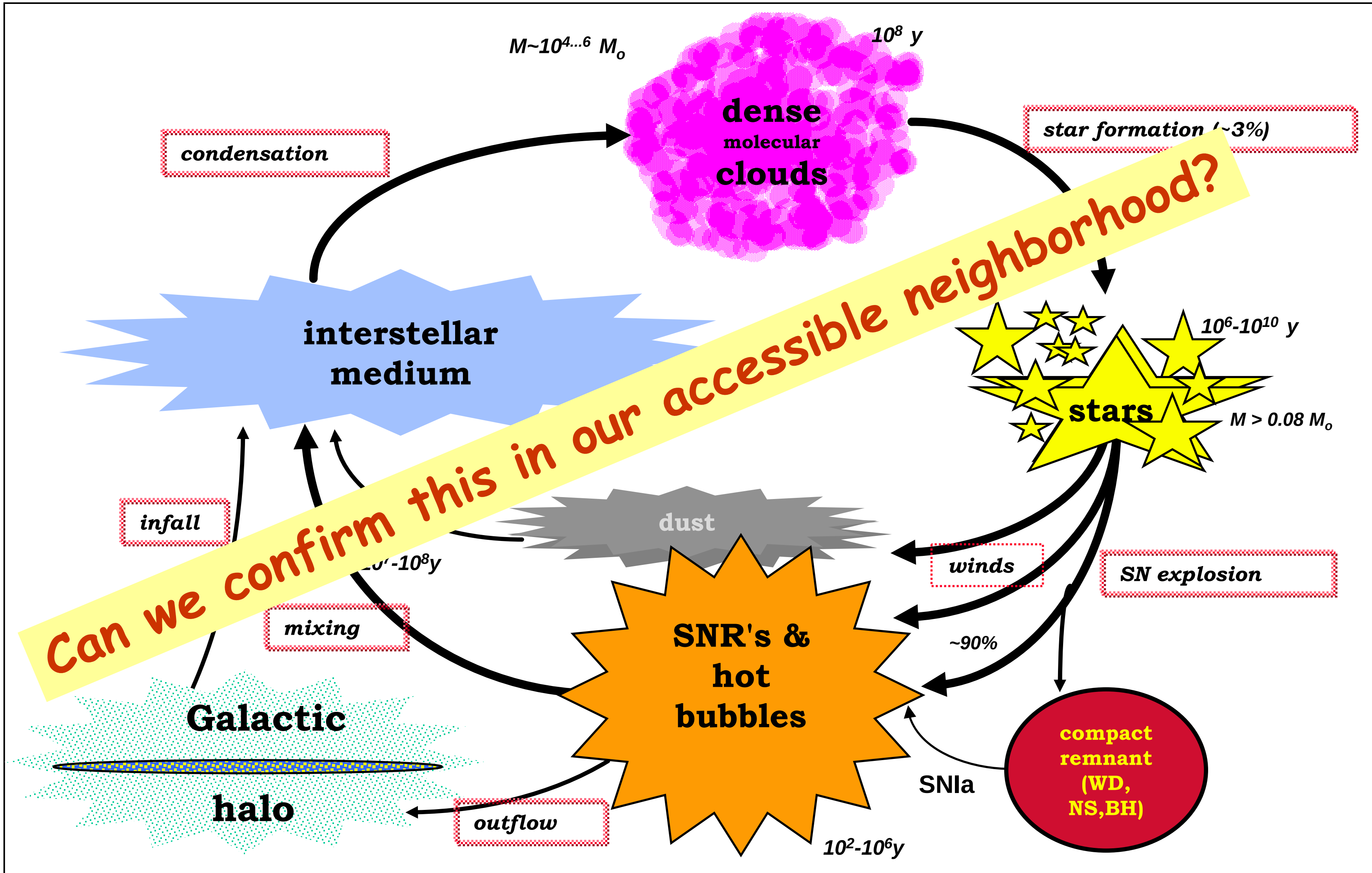

☆ Cosmic Chemical Evolution , Intertwined with Galaxy Evolution!

Abundance Evolution in the Solar Neighborhood

- ☆ Determination of Fe Abundances for Stars of Different Ages
  - ☞ Select Sufficiently-old Stars (F,G)
  - ☞ Determine Stellar Parameters:
    - Intrinsic Brightness (from Distance, interstellar Reddening, and Brightness)
    - Effective Temperature (from IR Flux)
    - Age (from HRD and M_v,T_{eff}; or from Chromospheric Activity)
    - Metallicity (from Absorption Lines, or Colors through Strömgren Photometry)

- ☆ Results:
  - ☞ ...
  - ☞ Substantial Abundance Evolution of Galactic Disk
  - ☞ Star Formation Rate History ~ok
  - ☞ Nucleosynthesis = Massive Stars and SNIa
  - ☞ ...

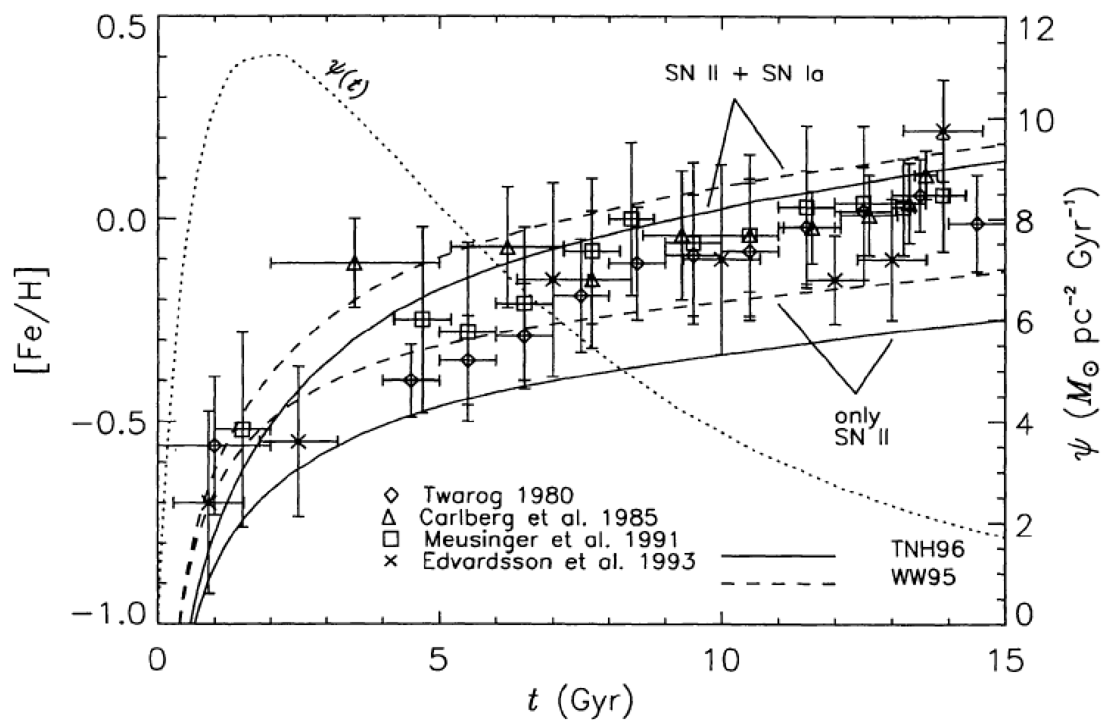

Abundance Evolution in Solar Neighborhood

- ☆ Birthrate of Stars per 'Metallicity'
- ☆ Models for Chemical Evolution, using:
  - ☞ Stellar Birth Rate Model (Schmidt-Law)
  - ☞ Stellar Metal-Yield Models
  - ☞ Chemical Mixing Models (incl. Infall)

Parameter	Observational constraint
Stellar yields	Element abundances of the Sun
IMF slope x	Solar abundance ratios
Close binary fraction A	Relative frequency of Type II and Ia SNe
	AMR
Star formation efficiency ν	current fraction of gaseous mass
Schmidt exponent k	ADF
Accretion time-scale τ_{disc}	current infall rate
	ADF

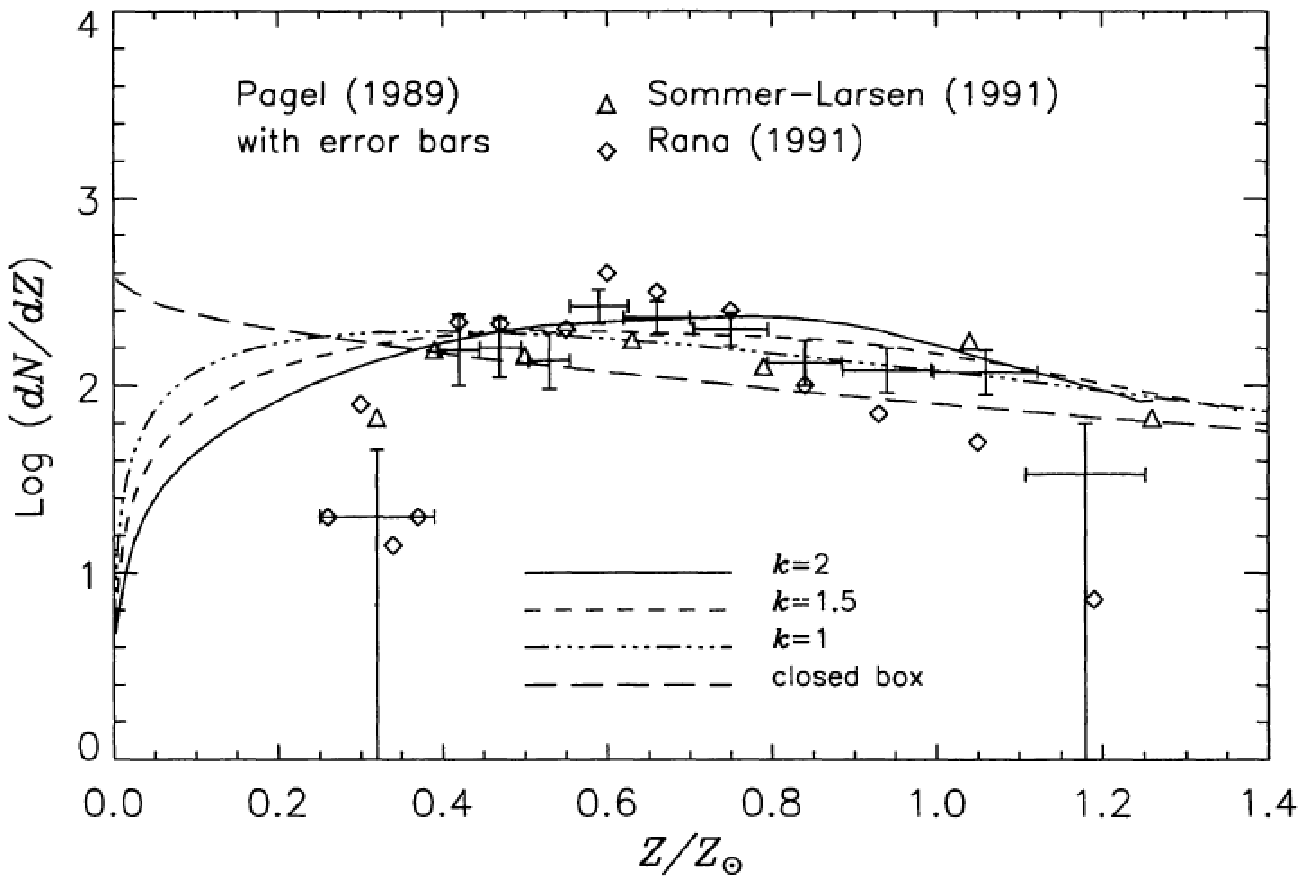

- ☆ Results:
  - ☞ ...
  - ☞ Closed-Box Models are Inadequate
  - ☞ ...

Age~Metallicity: Sample Biases?

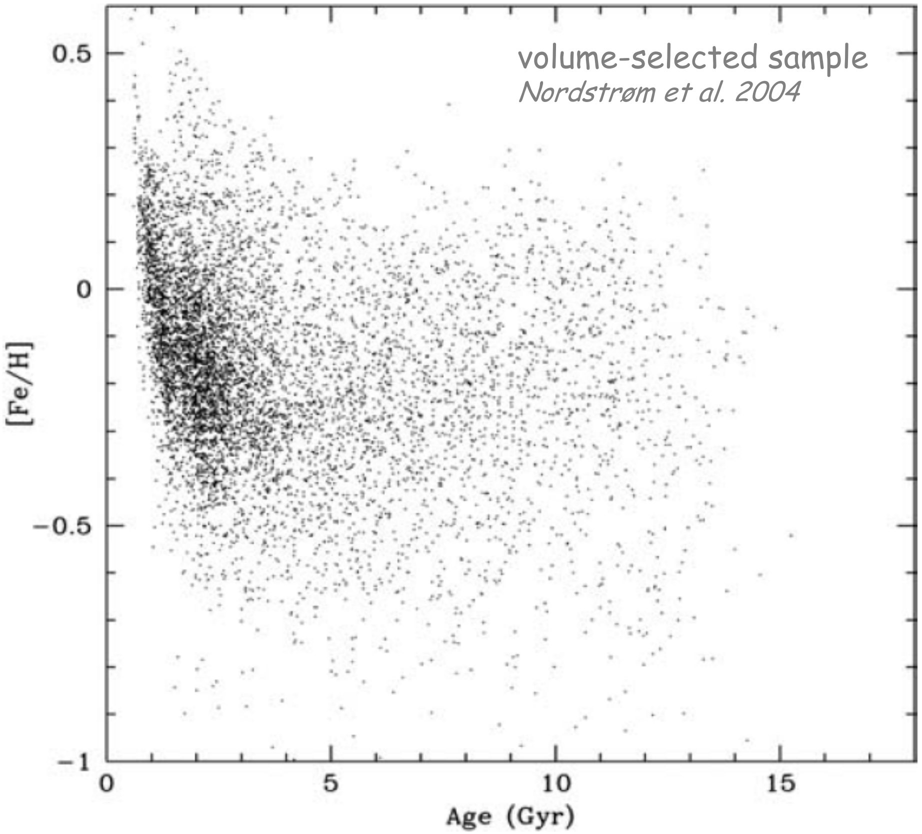

Fig. 27. Age–metallicity diagram for 7566 single stars with "well-defined" ages in the magnitude-limited sample. Note that individual age errors may still exceed 50% (cf. Fig. 16).

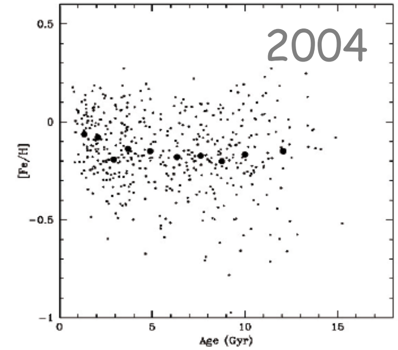

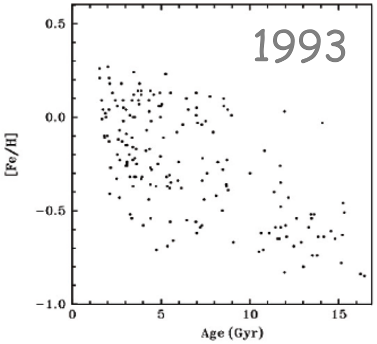

- ☆ Solar-Neighborhood Stars are a Mixture of Ages and Metallicities
  - ☞ Different Origins (Galaxy Encounters, ...)
  - ☞ Different Enrichments of Star-Forming Sites
- ☆ There is NO Simple Age/Metalicity Relation
  - ☞ Earlier Samples of Stars were Selected to Equally Expose the Galactic range of Metalicities *(Edvardsson et al. '93)*

Understanding the Abundances in Our Galaxy

(10^{11} Stars…)

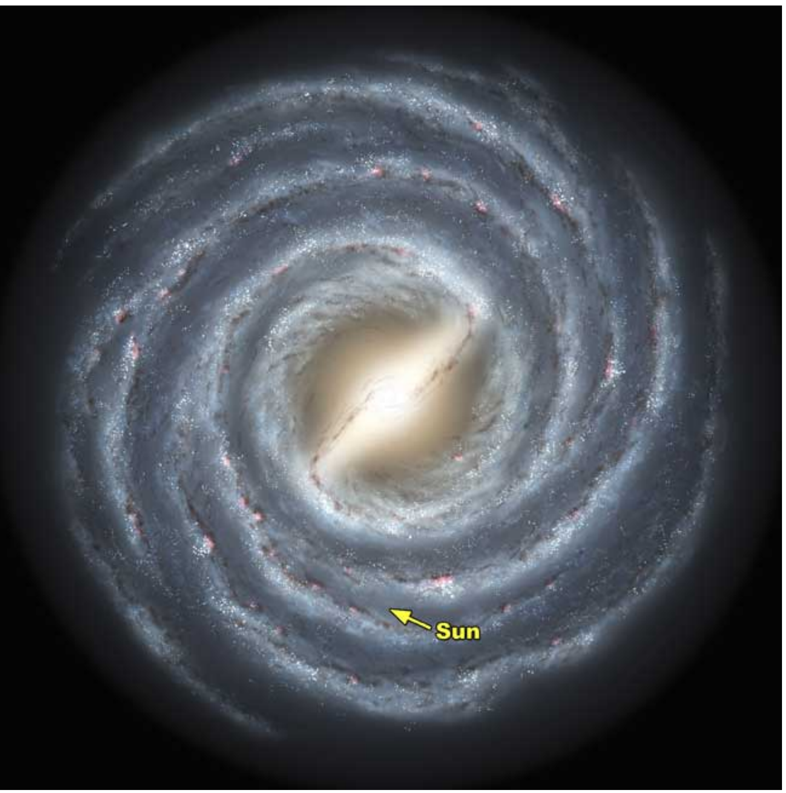

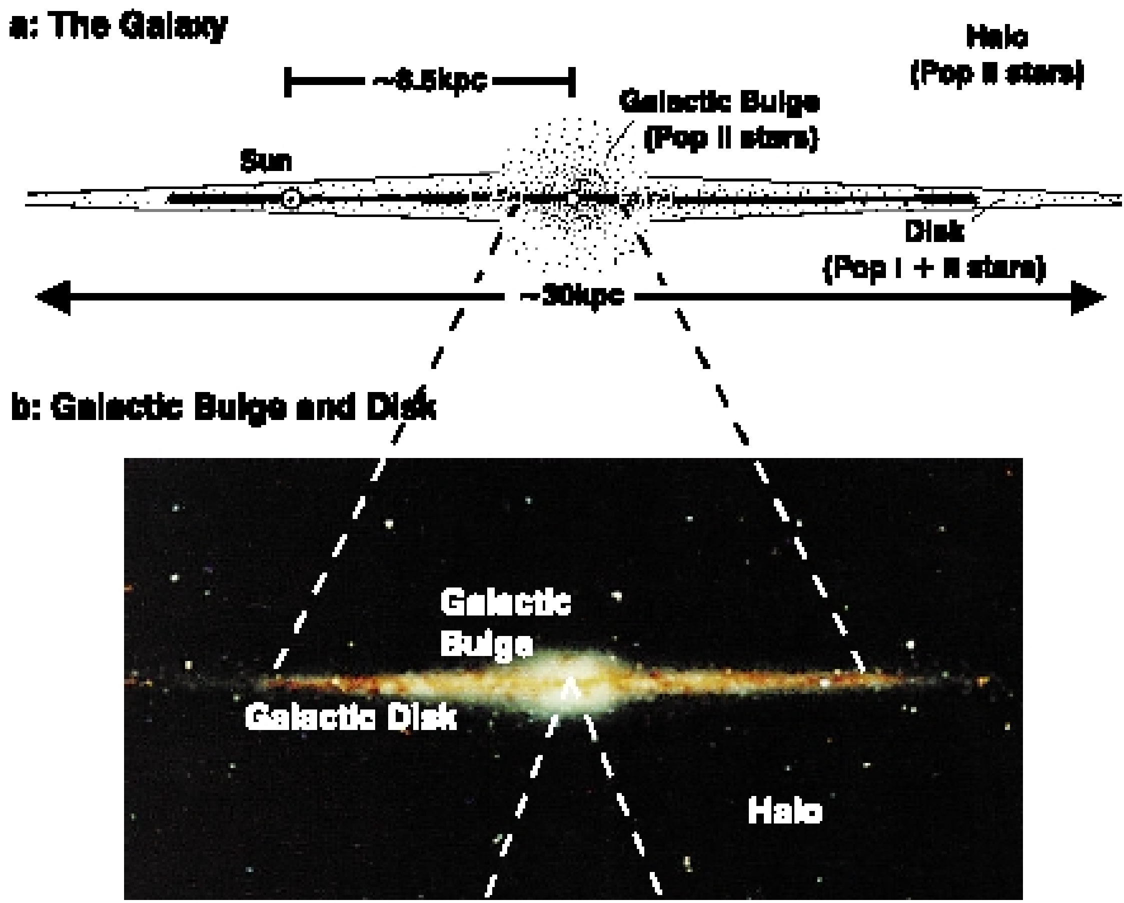

Spatio-temporal Evolution of the Galaxy

☆ Radial Gradients Provide a Key Diagnostic of Evolution

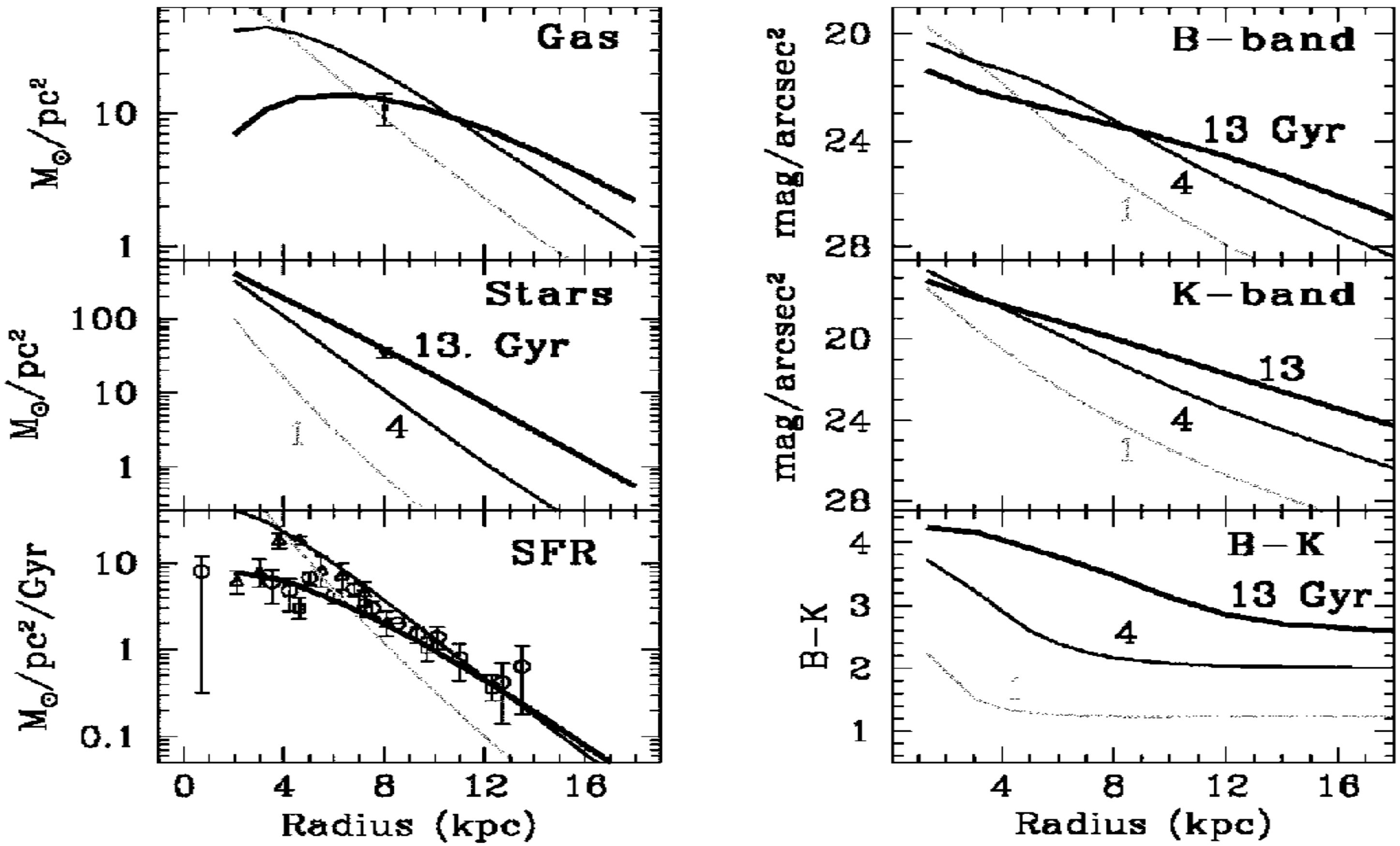

☞ *Prantzos & Boissier 1999, 2003*

Figure 1. Chemical (*left*) and photometric (*right*) evolution of the Milky Way disk, according to the model of Boissier and Prantzos (1999). In all panels the solid curves correspond to model results at galactic ages of 1, 4 and 13 Gyr, respectively; the latter (*heavy curves*) are compared to observations of the present day disk (in the left panels: *shaded* regions for the gaseous and stellar profiles and *data points* for the Star Formation Rate). The model leads naturally to different scalelengths for the B-band (4 kpc) and the K-band (2.6 kpc), in agreement with observations.

Chemical Evolution of the Galaxy

- Modeling Abundance Evolutions
  - ☆ Star Formation History
  - ☆ Source Yields
  - ☆ Mixing and Infall
  - ☞ Works for Some Elements, not for Others...

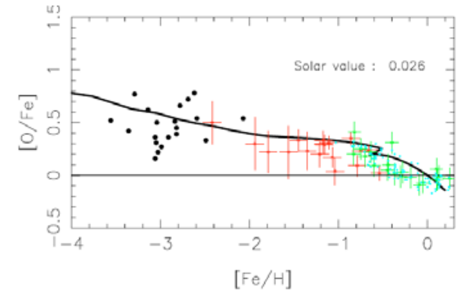

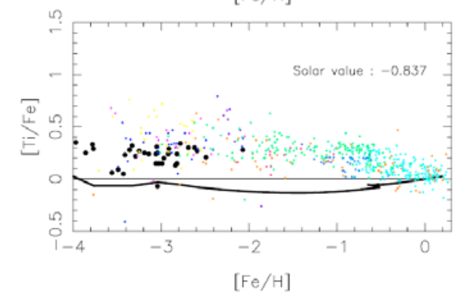

- Modeling Standard Abundances
  - ☆ (same ingredients)
  - ☞ Agreement is Good, ~Factor 2

- There are Missing Pieces...
  - ☞ Nuclear Reactions?
  - ☞ Stellar & SN Models?
  - ☞ Matter Cycling / ISM Flows?

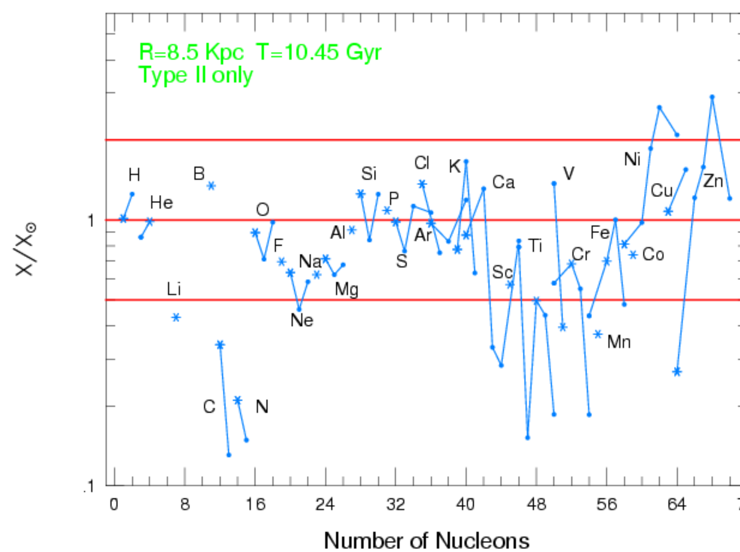

Roland Diehl

Abundances within the Galaxy: Inside-Out

Observations->

- ☆ Metallicity Reduces with Galactocentric Distance
- ☆ The Sun Appears Enriched wrt. its Environment

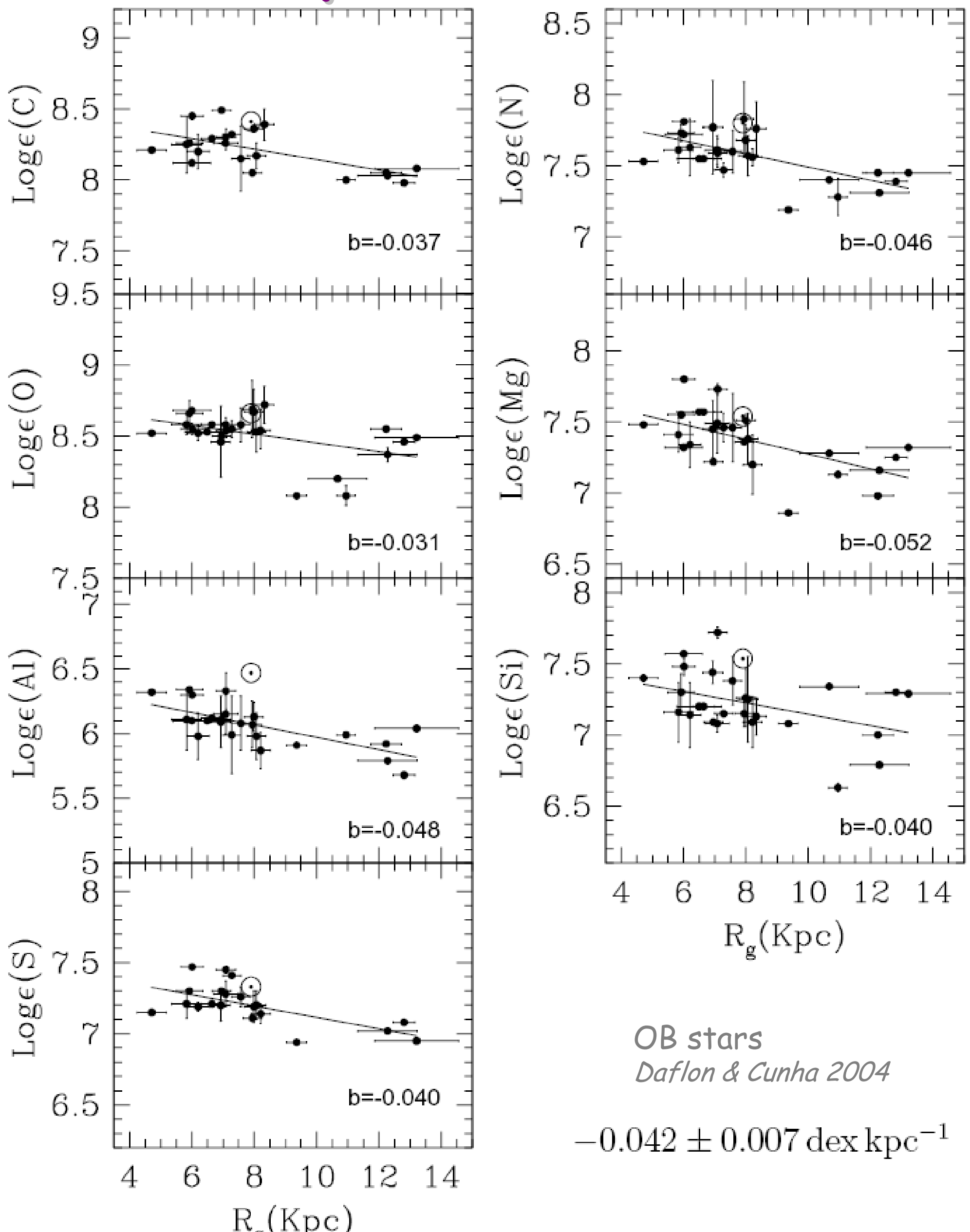

OB stars
Daflon & Cunha 2004

$-0.042 \pm 0.007\,\mathrm{dex\,kpc^{-1}}$

Chemical Evolution Model for the Galaxy

- "Two-Infall Model", *Chiappini, Matteucci, Gratton 1997, 2001*
- ☆ Treat Gas-to-Star Formation, Evolution, Yields & Recycling
- ☆ Two Major Episodes of Material Infall
  - Early, Short: τ~0.7 Gy -> halo and thick disk are formed
  - Later, Extended: τ~7 Gy for solar vicinity-> thin disk is formed, inside-out
  - Infall: Functional Model of galactocentric radius and time:

$$A(r,t) = a(r)e^{-t/\tau_H} + b(r)e^{(t-t_{max})/\tau_D(r)}$$

    - » using t_{max}=1 Gy as time of maximum thin-disk infall, and for the thin-disk formation time scale:

$$\tau_D = 1.033r(\text{kpc}) - 1.267\,\text{Gyr}.$$

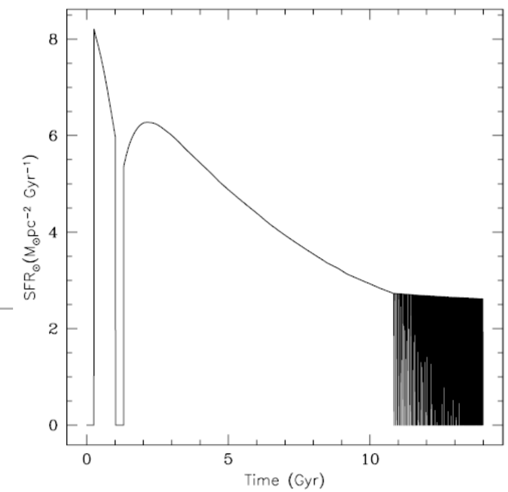

- ☆ Characteristics
  - Halo and thin disk are formed independently
  - Star Formation Ceases Below a Threshold Density of 7 $M_\odot$ pc^{-2}
  - Material Recycling Approximated
  - Instantaneous Mixing Assumed

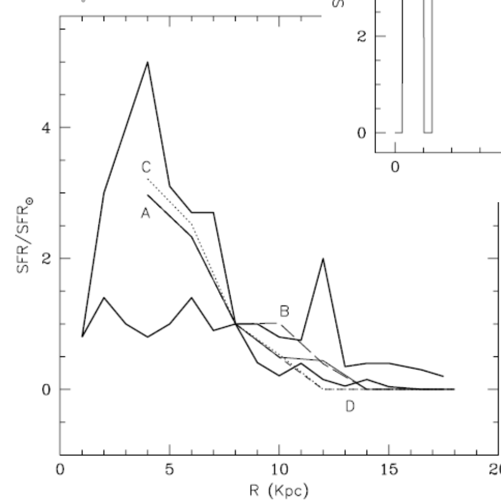

- ☆ Obtain
  - spatio-temporal gas, stars, abundances

Inverting the Argument:

What the Galaxy Tells Us About Yields

- ☆ Fitting GCE-Model Predictions to Observation-Inferred Abundance Histories
  - assuming Star-Formation and Infall Histories and IMF are Fixed by Various Constraints (e.g. star & gas distributions, spatial abundance gradients)

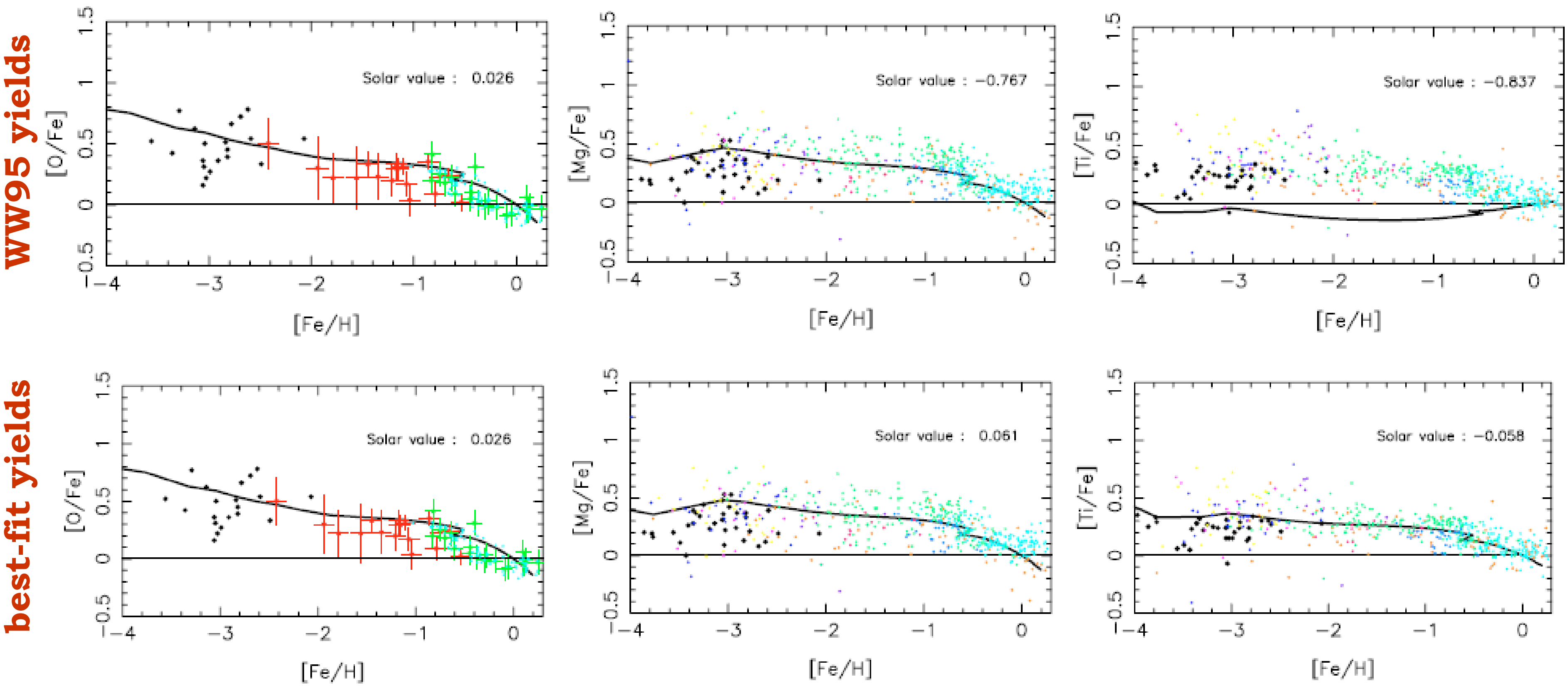

Yield Consistency Check

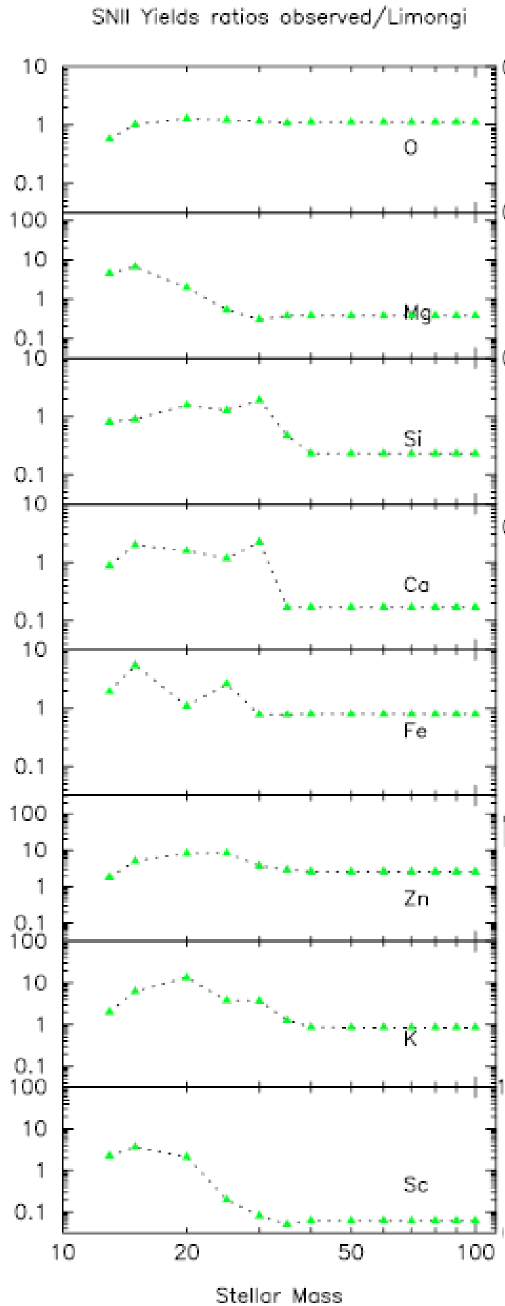

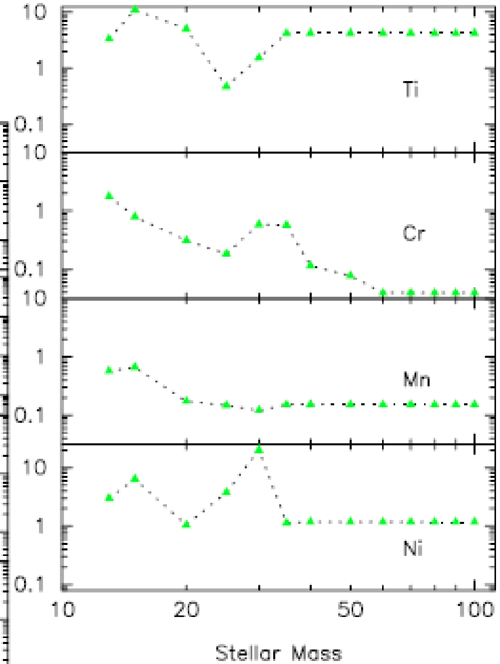

- ☞ Ref.: Limongi & Chieffi 2003
- ☆ Same as WW95: most ~ok
  - ☞ Massive Stars & cc-SNe ~ok
- ☆ Corrections Suggested for SNIa Yields

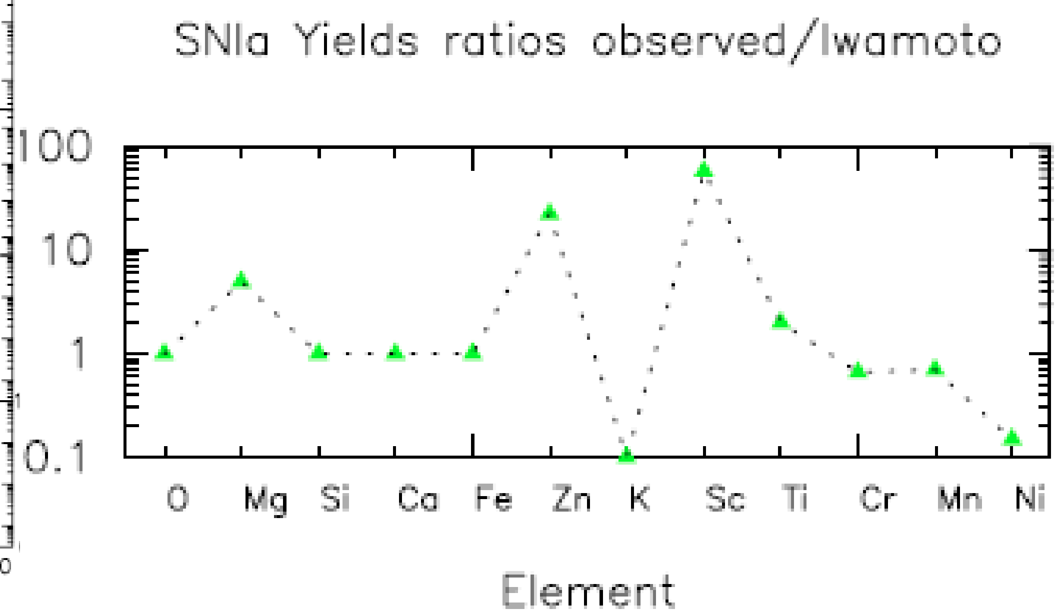

Separating Galactic Stellar Populations (I)

- Combine Kinematic with Metallicity Signatures
  - ☆ Characterize the General Sample Properties
    - ☞ Spatial Distribution

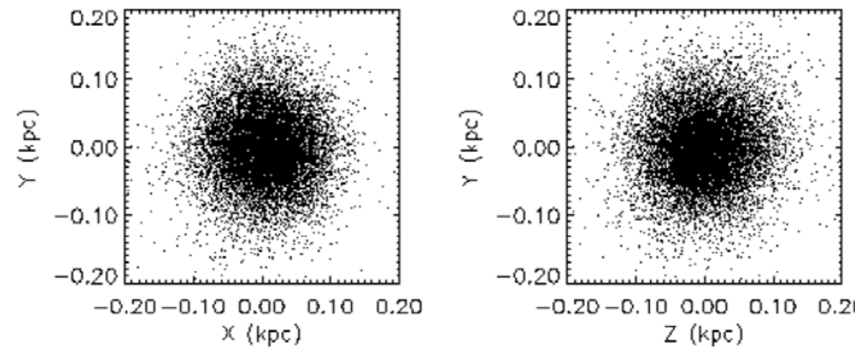

    - ☞ Distribution in Velocity Space

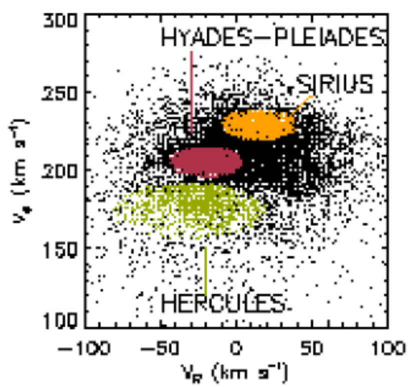

    - ☞ Distribution in Metallicities

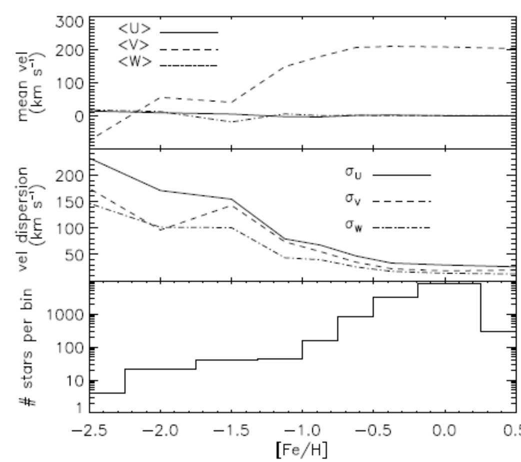

Figure 3. Mean velocity components and dispersion as function of metallicity [Fe/H] for the stars in the N04 sample. The bottom panel shows that there are only a handful of objects in the most metal-poor bins, which makes less reliable the characterization of the velocity ellipsoid.

Metal-Poor Stars

Stars with Unusually-low Metal Enrichments

- ☆ Access to:
  - ☞ **First Stars in Universe/Galaxy**
  - ☞ **Primordial Abundances (Li)**
  - ☞ **Supernova-II Abundances**

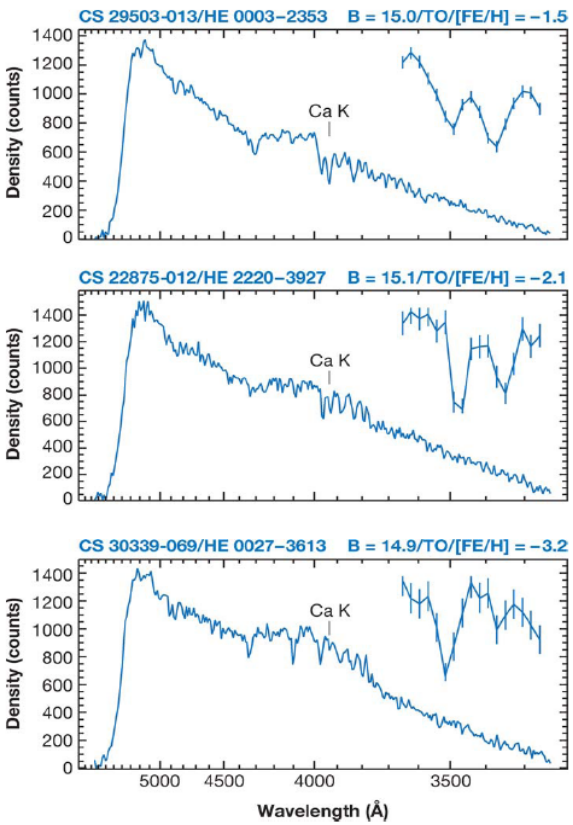

TABLE 1 Nomenclature for stars of different metallicity

[Fe/H]	Term	Acronym
$> +0.5$	Super metal-rich	SMR
~ 0.0	Solar	—
< -1.0	Metal-poor	MP
< -2.0	Very metal-poor	VMP
< -3.0	Extremely metal-poor	EMP
< -4.0	Ultra metal-poor	UMP
< -5.0	Hyper metal-poor	HMP
< -6.0	Mega metal-poor	MMP

TABLE 2 Definition of subclasses of metal-poor stars

Neutron-capture-rich stars	
r-I	$0.3 \leq$ [Eu/Fe] $\leq +1.0$ and [Ba/Eu] < 0
r-II	[Eu/Fe] $> +1.0$ and [Ba/Eu] < 0
s	[Ba/Fe] $> +1.0$ and [Ba/Eu] $> +0.5$
r/s	$0.0 <$ [Ba/Eu] $< +0.5$
Carbon-enhanced metal-poor stars	
CEMP	[C/Fe] $> +1.0$
CEMP-r	[C/Fe] $> +1.0$ and [Eu/Fe] $> +1.0$
CEMP-s	[C/Fe] $> +1.0$, [Ba/Fe] $> +1.0$, and [Ba/Eu] $> +0.5$
CEMP-r/s	[C/Fe] $> +1.0$ and $0.0 <$ [Ba/Eu] $< +0.5$
CEMP-no	[C/Fe] $> +1.0$ and [Ba/Fe] < 0

Finding Metal-Poor Stars

- ☆ Surveys and Follow-Ups
  - ☞ Surveys Identify Stars with Weak Lines from Clearly-Visible Metals (Ca)
  - ☞ Follow-Up High-Res Spectroscopy Determines Metal Content

Beers & Christlieb 2005

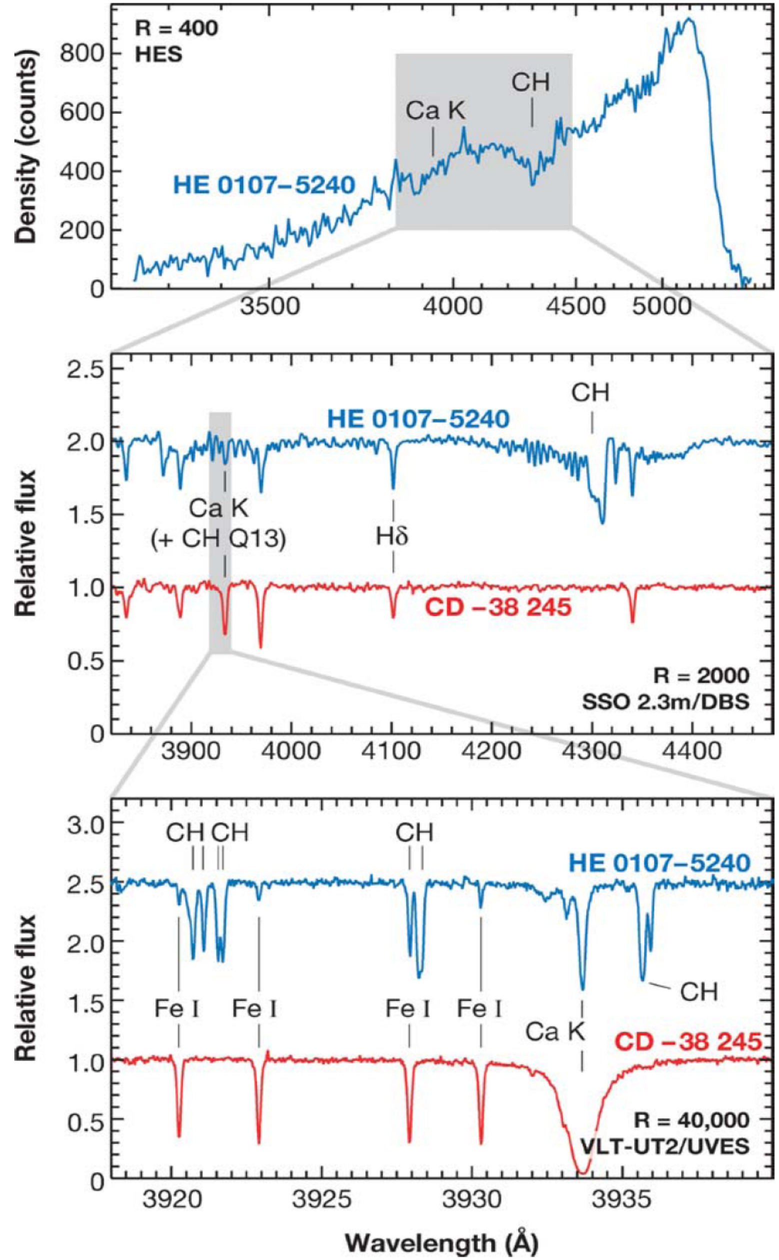

Figure 1 The three major observational steps toward obtaining elemental abundances of metal-poor stars: (*a*) Wide-angle surveys (e.g., objective-prism surveys) yield candidate metal-poor stars; (*b*) vetting of the candidates by moderate-resolution follow-up spectroscopy; and (*c*) high-resolution spectroscopy of confirmed metal-poor candidates. The star shown in this example, HE 0107−5240, is one of the most iron-poor stars yet discovered. The strengths of its absorption lines are compared with the formerly most iron-poor giant known, CD −38° 245. The spectra shown in the *lower two panels* have been divided by the continuum. The resolving power, $R = \lambda/\Delta\lambda$, of the spectra is indicated along the right-hand side of each panel. Prominent atomic and molecular species are labeled.

Elemental Abundance Pattern in Halo Stars

☆ Metal-Poor Halo Stars ([Fe]/[H]~-3!) Show Same Elemental Patterns as Solar System!

☞ Is This A Unique Physical Process (Primary)? Do Old Stars Sample Single r-Process Events?

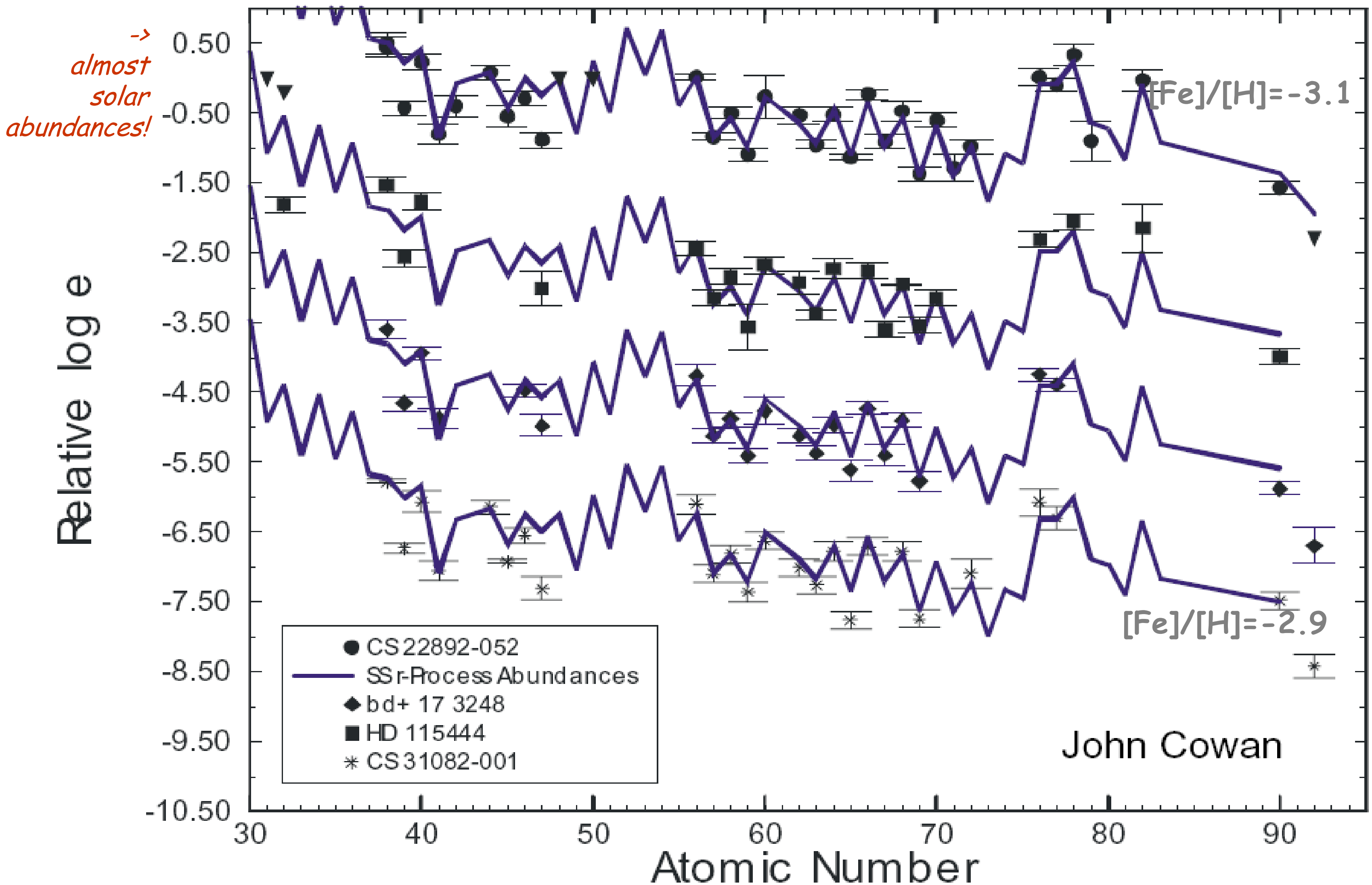

Reminder: The r-Process

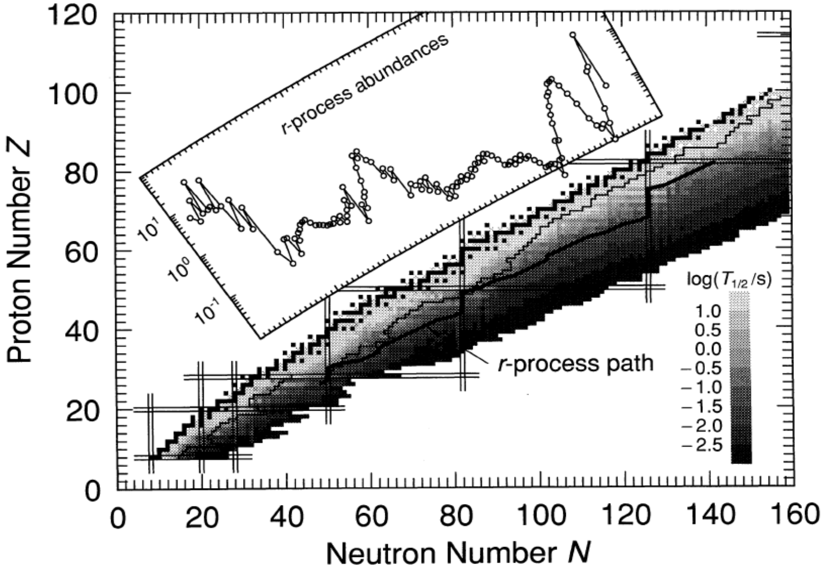

$\dot{Y}(Z, A) =$ *n captures, photodisintegration, and β decays =*

$$n_n Y(Z, A-1)\sigma_{A-1} + Y(Z, A+1)\lambda_{A+1}$$
$$- Y(Z, A)(n_n \sigma_A + \lambda_A + \lambda_\beta^A + \lambda_{\beta n}^A + \lambda_{\beta 2n}^A + \lambda_{\beta 3n}^A)$$
$$+ Y(Z-1, A)\lambda_\beta^{Z-1,A} + Y(Z-1, A+1)\lambda_{\beta n}^{Z-1,A+1}$$
$$+ Y(Z-1, A+2)\lambda_{\beta 2n}^{Z-1,A+2} + Y(Z-1, A+3)\lambda_{\beta 3n}^{Z-1,A+3}$$

"Detailed Balance" for (n,γ), (γ,n)
-> nuclear properties! (B_n)

$$\lambda_{A+1} = \left[\frac{2G(Z, A)}{G(Z, A+1)}\right]\left(\frac{A}{A+1}\right)^{3/2} \times \left(\frac{m_u kT}{2\pi\hbar^2}\right)^{3/2} \sigma_A \exp\left[\frac{-B_n(Z, A+1)}{kT}\right]$$

$$\frac{Y(Z, A+1)}{Y(Z, A)} = n_n \frac{G(Z, A+1)}{2G(Z, A)} \left(\frac{A+1}{A}\right)^{3/2} \times \left(\frac{2\pi\hbar^2}{m_u kT}\right)^{3/2} \exp\left[\frac{B_n(Z, A+1)}{kT}\right]$$

i.e., abundance pattern determined by:
neutron density, temperature, and nuclear masses

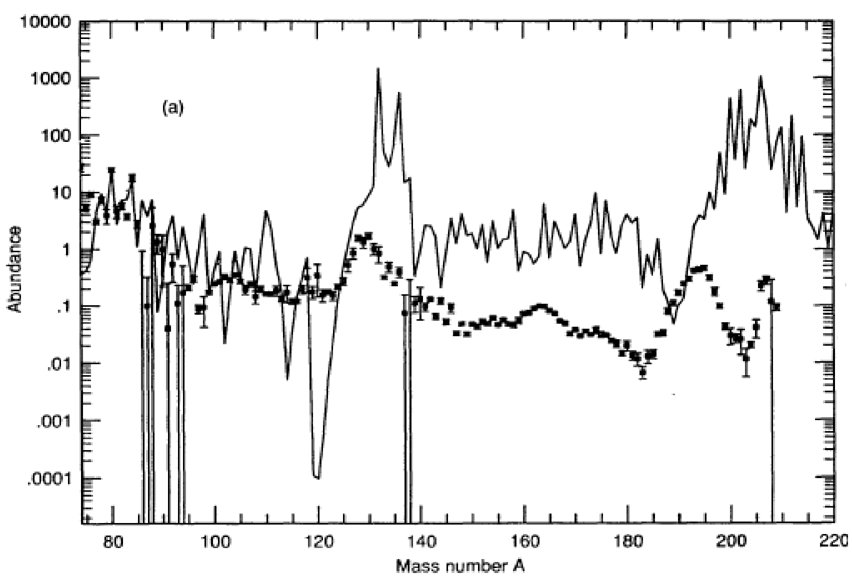

"Waiting Point" Approximation:

β Decay of n-richest Isotope limits Flow

Flow Continuity

->

r Process Pattern Completely Determined by:

- neutron density
- temperature
- nuclear masses
- seed nucleus abundance

(-> nuclear properties far from stability by astronomy?)

"Shell Quenching" and the r-Process

- r-Process Elemental Abundance Pattern is Sensitive to n Shell Closure Effects
  - Closed Shells = "Waiting Points" of r Process Path
  - Pronounced Shell Structure Would Make Shell Crossings More Difficult
  - Increased Abundances Around Closed Shells During r-Process
  - r-Process Reaction Flow Times Would Be Increased

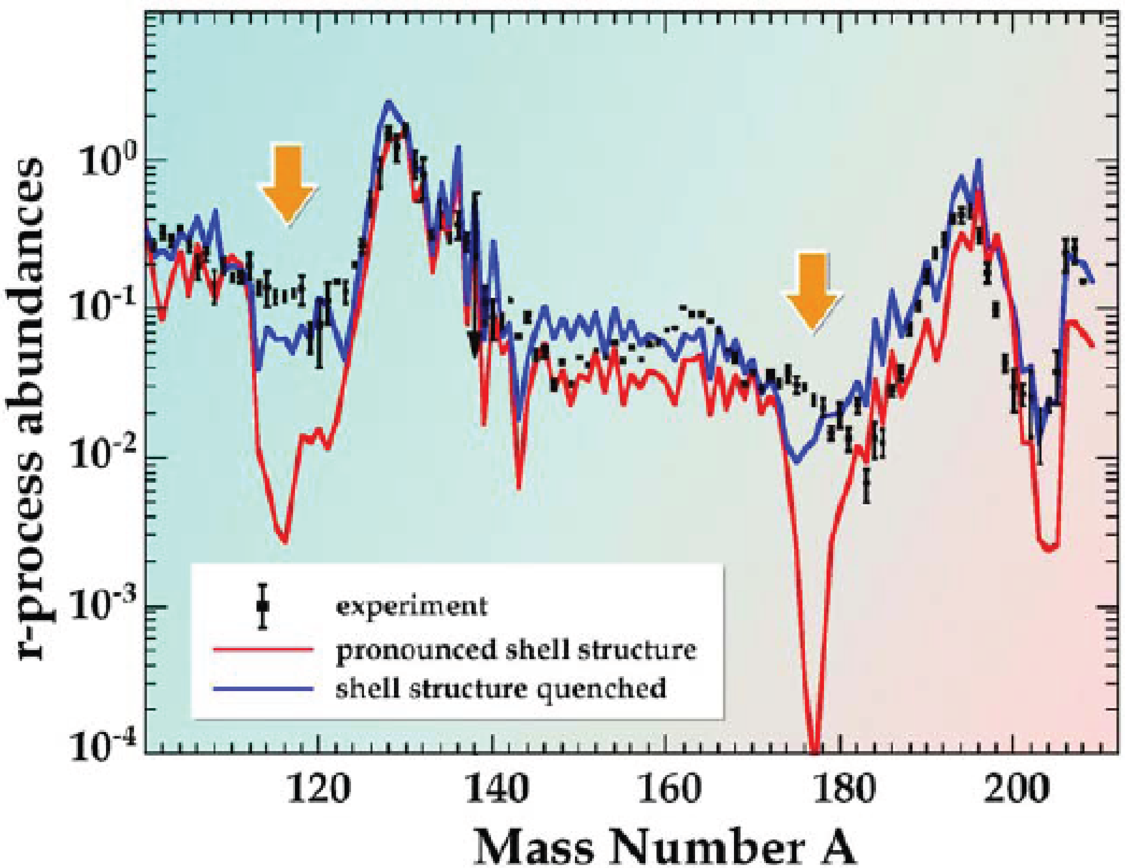

MPS Puzzles from Early Nucleosynthesis

- SNII Nucleosynthesis in the Early Galaxy: Yield Ratios ~SNII?
  - ☞ *...apart from the r-process pattern...*
- ☆ Metal Lines in Halo Stars
  - ☞ Now Down to Metallicities <5.4!
  - ☞ But: Surprises...

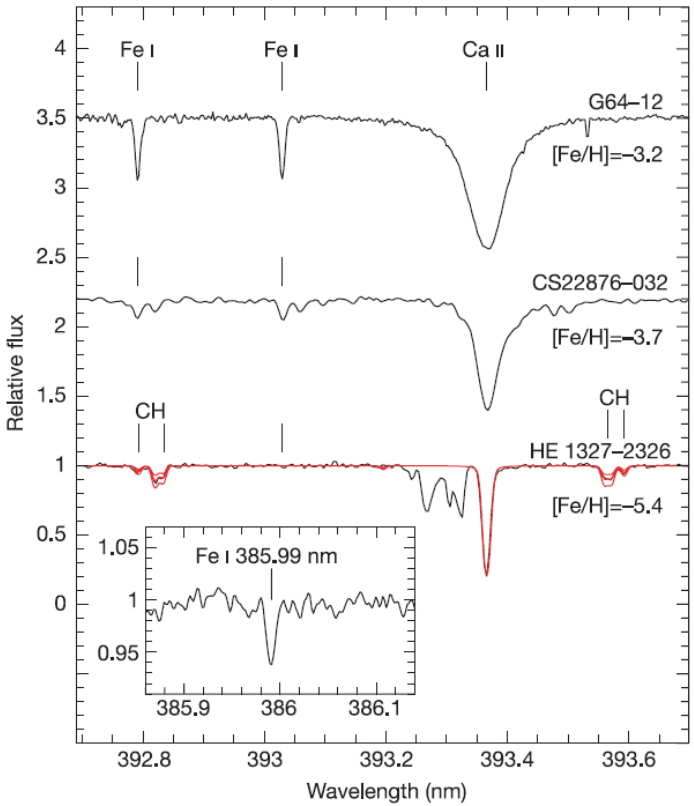

find surprisingly high CNO (CH lines!), while Ca..Ti are low

Unusual Early SNe, richer in CNO??

Frebel et al. 2005

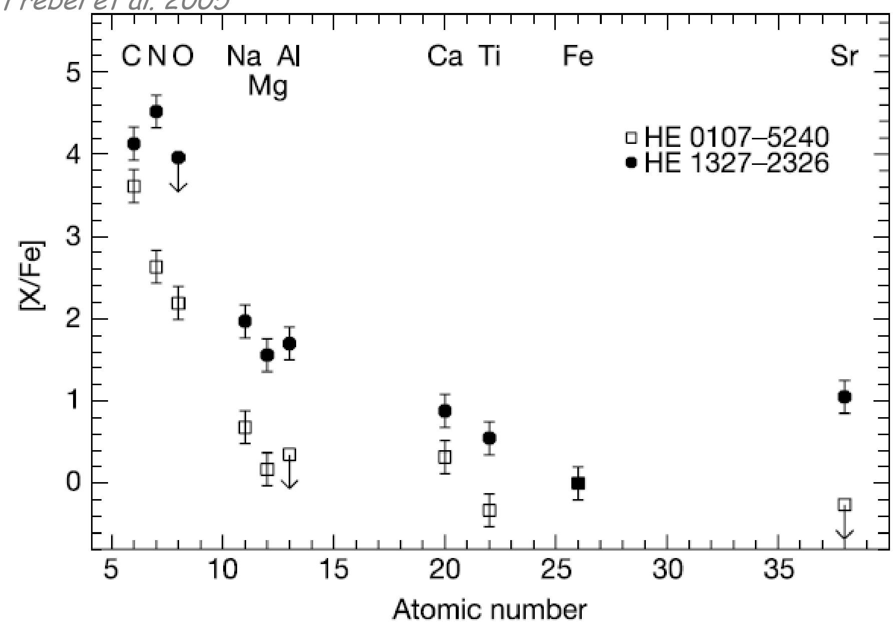

Metal-Poor Stars: Primary/Seconday Diagnostics

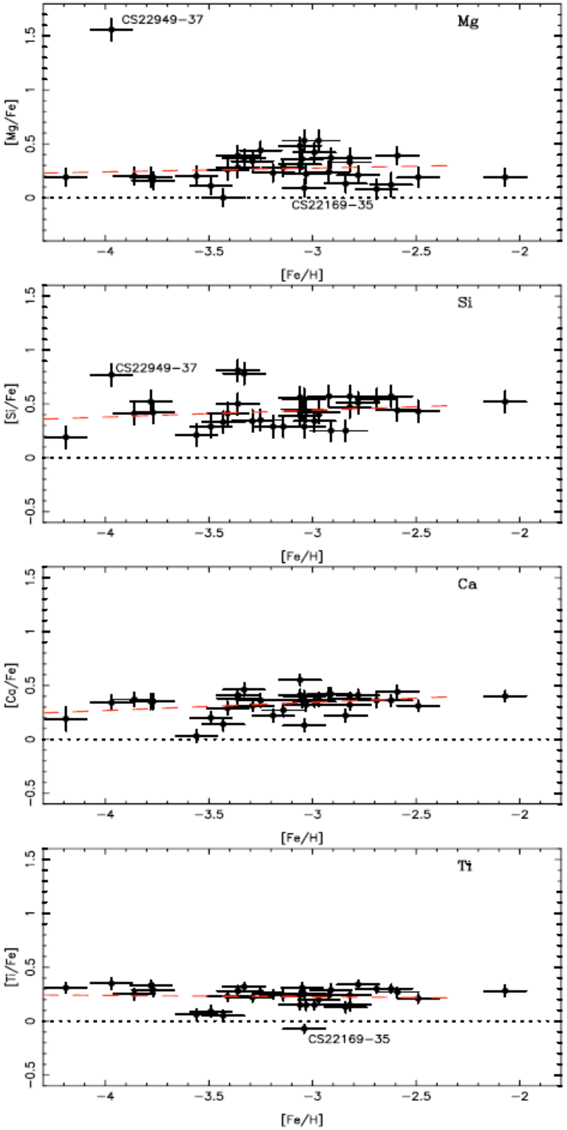

Fig. 7. [Mg/Fe], [Si/Fe], [Ca/Fe] and [Ti/Fe] plotted vs. [Fe/H]. The peculiar star CS 22949–037 is not included in the computations of the scatter and of the regression line (dashed) for Mg. The star CS 22169–035 is deficient in all the light "even" elements.

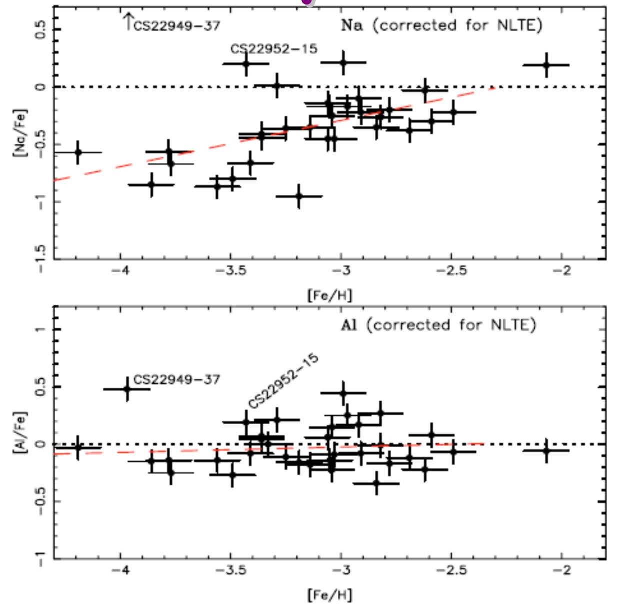

Fig. 8. [Na/Fe] and [Al/Fe] plotted vs. [Fe/H]. The LTE abundances of these elements have been determined from resonance lines, but corrections for NLTE effects have been applied.

☞ Na,Al are dominated by n-rich isotopes
-> expect 'secondary' behaviour
([X]~[n-rich matter])
-> only seen for Na, not for Al

Are We Seeing Individual Supernovae?

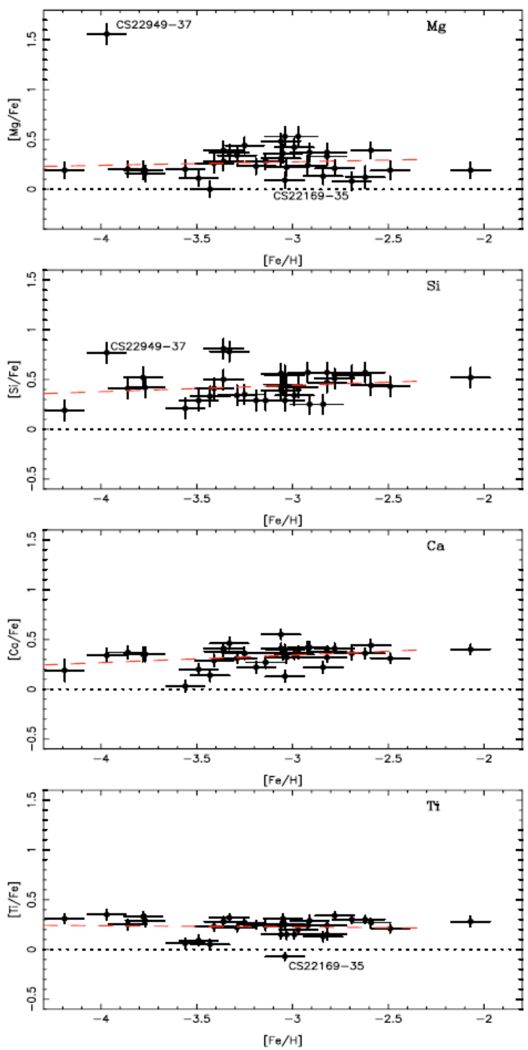

Fig. 7. [Mg/Fe], [Si/Fe], [Ca/Fe] and [Ti/Fe] plotted vs. [Fe/H]. The peculiar star CS 22949–037 is not included in the computations of the scatter and of the regression line (dashed) for Mg. The star CS 22169–035 is deficient in all the light "even" elements.

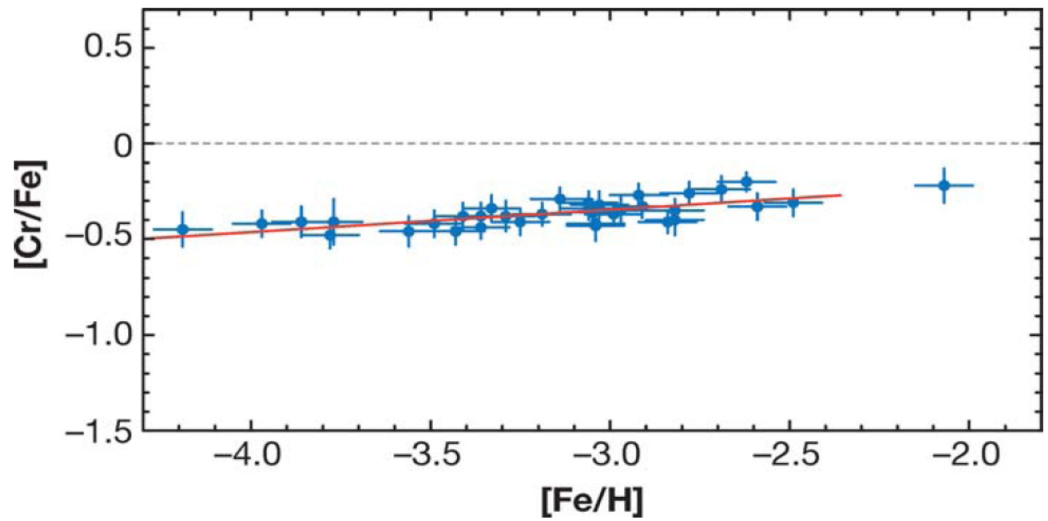

Figure 6 [Cr/Fe] as a function of [Fe/H] for 35 VMP giants from the HK survey observed with VLT/UVES (Cayrel et al. 2004). The error bars are one-sigma estimates. Note the extremely small scatter about the trend line.

- ☆ Typical SN Products Seem 'Primary'
- ☆ Absence of Scatter
  - ☞ Well-Mixed Multi-SN Composition (NOT Individual SNe)
- ☆ [Eu/Fe] Scatter Suggests the Opposite
  - ☞ r-process yields more variable?

Abundances from Metal-Poor Stars

☆ Applications/Lessons:

- ☞ Estimating the Age of the Galactic Disk
- ☞ Tracing the Chemical Evolution in the Early Galaxy
- ☞ Testing for Interstellar Mixing
- ☞ Identifying an Apparently Robust Nucleosynthesis Process from Individual Sources

Galaxy Interactions

- ☆ Suggested by
  - ☞"Infall" Component as Required by all Chemical-Evolution Descriptions
  - ☞Different Stellar Subgroups
  - ☞DM-Dominated Galaxy Evolution Simulations
  - ☞Galaxy Surveys

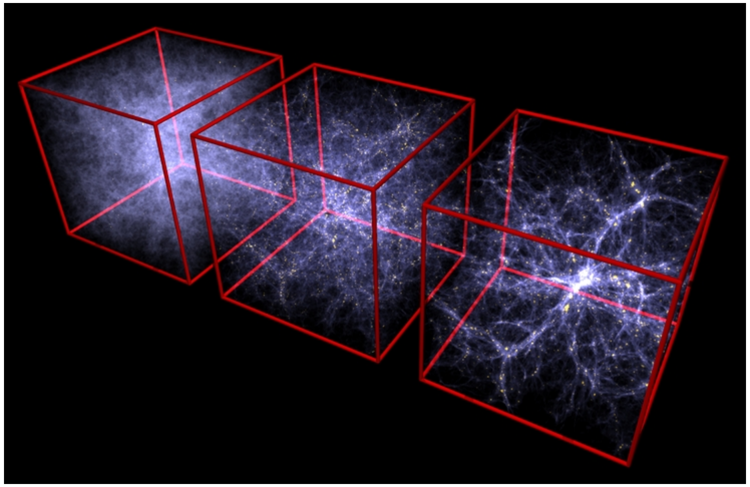

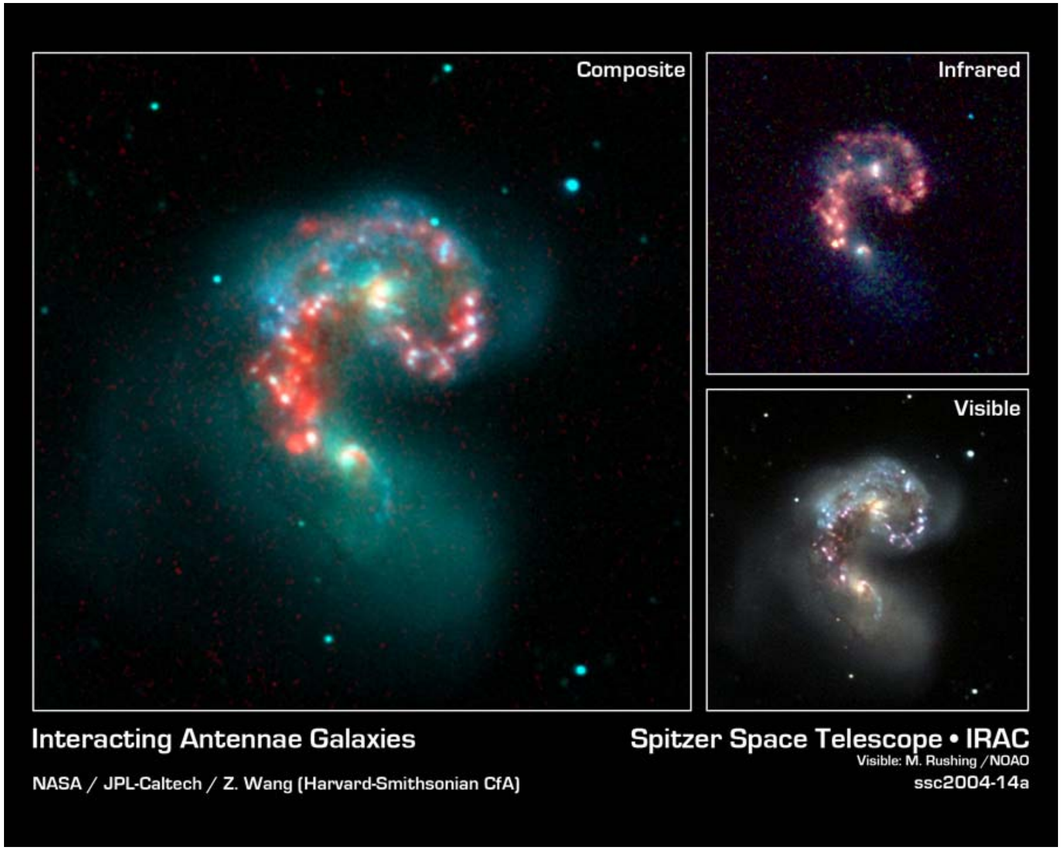

Lessons from Dwarf Galaxies?

☆ The Galaxy's Companions:

- ☞ Same Origin, Different/Separate Evolution?
- ☞ Dwarf Galaxies (& Globular Clusters in Halo)
  - » many clearly associated with major galaxies (MW, M31)

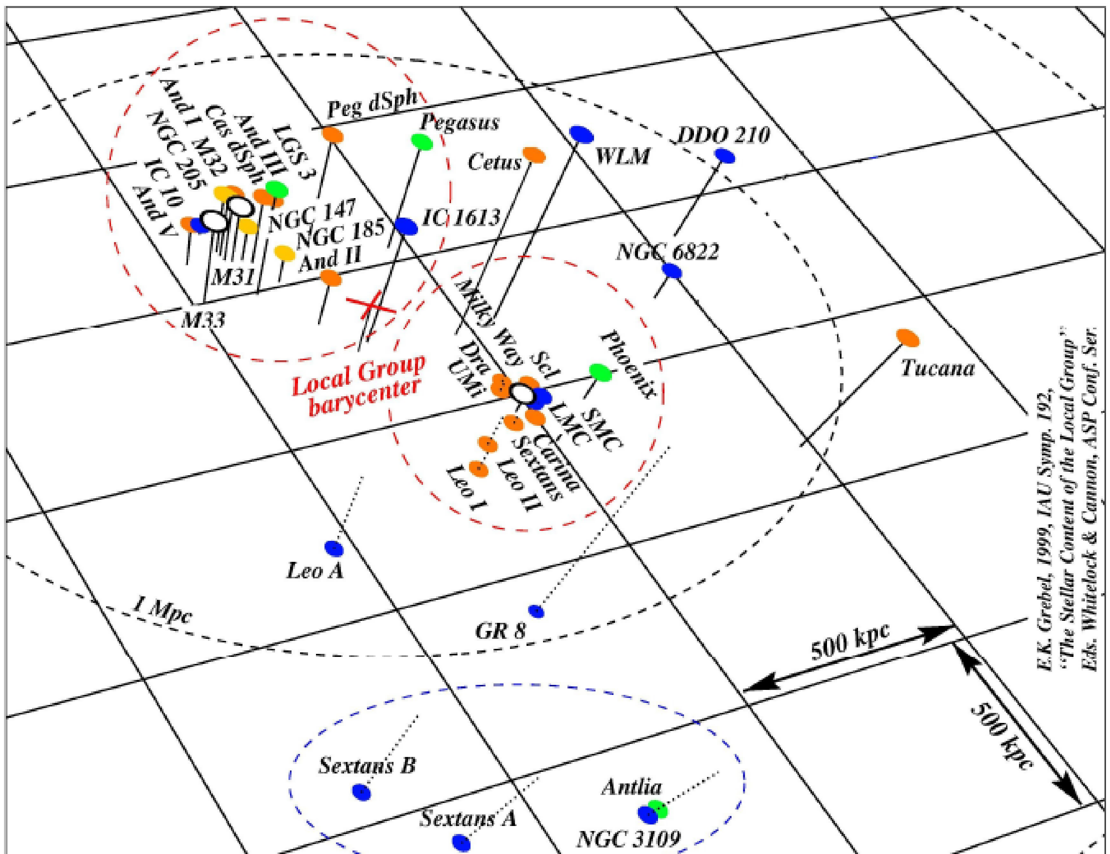

  - » smaller scale -> less confusing / simpler evolution??

Comparing Trends for Different Stellar Samples

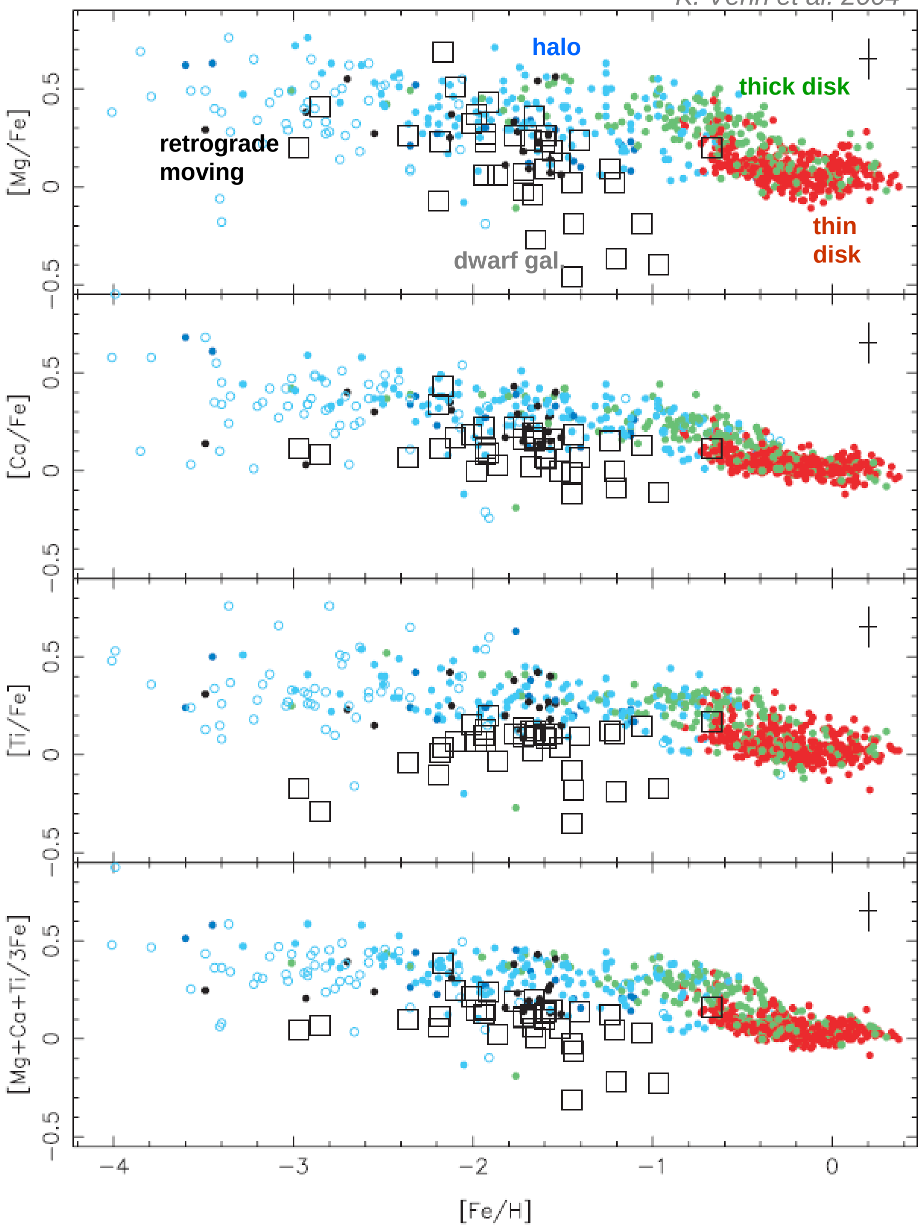

☆ Separation of Stellar Groups:

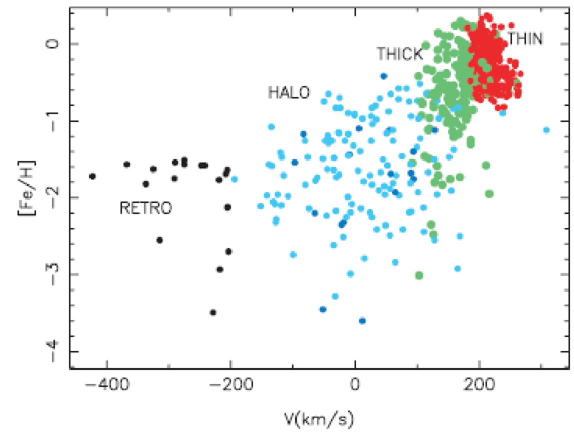

- 'normal' Milky Way Stars
- 'retrograde' Stars (accreted from merger??)
- Dwarf Galaxies' Stars

☆ Similar Evolutionary Principles

☆ Discrepancies & Offsets

- Implausible Common Origin (merger)
  - α/Fe is lower in dSph's
- Dwarf Galaxies: Differences in
  - SF Histories
  - Relative Contributions of
    - cc-SNe
    - SNIa
    - AGB Stars

Roland Diehl

Galactic Halo vs. Nearby Dwarf Galaxies

☆ Low-Mass & Nearby Dwarf Galaxies are Dominated by a Single, Early Star-Formation Burst

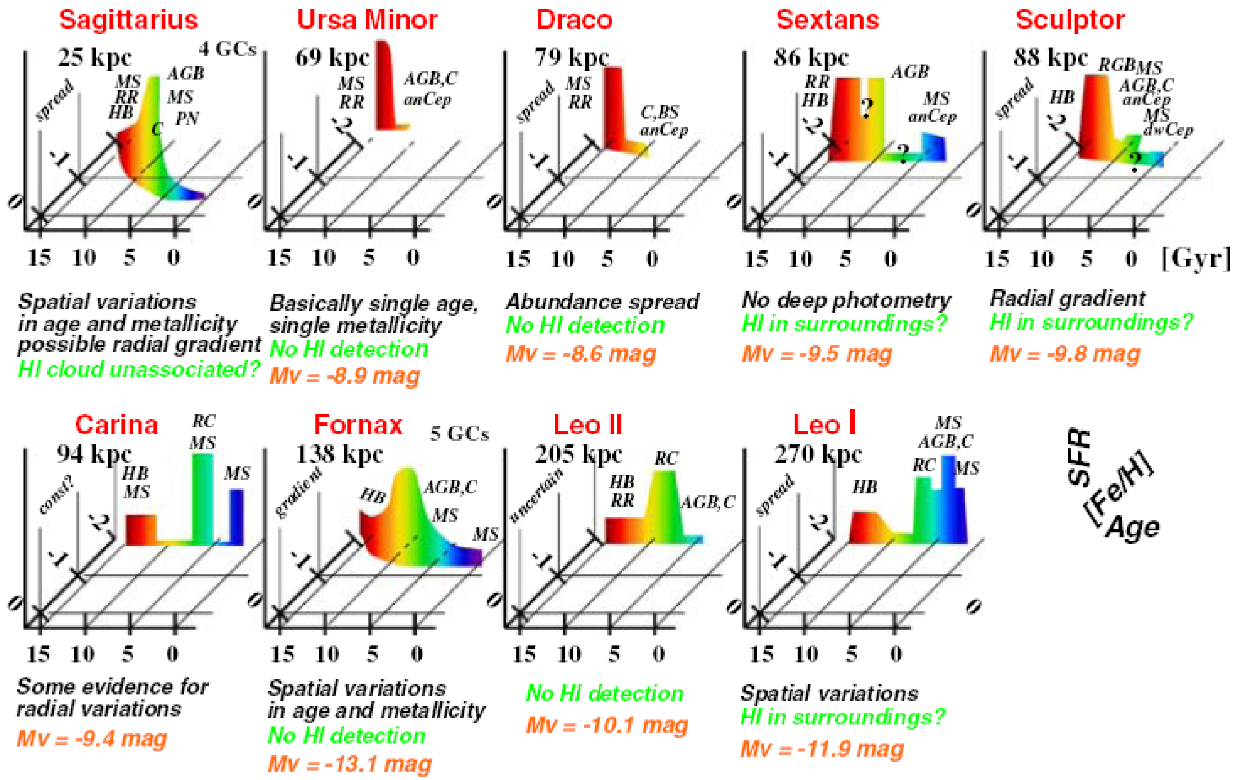

☆ Chemical Evolution is Slower in Dwarf Galaxies

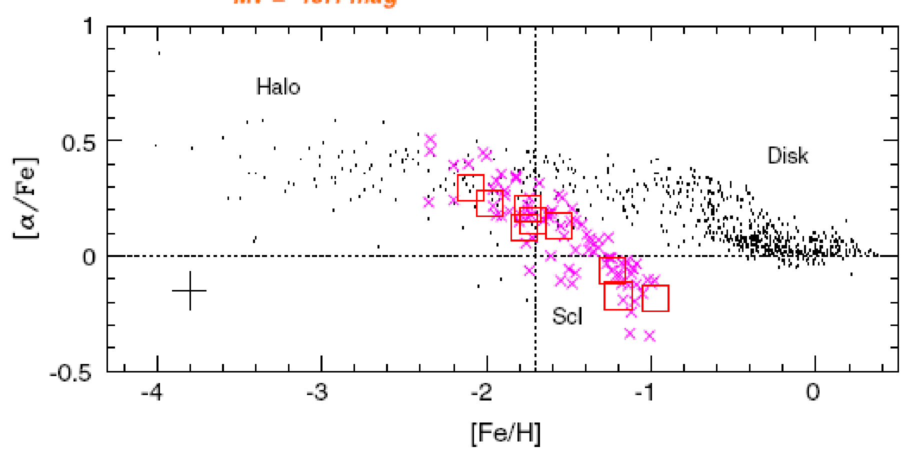

Quasar Absorption Line Spectroscopy

- ☆ Quasar:
  - ☞ Bright, Distant Light Source
  - ☞ Emission Line Spectrum
- ☆ Less-Distant Gas Clouds & Galaxies:
  - ☞ Lower Redshift
  - ☞ Absorption Line Pattern (shifted)
    - » "Ly α forest"
  - ☞ Analysis Task:
    - » Extract Absorption-Line Pattern Attributed to Specific/One Galaxy/Cloud
    - » Evaluate Relative Abundances

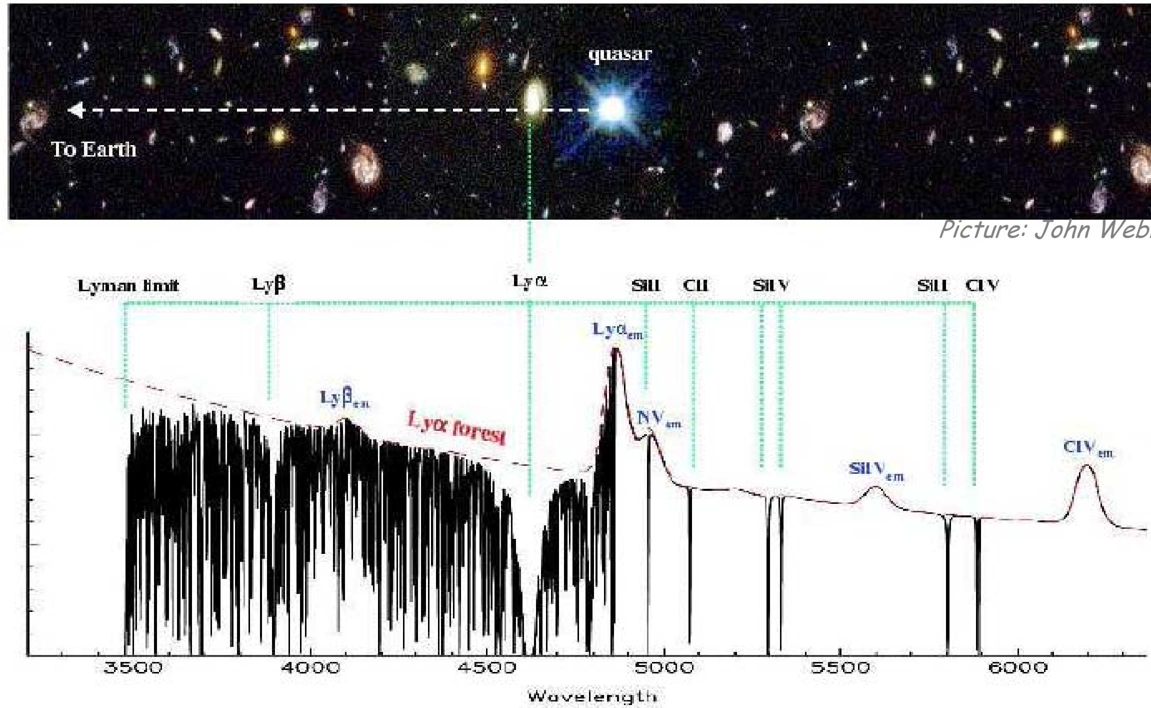

Redshift	Lookback Time (Gyr)	Lookback time (t/t_∞)
0	0	0
0.5	5.4	0.37
1	8.3	0.57
2	11.0	0.76
3	12.2	0.84
4	12.9	0.89
5	13.3	0.92
6	13.5	0.93
10	14.0	0.97
∞	14.5	1.00

Chemical History of Earlier Universe

J. X. Prochaska

- ☆ Suggest Evolution with
  $m \approx -0.25$ dex/Δz
- ☆ Metallicity Inconsistent with CII Line-Inferred Metallicity (missing metals)

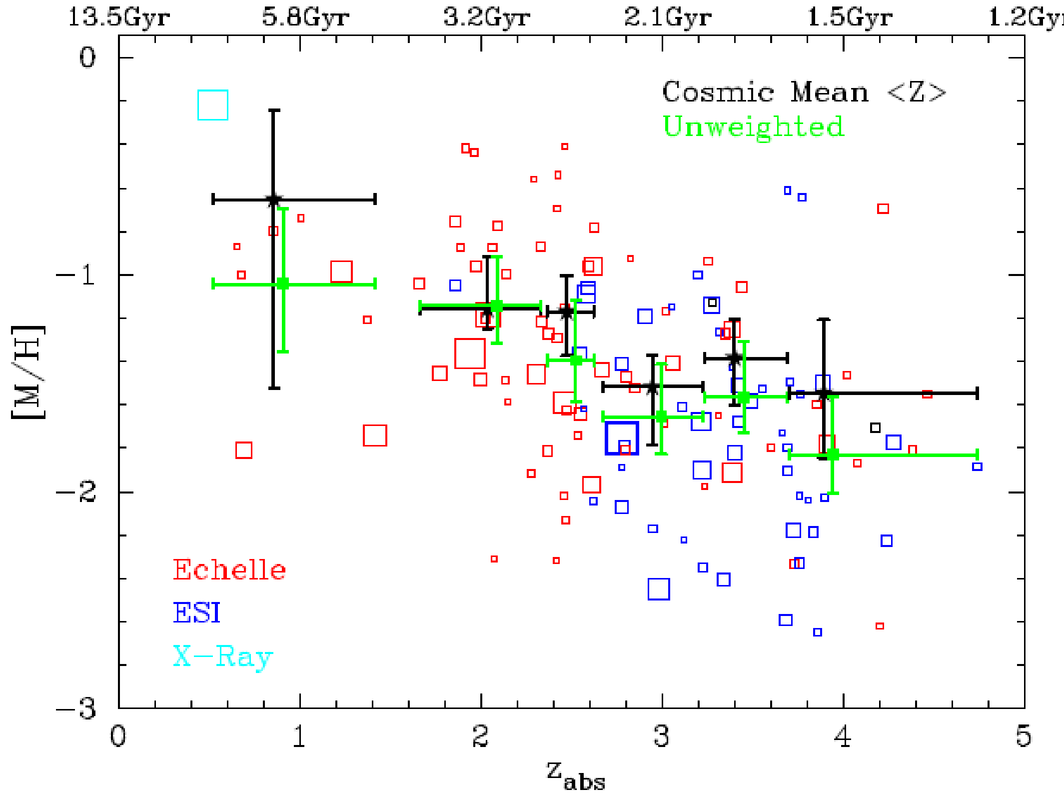

Fig. 1.3. Summary of the metallicity measurements vs. redshift for the 121 DLAs comprising the full, current sample. The area of the data points (squares) scales with the N(H I) values of the DLAs. The dark binned values with stars correspond to the cosmic mean metallicity $\langle Z \rangle$, which is the metallicity of the Universe in neutral gas.

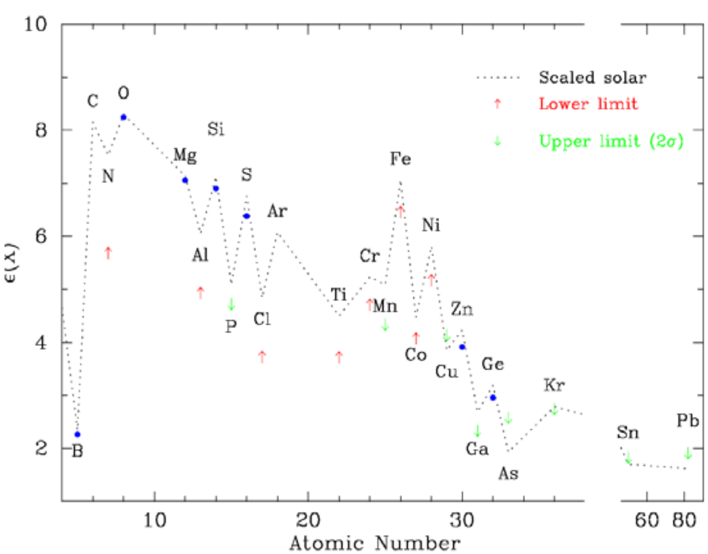

<- eventually compare to nucleosynthesis / chem. Evol. models

Early Nucleosynthesis: DLA System Spectra

- ☆ DLA Systems
  - ☞ Redshift -> Background Galaxy's Age Limit (here:<2.5 Gy)
  - ☞ Compare Observed Abundance Patterns with Models of Different Evolutionary Ages
    - – Rapid Enrichment, Time Scale (<1Gy)
    - – Enrichment of α Elements (from intermed-mass stars)
      - » Analysis: Compare Patterns to Models, varying e.g. Age, Metallicity -> Consistency Check of Chemical Evolution
  - ☞ *Fenner et al. 2004*

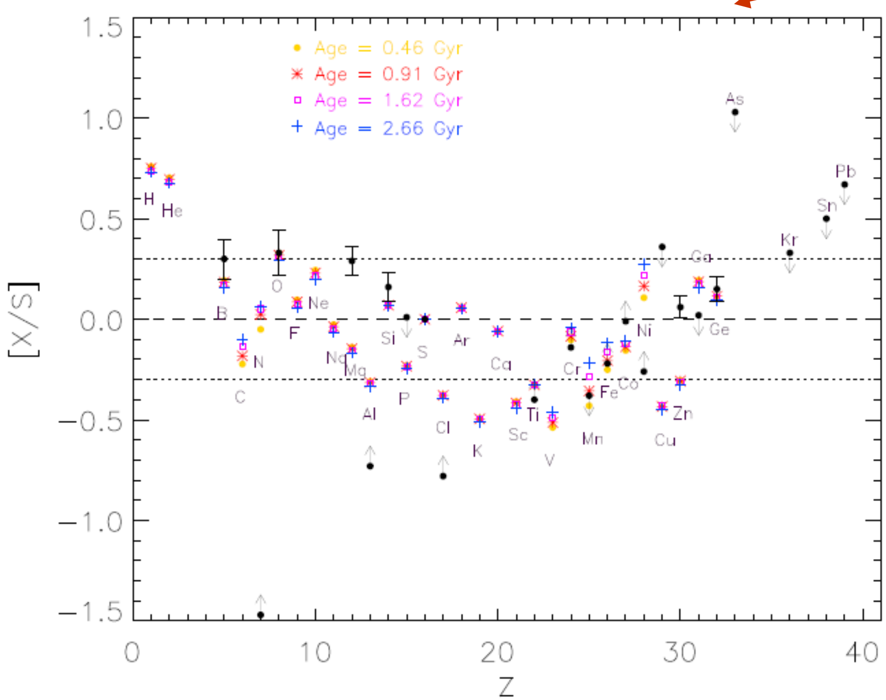

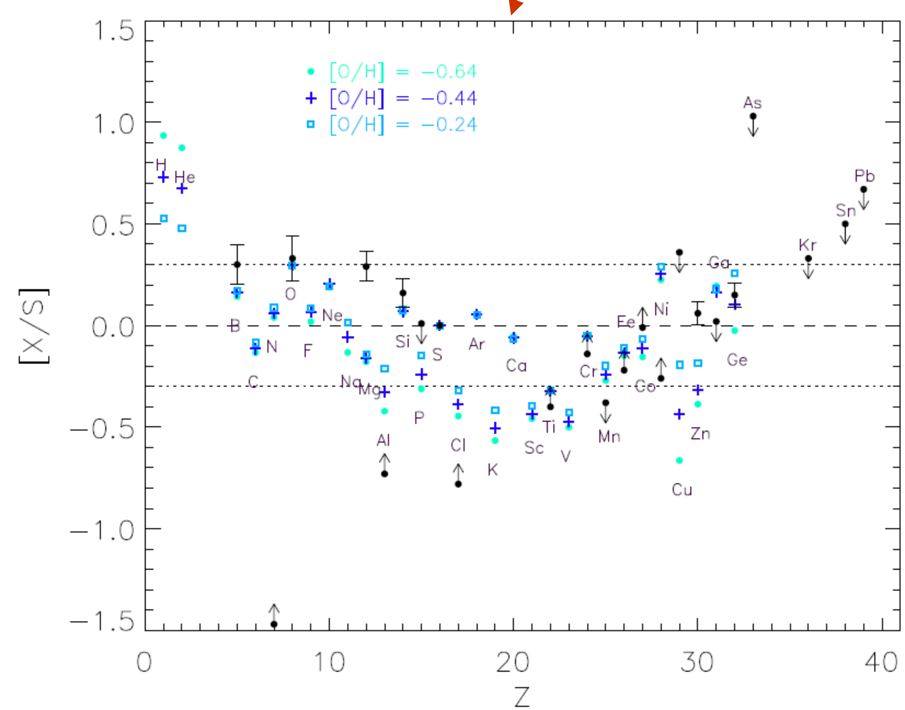

Abundance Constraints/Hints from Galaxy Clusters

- ☆ Spatial Mapping of X-ray Lines from Fe, Si, C, O is Possible
- ☆ If Fe,Si is Attributed to SNIa Production & Ejection from Central Galaxy
  - ☞ Extent of Fe Features Beyond Central Galaxy Measures ICM Transport
  - ☞ Ratio of Fe&Si to cc-SN Elements (O, S) Measures SNIa/SNII Rates
  - ☞ Multiple Clusters Provide Checks / Hints for SNIa Nucleosynthesis

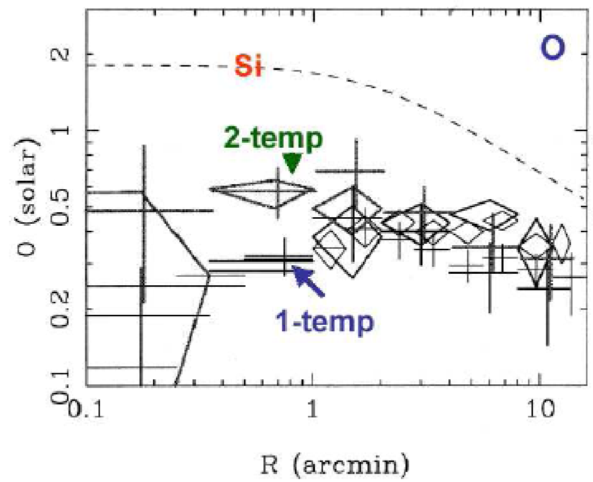

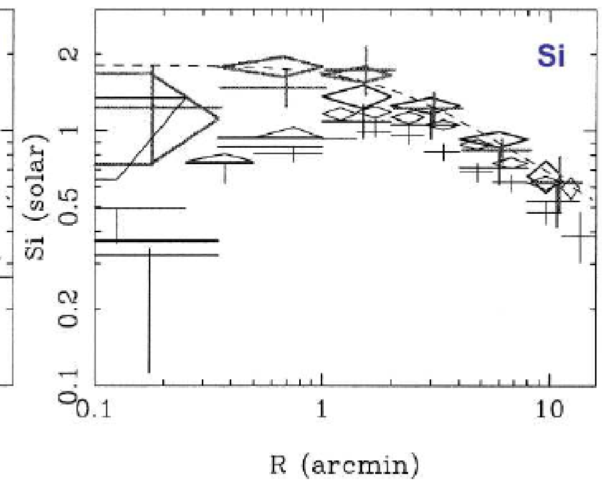

Matsushita et al. 2003; 2006

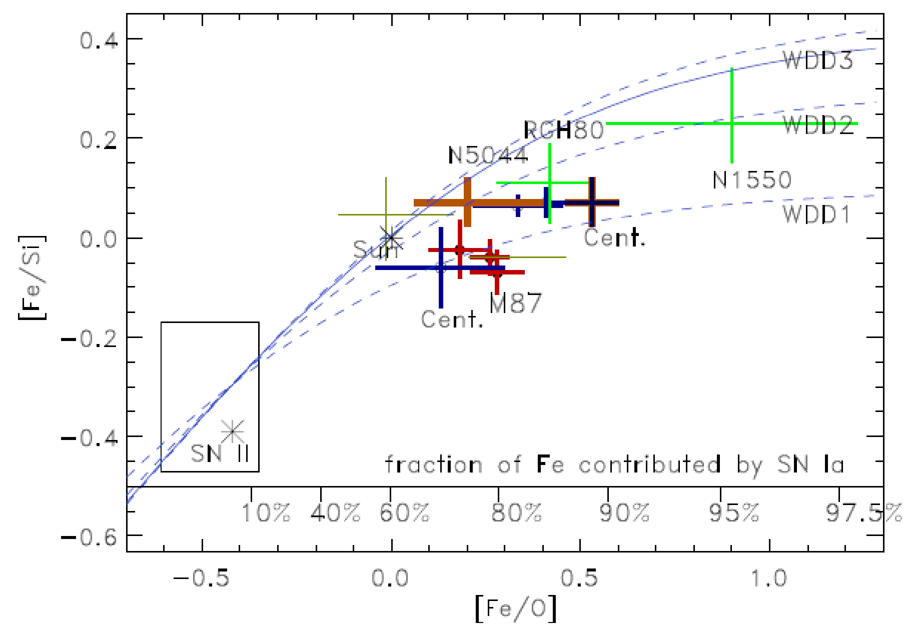

Time Domains of Cosmic Nucleosynthesis

$\tau_{mixing(ISM)}$?

1 First Stars

τ_{delay}?

3 First Type Ia Supernovae

7 Galactic Disk Formation

τ_{disk}?

....? ? Collisions with other Galaxies?

....? $\tau_{coll,i}$?

Latest Star Forming Episode

τ_{SF}?

T_G-0.01 [Gy]

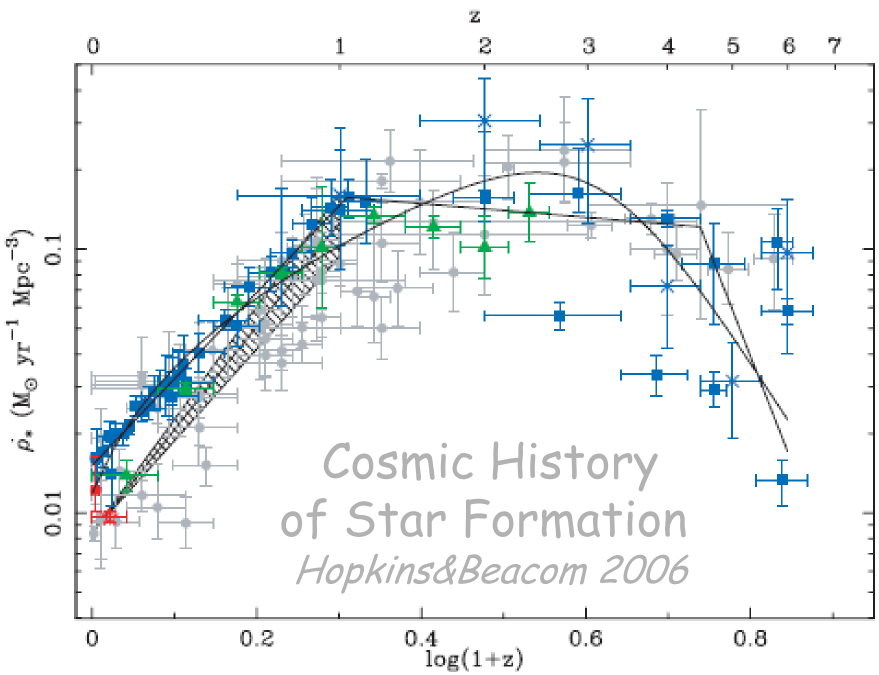

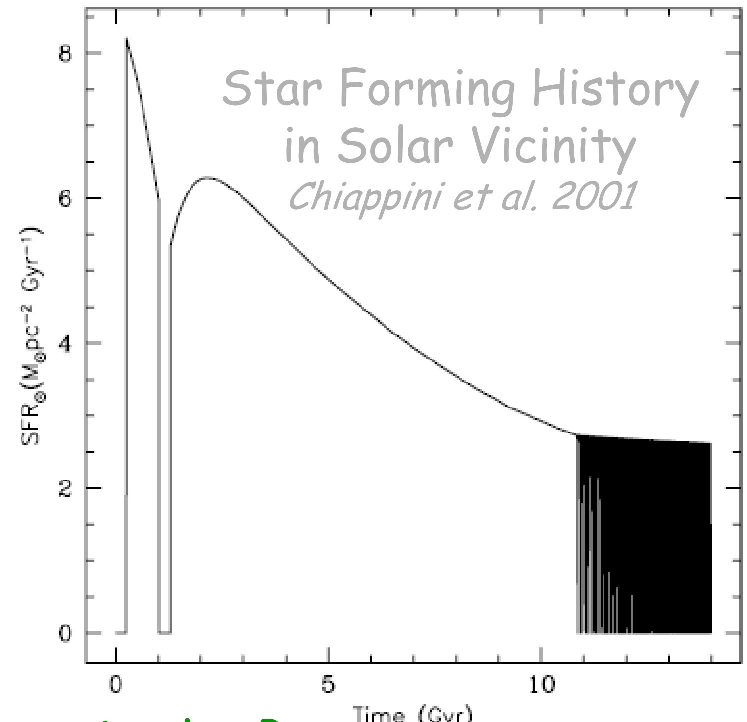

- ☆ Star Formation was More Violent in the Past
- ☆ Details are very Uncertain

How Do Nucleosynthetis Sources Enrich the Universe with Heavy Elements?

☆ Individual Objects/Sources

- ☞ Meteoritic & Gamma-Ray Isotopic Ratios
- ☞ r-process pattern in metal-poor stars

☆ Stellar Groups

- ☞ Abundance Patterns -> Star-Formation History Variety
- ☞ Kinematic Disentanglement in Progress -> Attribute Origins

☆ Chemical Evolution

- ☞ Models Reproduce First-Order Effects
- ☞ Feedback of SN-Activity on SF History Unclear/Difficult

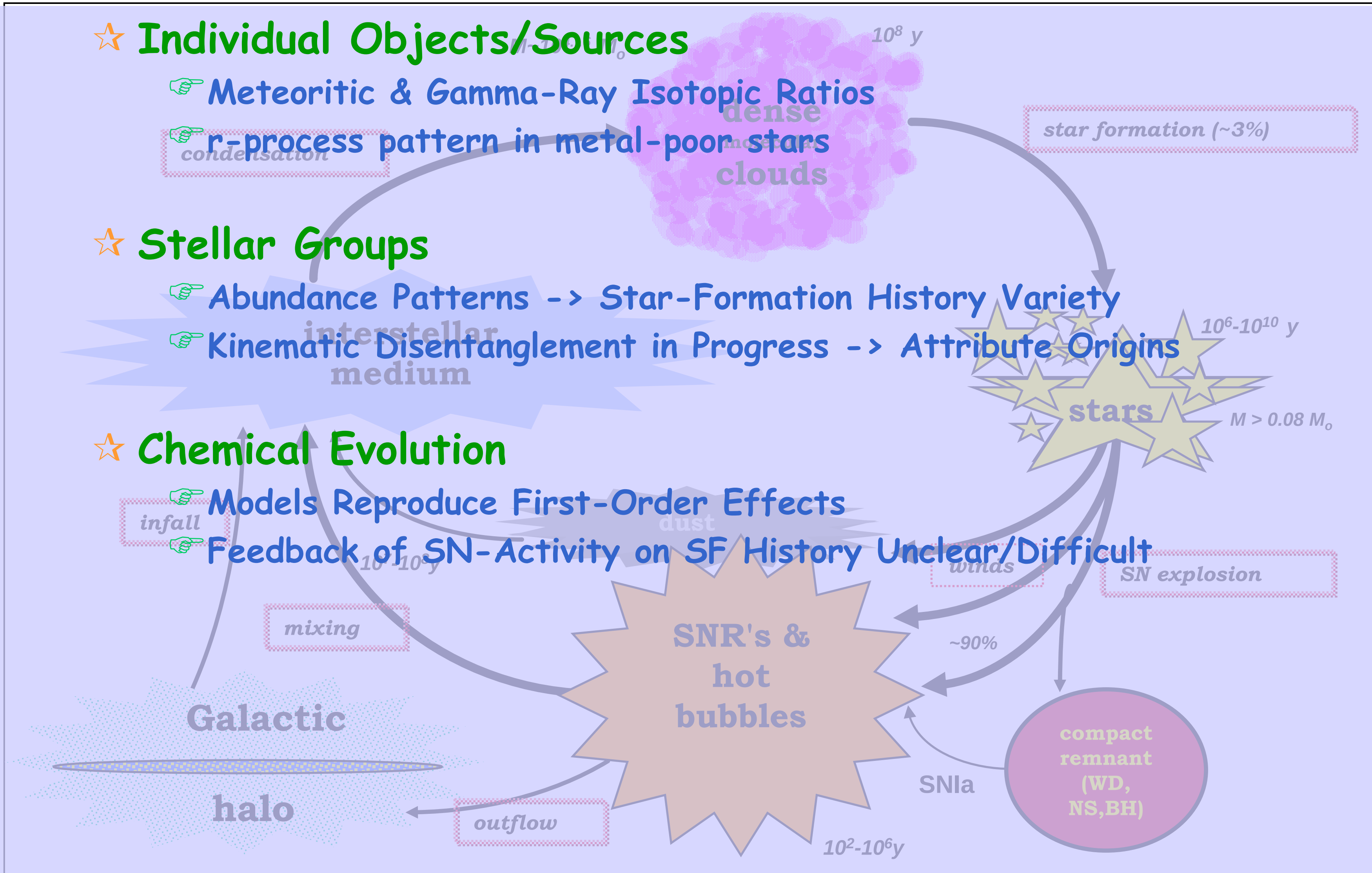

☆ Cosmic Chemical Evolution , Intertwined with Galaxy Evolution and Individual-Object Characteristics - Abundance Details Provide the Key Observational Tools